



## **SkyTEM Survey: Colorado, USA Data report**

Client: USGS OAG Denver Acquisition Branch

Date: January 2012

# Contents

Introduction .....	3
Definition of the areas .....	6
Instruments and parameter setup .....	6
Synchronizing the data .....	7
Calibration of the TEM system.....	7
Special note on Calibration (50/60 Hz) .....	7
Calibration at the National Danish Reference Site.....	9
High altitude test .....	10
Data acquisition .....	12
Ground Base Stations .....	16
DGPS base station .....	16
Magnetometer base station .....	16
Flight reports.....	17
Daily production diary, including weather conditions.....	17
Processed data .....	18
EM processing .....	19
Tilt processing .....	19
Height processing .....	19
DGPS processing .....	20
Digital elevation model.....	20
EM GDB-files.....	22
Presentation of GDB-files .....	24
Mag processing.....	24
Processing of base station magnetic data.....	25
Processing and Filtering of airborne magnetic data.....	25
Corrections to the magnetic data .....	25
IGRF correction .....	26
Tie-line levelling and micro-levelling of magnetic data .....	26
TMI recalculation .....	27
MAG GDB-files.....	28
Gridding of magnetic data.....	29
Inversion of SkyTEM data.....	31
Initial model and optimization norm .....	37
Regularization .....	39
Noise model.....	39
Inversion results.....	40
Presentations - Model sections and grids.....	41
Residuals .....	41
References .....	44
Appendix list.....	45
Appendix 1: Instruments .....	45
Appendix 2: Time gates.....	45
Appendix 3: Calibration .....	45
Appendix 4: Control parameters .....	45
Appendix 5: Modelling and inversion of TEM data.....	45
Appendix 6: Inversion results.....	45
Appendix 7: Digital data .....	45

## Introduction

This data report covers the data acquisition pertaining to a time domain electromagnetic and magnetic survey carried out in Colorado, USA, by SkyTEM Surveys ApS in 2011.

Contact person at SkyTEM: Bill Brown Tel. +1 519-502-1436

Email: bb@skytem.com

From October 11th to 23rd 2011 a combined time domain electromagnetic and magnetic survey was performed by SkyTEM Surveys ApS in Colorado, USA. The survey outlines seen in Figure 1 represent the Paradox, Buckey, and Doloras Canyon survey areas and are outlined in red, orange, and yellow respectively (line spacing 150 m). Figure 2 displays the survey outline for the SanLuis project as a single red polygon (line spacing 300 m).

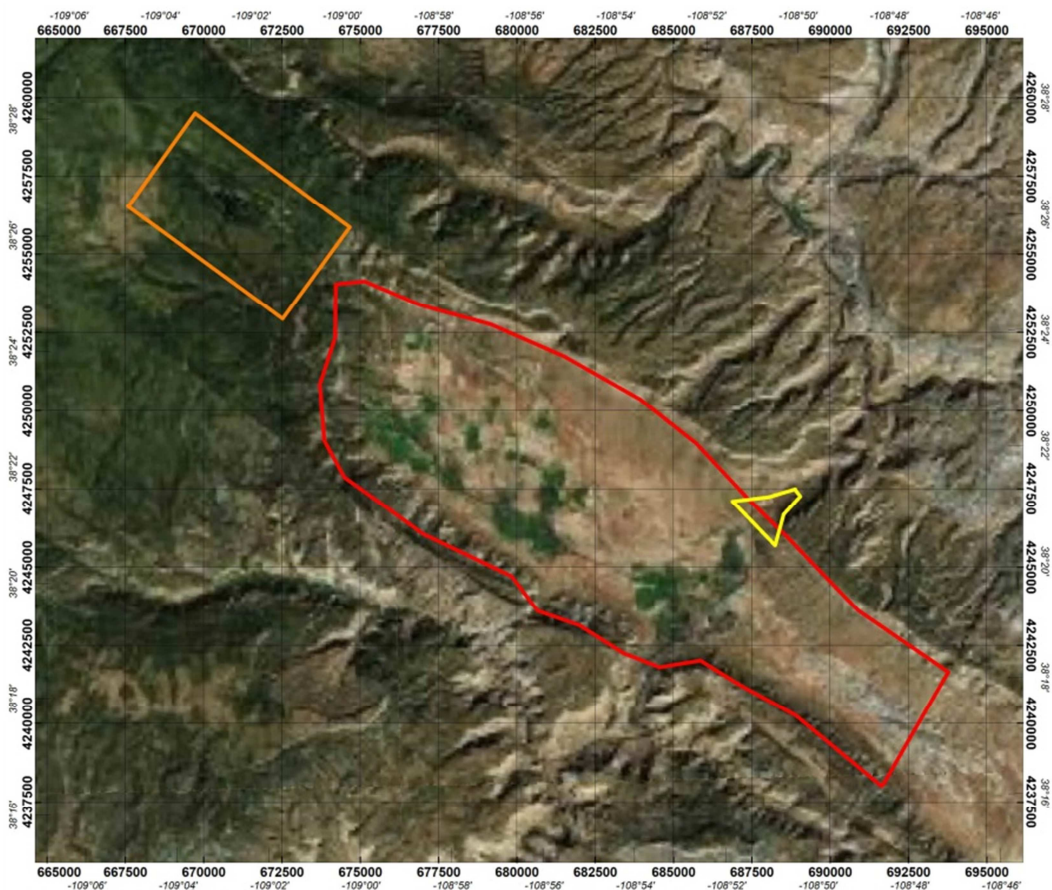


*Figure 1 Project overview with the location of the Paradox survey area. The Paradox, Buckey, and Doloras Canyon survey areas are outlined in red, orange, and yellow respectively. UTM Zone 12N NAD83*

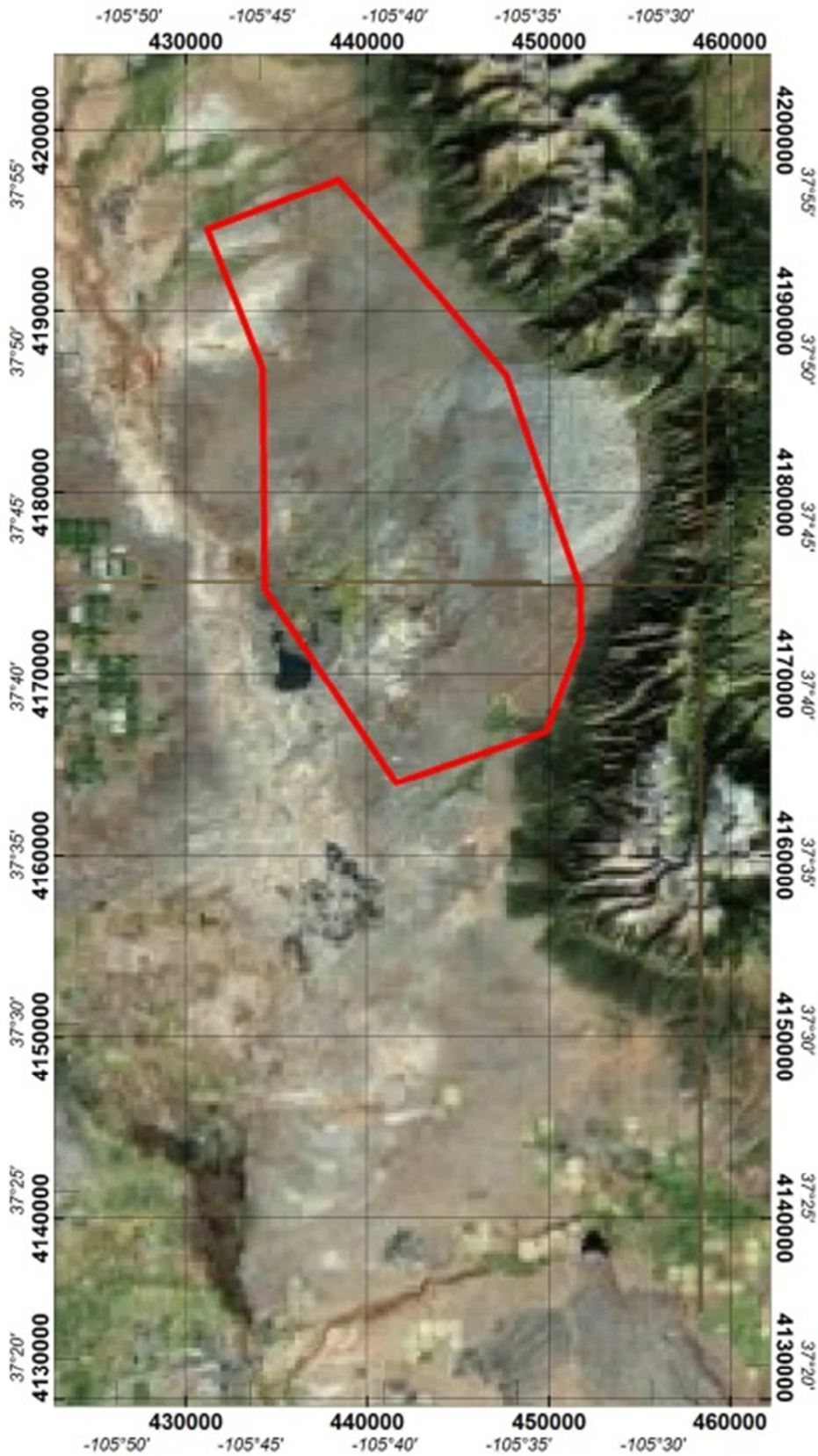


Figure 2 Project overview with the location of the San Luis survey area. The survey boundary is displayed as a red outline. UTM Zone 13N NAD83.

The survey requested by USGS OAG Denver Acquisition Branch was planned to consist of 2657 line kilometers in total.

SkyTEM Surveys ApS has agreed to deliver the electromagnetic and magnetic raw data measured during the flights together with the standard SkyTEM processing and inversion.

This report does not include any geological interpretations of the geophysical datasets.

Client		USGS OAG Denver Acquisition Branch PO Box 25046 204 Denver Federal Center, Denver CO 8225-0046
Field crew		Ib Faber Jean Christophe Ricard
Field work		October 11th to 23rd 2011
Flown line km		2732 km
Flight operation	Helicopter type	Eurocopter AS350FX2, operated by Abitibi Helicopters Ltd
	Average flight speed	50-80 km/h
	Nominal terrain clearance (above any obstacles or hazards)	30 - 40 m
Pilot		Pierre Otis
Report	Data processing and presentation	Russell John Eade
	QC by	Rasmus Teilmann
Contact Person at SkyTEM		Bill Brown Email: bb@skytem.com

## Definition of the areas

The survey is obtained by the two areas referred to as San Luis and Paradox (Figure 1 and Figure 2). In addition to this calibration lines are performed in connection with both areas. The calibration lines are described in detail below in Data Acquisition.

Coordinate systems used are UTM Zone 12N (Paradox) / 13N (San Luis) NAD83.

## Instruments and parameter setup

The instrumentation includes a time domain electromagnetic system: a data acquisition system, a magnetometer, two DGPS', two inclinometers and two altimeters (Figure 3).

A more thorough description of the setup is given in Appendix 1.

The equipment setup operates in dual moment configuration including a Low moment (LM) with a peak moment of  $\sim 3,140$  NIA and a High Moment (HM) with a peak moment of  $\sim 150,000$  NIA.

The main benefit of the dual moment system is the concurrent measurement of early time gates (LM mode) and late time gates (HM mode), providing near-surface solution as well as deep penetration.

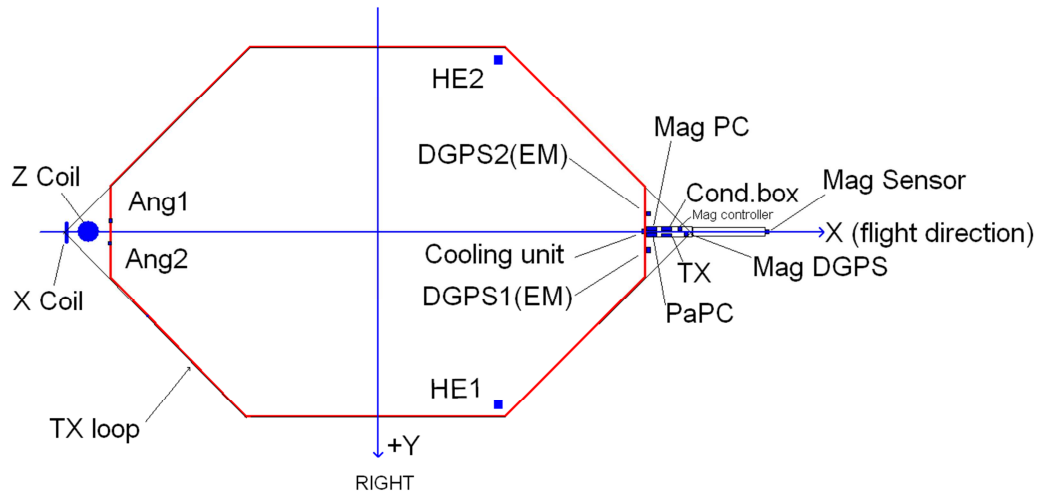


Figure 3 Sketch showing the frame and the position of the instruments. The red line defines the transmitter loop. The horizontal plane is defined by  $(x, y)$ .

The location of instruments in respect to the frame is shown in Figure 3.

X and Y define the horizontal plane. Z is perpendicular to  $(X, Y)$ . X is positive in the flight direction, Y is positive to the right of the flight direction, and Z is positive downwards.

The DGPS systems are mounted in the front of the frame.

The generator used for powering the transmitter is positioned 10 m below the helicopter.

A more thorough description of the system and individual instruments can be found in ref /1/ and Appendix 1.

## Synchronizing the data

All recorded data are marked with a time stamp used to link the different data types. The time stamp is in UTC/GMT.

The time stamp formats are either

1. yyyy/mm/dd hh:mm:ss.sss – Values defined as year/month/day/hours/minutes/seconds.

or

2. Dddd.ssssssssss - Datetime values defined as the number of days since 1900-01-01 and seconds of the day.

## Calibration of the TEM system

### Special note on Calibration (50/60 Hz)

Due to the fact that the electrical power supply grid in North America runs with a frequency of 60Hz, whereas the European grid uses 50 Hz, the calibration at the Danish National Reference site has not been conducted with the exact same timing for the transmitter and receiver (referred to as "the script"). This is done in order to avoid noise from the 50 Hz power grid while calibrating the system.

The following table describes the difference between the script used for calibration in Denmark and the script used for production in North America.

Parameter	50 Hz script	60 Hz script
ON-time HM	10000 $\mu$ s	8000 $\mu$ s
OFF-time HM	10000 $\mu$ s	8667 $\mu$ s
ON-time LM	800 $\mu$ s	800 $\mu$ s
OFF-time LM	1450 $\mu$ s	1283 $\mu$ s
Base frq. HM	25 Hz	30 Hz
Base frq. LM	222.2 Hz	240 Hz

The calibration parameters found at the reference site are not dependent on the timing and can be used regardless of the frequency setup. The following paragraphs and Appendix 3 hence refer to the 50 Hz script calibration, but the parameters are valid for the 60 Hz script as well.

## Calibration at the National Danish Reference Site

The complete SkyTEM equipment has been tested and calibrated at the Danish National Reference Site in March 2011.

The calibration includes measurements of the transmitter waveform and data level in different altitudes. By these measurements it has been documented that the instrumentation can reproduce the reference site using constant calibration parameters independent of the flight altitude.

The calibration results and parameters are shown below:

Low moment:

Shift factor: 0.96 (on the raw dB/dt data)

Time shift:  $-1.1e-6$

High Moment:

Shift factor: 0.96 (on the raw dB/dt data)

Time shift:  $-1.1e-6$

All data has been processed using the above stated calibration parameters.

SkyTEM inversion software (iTEM) handles time shift calibration during import of data. If third party processing or inversion software is used the calibrated gate center times in Appendix 2 should be used.

The waveforms, as well as the reproduced soundings in different altitudes, are shown in Appendix 3.

## High altitude test

A high altitude test was performed on November 11<sup>th</sup>, 2011 prior to survey flying in which the system was raised above 1000 masl. The same equipment and configuration was used for the duration of the survey.

The test was performed in order to establish that system signal to noise level was below an acceptable level on all used gates, and that no drift was present in the system. The data acquired was compared to internal standards and was well below the maximum allowable signal to noise level.

Figure 4 displays the data used for the high altitude test. Test data is acquired at a height of 1000m above ground level over a period of at least 60 second, often longer. Each decay collected at high altitude can be seen in Figure 4 as a grey curve. The solid blue line represents the mean of all decays and the sign of each gate is indicated by the colored circle with positive and negative values being represented by red and blue circles respectively. The dashed blue line indicates the standard deviation of the data calculated for each gate. Gates 5 to 26 are displayed in the LM plot and gates 18 to 34 are displayed in the HM plot.

In order to confirm that no drift was present in the system 'semi' high altitude data is collected on each flight. This is done by raising the system to 400m above ground level. Inspection of the semi high altitude data from each flight occurs on a daily basis. It has been observed that the system reproduces itself and that no drift is present in the system.

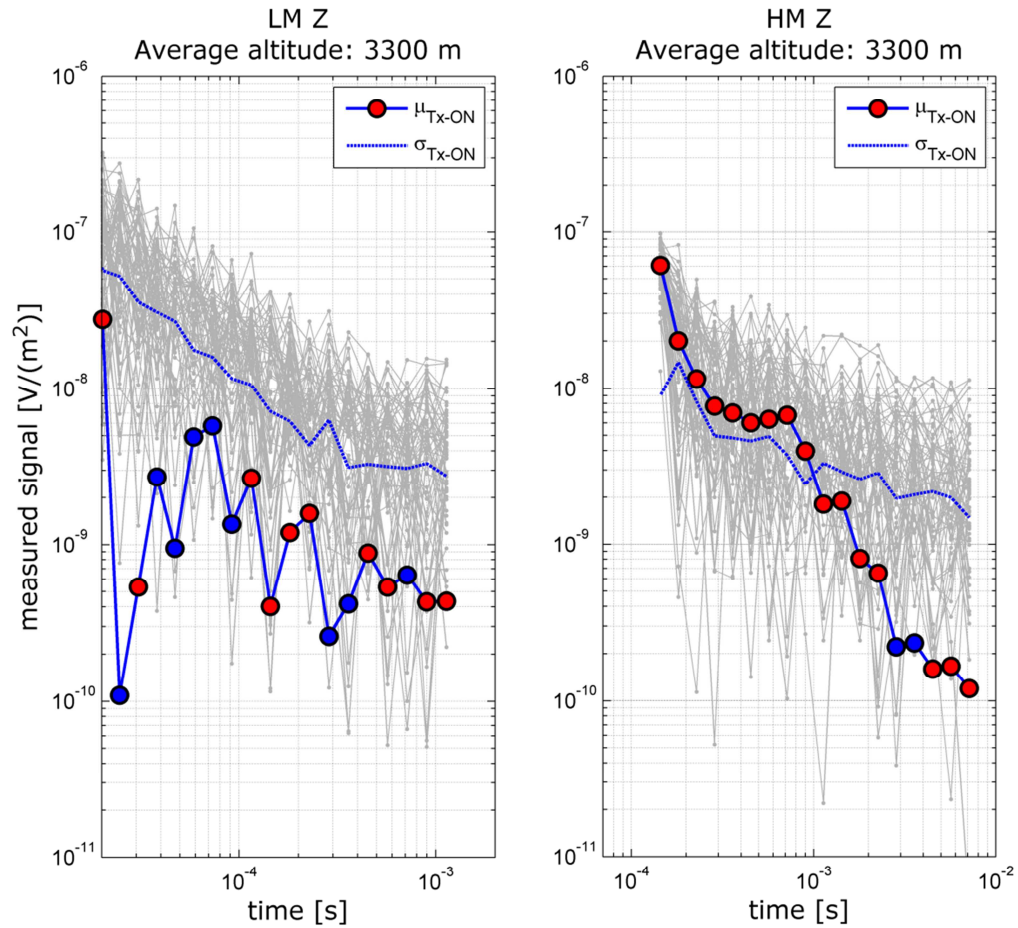


Figure 4 High altitude tests data collected on November 11'th, 2011 at 1000 masl. A comparison of all decays acquired during the high alt test (grey curves) with the mean response (solid blue curve) and standard deviation (dashed blue curve) for each gate. The sign of each gate is indicated by the color and fill of the circle with positive and negative values being represented by red and blue color fill respectively. The LM plot displays Gates 5 to 26 while the HM displays gates 18 to 34.

# Data acquisition

The planned flight lines covering the Colorado area are shown in Figure 5 and Figure 6 (blue lines). The in-lines of San Luis strike 70 degrees (WSW/ENE), line spacing is 300 m. The Paradox area is obtained by two sub-areas, the in-lines are oriented 54 degrees (NW/SW) in the northern area and 44 degrees (NW/SW) in the southern area, line spacing is 150 m. Calibration lines (calc-lines) are performed in connection with both areas. The table below contains an explanation of the flight line numbers.

Block	In-line	Tie-Line	Calc-line
San Luis - Regional	100101 - 110801 300101 - 300501	200201 - 200401	990101 - 990106
Paradox -Buckey -Doloras -Regional	100202 - 106302 150101 - 152401 350101 - 351301 600100 - 600103	200101 - 200801 250101 - 250301	990101 - 990106

The nominal terrain clearance is 30 m above any obstacles or hazards, with an increase over forests, power lines, etc. The safe flying height during survey is always based on the pilot's assessment of risk and deviations from nominal values are at the discretion of the pilot.

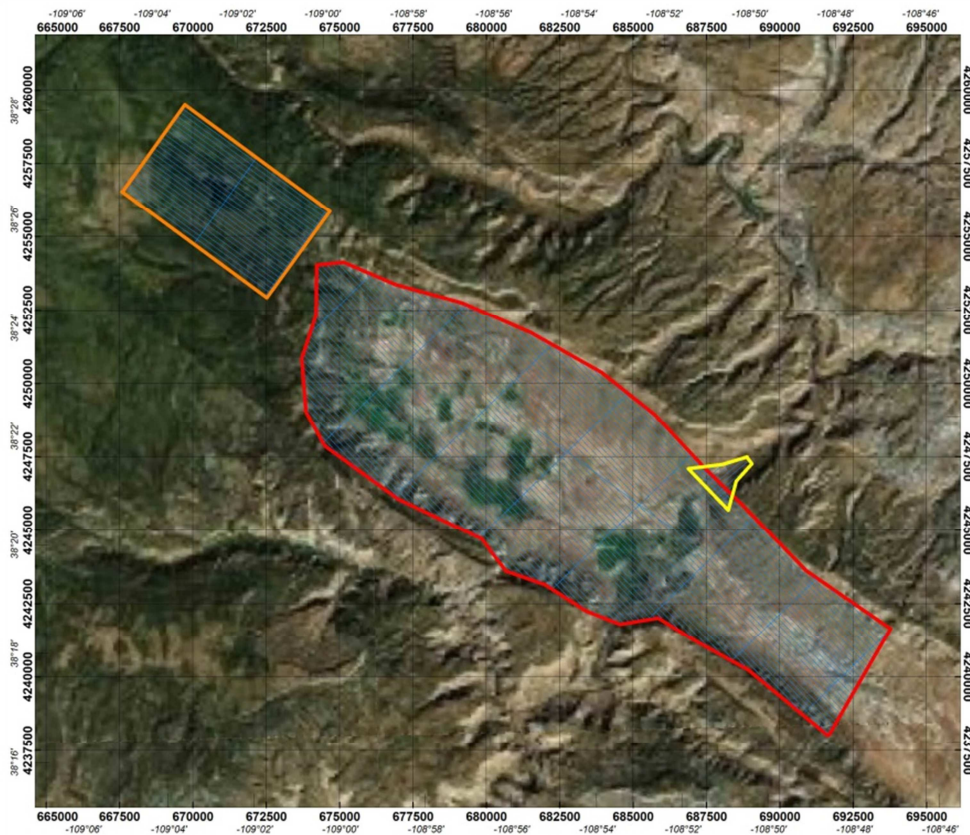


Figure 5 Planned flight lines (blue) for the Paradox survey area. Coordinate system: UTM Zone 12N NAD83.

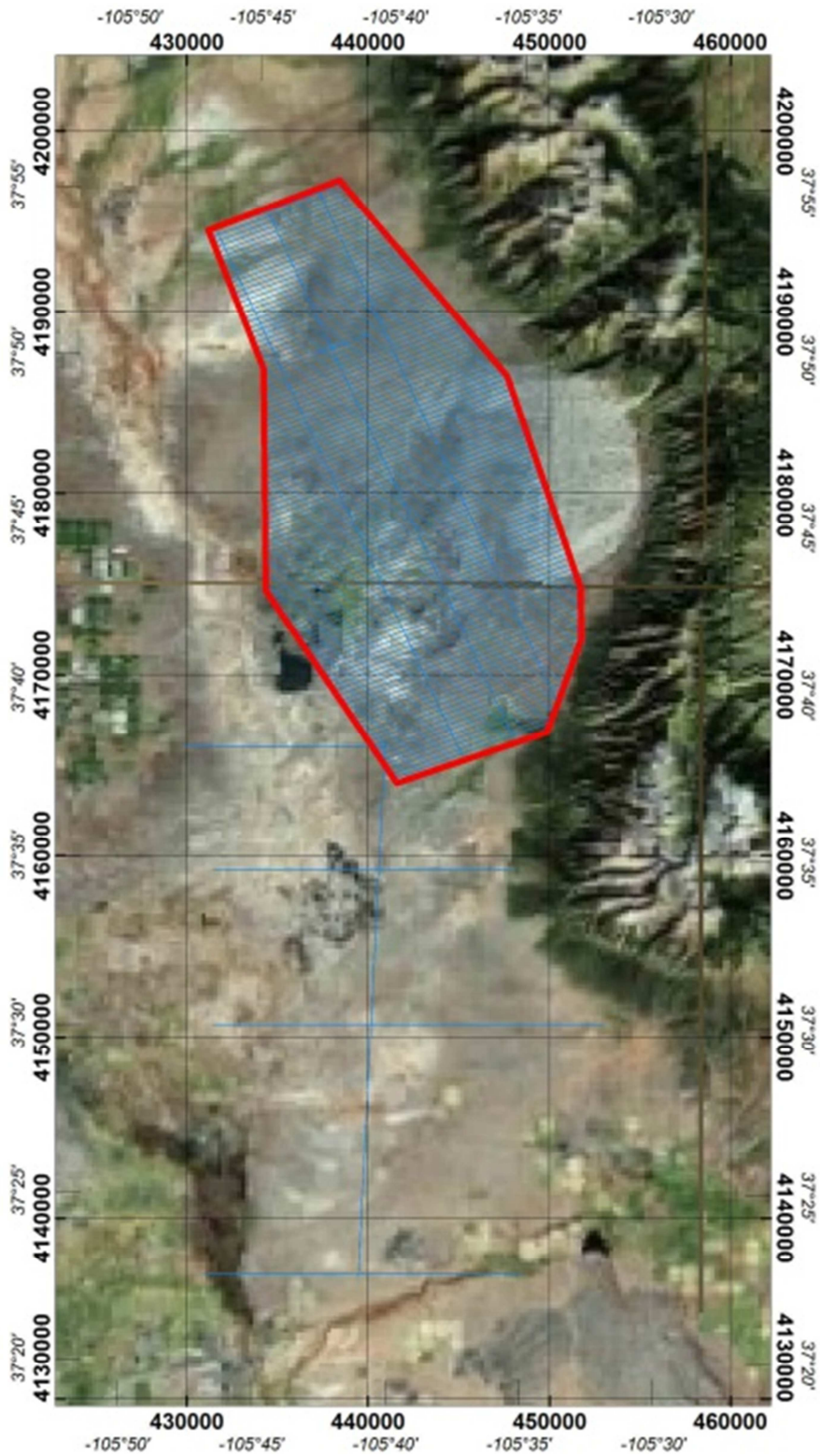


Figure 6 Planned flight lines (blue) for the San Luis survey area. Coordinate system: UTM Zone 13N NAD83.

The planned helicopter airspeed is 85 km/h for flat topography with no wind. This may vary in areas of rugged terrain and/or windy conditions.

The surveyed flight path (what was actually flown) can be seen as red lines in Figure 7 for the Paradox area and Figure 8 for the San Luis area. Discrepancies from the planned lines occur when possible noise sources are present or cultural features such as roads, buildings, and antennas necessitate a diversion. This can also result in the survey lines being broken into pieces and flown in multiple passes or flights.



Figure 7 Red lines represent the GPS recorded flight path of the survey instrument while blue lines indicate the planned flight lines. Coordinate system: UTM Zone 12N NAD83.

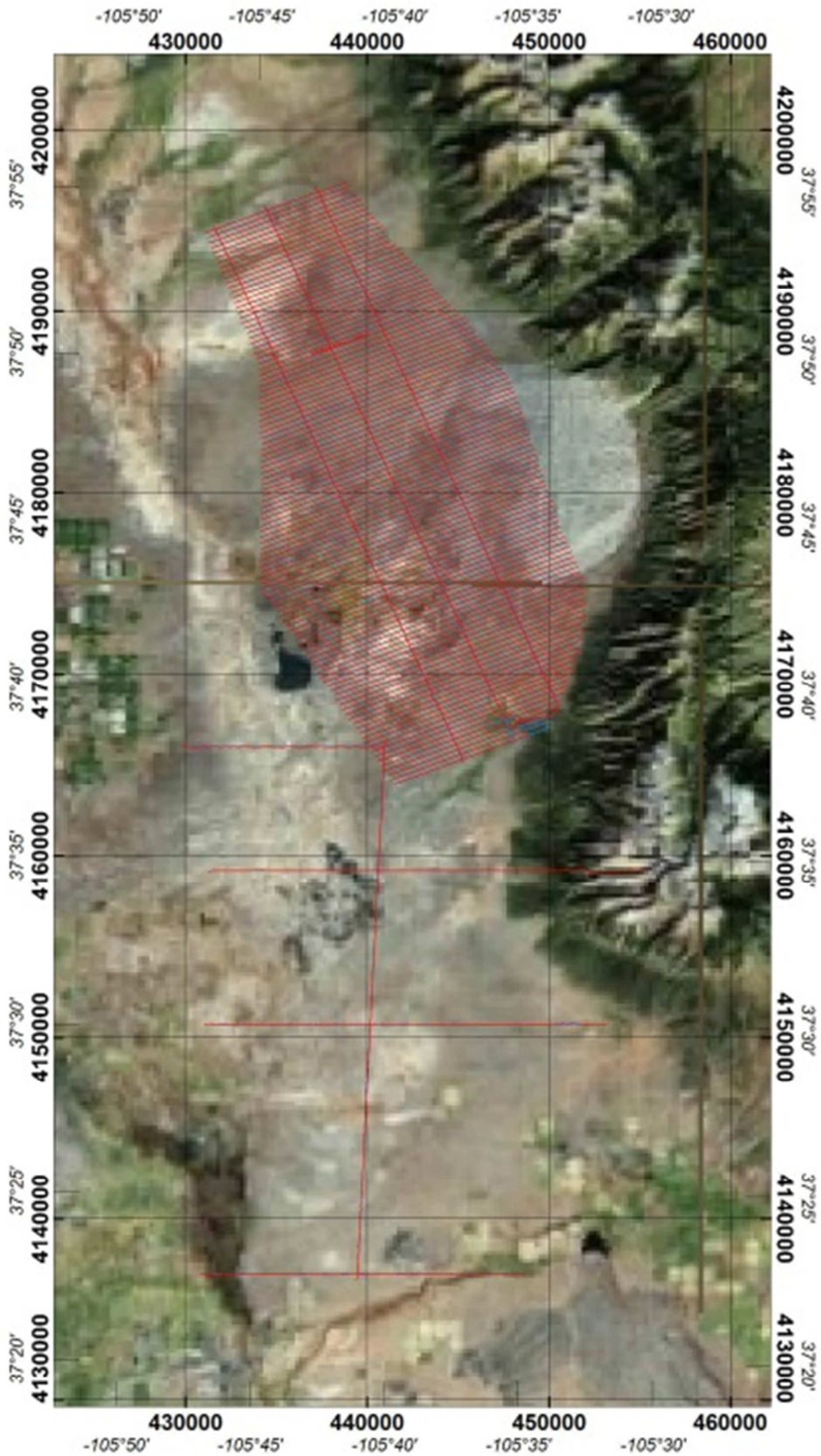


Figure 8 Red lines represent the GPS recorded flight path of the survey instrument while blue lines indicate the planned flight lines. Coordinate system: UTM Zone 13N NAD83.

## Ground Base Stations

The DGPS and magnetic base stations were positioned at the closest accessible place to the survey areas.

### DGPS base station

Utmost effort was made to ensure that the DGPS base station was placed at a location of maximum possible view to satellites and out of any metallic objects that could influence the GPS antenna.

Table showing DGPS base station location (Lat/Lon (WGS84)):

Area	Lat	Lon	Ell. Height
San Luis	37° 41' 38.84"	-105° 32' 56.49"	2403.5 m
Paradox	38° 19' 10.03"	-108° 51' 07.40"	1497.6 m

### Magnetometer base station

Great effort was made to ensure that the base station magnetometer was placed in a location of low magnetic gradient, away from electrical transmission lines and moving metallic objects, such as motor vehicles and aircrafts.

The location of the magnetic base stations can be seen in the table below (Lat/Lon, WGS84, degrees, minutes, seconds).

Magnetometer Base station	Lat	Lon
San Luis	37° 41' 39.11"	-105° 32' 55.99"
Paradox	38° 19' 10.50"	-108° 51' 07.94"

## Flight reports

For each flight, a report with key information regarding the data gathering was made. Listed in the reports are details on the weather, special data parameters and other events which may influence the data. Selected information from the flight reports are shown in the table below:

### Daily production diary, including weather conditions

Date	Temperature (°C)	Wind (m/s)	Visibility	Description
20111011.06	14-18	4 - 6	Good	Production Calibration and recon
20111012.01	14-18	2 - 6	Good	Production
20111012.02	14-18	1 - 4	Good	Production
20111012.03	14-18	1 - 4	Good	Production
20111013.01	14-18	1 - 4	Good	Production
20111013.02	3-8	2 - 8	Good	Production
20111013.03	16-20	2 - 8	Good	Production
20111014.01	16-20	1 - 4	Good	Production
20111014.02	4-10	1 - 4	Good	Production
20111014.03	12-15	2 - 4	Good	Production
20111015.01	14-18	1 - 3	Good	Production
20111015.02	3-8	1 - 4	Good	Production
20111015.03	15-20	1 - 4	Good	Production
20111016.01	15-22	1 - 2	Good	Production
20111016.02	5-12	3 - 7	Good	Production
20111020.01	18-22	1 - 3	Good	Production
20111020.02	5-19	2 - 4	Good	Production
20111020.03	15-22	4 - 7	Good	Production
20111021.02	15-22	4 - 7	Good	Production
20111021.03	15-22	4 - 7	Good	Production
20111022.01	15-22	4 - 7	Good	Production
20111022.02	15-22	4 - 7	Good	Production
20111022.03	15-22	4 - 7	Good	Production
20111023.01	15-22	4 - 7	Good	Production
20111023.02	15-22	4 - 7	Good	Production

## Processed data

All files needed for processing of EM data in Aarhus Workbench are delivered digitally, including, EM data files (skb-files), auxiliary data files (sps-files), mask file (lin-file) and geometry file (geo-file) describing all settings and the geometry of the system.

Selected control parameters are plotted in Appendix 4. The plots contain information about the flight altitude, speed, angle of the frame, transmitted current, transmitter voltage and transmitter temperature.

Mean values and standard deviations of control parameters are found in the table below.

Control parameter		Mean Value		Standard Deviation	
		San Luis	Paradox	San Luis	Paradox
Ground speed*)		80.4 km/h	71.8 km/h	10 km/h	13.4 km/h
Processed height		32 m	42.7 m	7.1 m	15.7 m
Tilt angle	X	-2.6 deg.	1.2 deg.	4.5 deg.	7.3 deg.
	Y	-0.9 deg.	-1.1 deg.	2.2 deg	2.8 deg.
Tx Voltage**)	Tx_off	70 V		-	
	Tx_on	67 V		-	
Low moment Current**)		9.46 A	9.41 A	0.1 A	0.1 A
High Moment Current**)		111.9 A	110.9 A	1.4 A	1.4 A
Tx temperature**)		45 °C		-	

\*) Actual speed varies as a function of day and flight direction due to different wind directions and magnitude.

\*\*) Few spikes are seen in the temperature, current and voltage data. These are not caused by errors in the instruments but are a matter of digital drop outs.

## EM processing

In the following the processing and inversion performed by SkyTEM Surveys are presented.

All data are resampled to 10 Hz using the SkyTEM in-house software SkyPRO.

The data are normalized in respect to effective Rx coil area, Tx coil area, number of turns and current giving the unit:  $\text{pV}/(\text{m}^4 \cdot \text{A})$ .

The raw HM EM data are filtered using a third order polynomial filter with varying filter width increasing at late gate times.

The raw LM EM data are filtered using a Box-car filter with a width of 3.6 s

All auxiliary devices (DGPS, Laser altimeters, inclinometers) are moved to the center of the frame as based on the values stated in Appendix 1.

After merging auxiliary data together with EM data in SkyPRO additional filters in Oasis Montaj Geosoft has been applied. This include for both LM and HM:

1. Gaps from HM/LM series are interpolated using B-Spline filter
  - a) Smoothness= 0.55
  - b) Tension= 0.0
2. Transferring data channels into Oasis Montaj Geosoft Array channels

## Tilt processing

The X and Y angle processing involves manual and automated routines using a combination of the SkyTEM in-house software SkyPRO and Oasis Montaj Geosoft.

The processing involves the following steps:

1. 3 sec box filter (SkyPRO)
2. Manual editing for spikes (Geosoft)
3. Akima interpolation of edited gaps (Geosoft)
4. Low pass filtering of 4.0 sec. (Geosoft)

## Height processing

The height processing involves manual and automated routines using a combination of the SkyTEM in-house software SkyPRO and Oasis Montaj Geosoft.

The processing involves the following steps:

1. Keeping the 2 highest values pr. second and discarding the rest to correct for the canopy effect (treetop filter)
2. 2 sec running box filter (smoothing filter)
3. Tilt correction

4. Averaging of the two laser values
5. Additional filters in Geosoft involving:
  - a. Editing of spurious data (i.e. missing data over lakes etc.)
  - b. Small data gaps interpolated (Akima interpolation)
  - c. Low pass filter of 4.0 sec

## DGPS processing

The DGPS has been processed using the Waypoint GrafNav Lite Differential GPS processing tool. The standard airborne settings have been used.

1. Import of base station (Master)
2. Import of Airborne files (Rover)
3. Calculation of forward and reverse DGPS solution
4. Export as .txt file

The DGPS.txt files are used as input to the SkyPRO software assuring DGPS corrected data in the processed files.

The ground speed, altitude, latitude and longitude from the processed DGPS are merged into the final GDB. Afterwards the coordinates are transformed into UTM Zone 12N (Paradox) / 13N (San Luis) NAD83.

A low pass filter of 4.0 sec has been applied to the above mentioned parameters.

## Digital elevation model

A digital elevation model (DEM) channel has been calculated by subtracting the filtered laser altimeter data from the DGPS elevation.

The Processing to the final DEM involves the following steps:

1. Filtering and processing of the laser altimeter height as described above
2. DEM data received by subtraction of final filtered laser data from final processed DGPS altitude data
3. Grids produced using the minimum curvature method – grid cell sizes are 50 m for Paradox, and 100 m for San Luis.

The DEM channel was gridded (see Figure 9 and Figure 10) in Geosoft format and included in the data delivery catalogue.

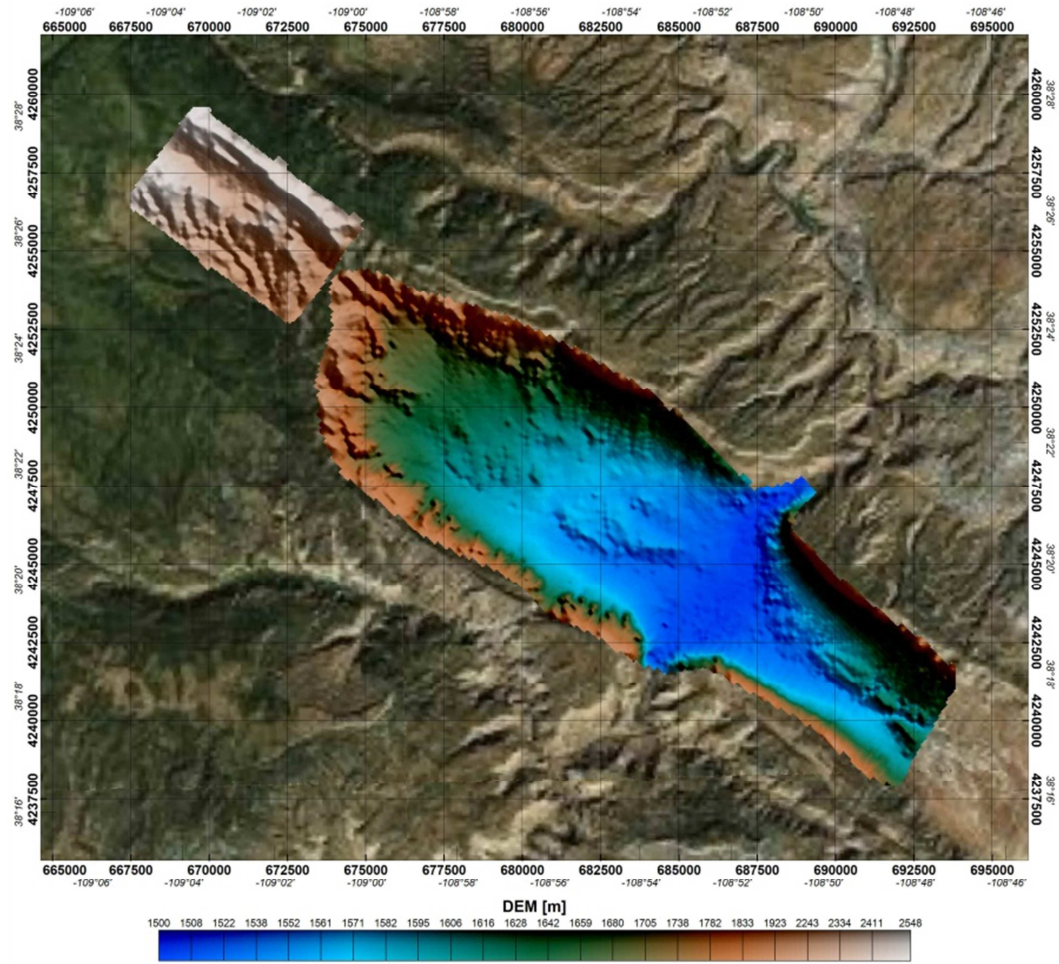


Figure 9 Digital Elevation Model of meters above sea level, cell size 50m UTM Zone 12N NAD83.

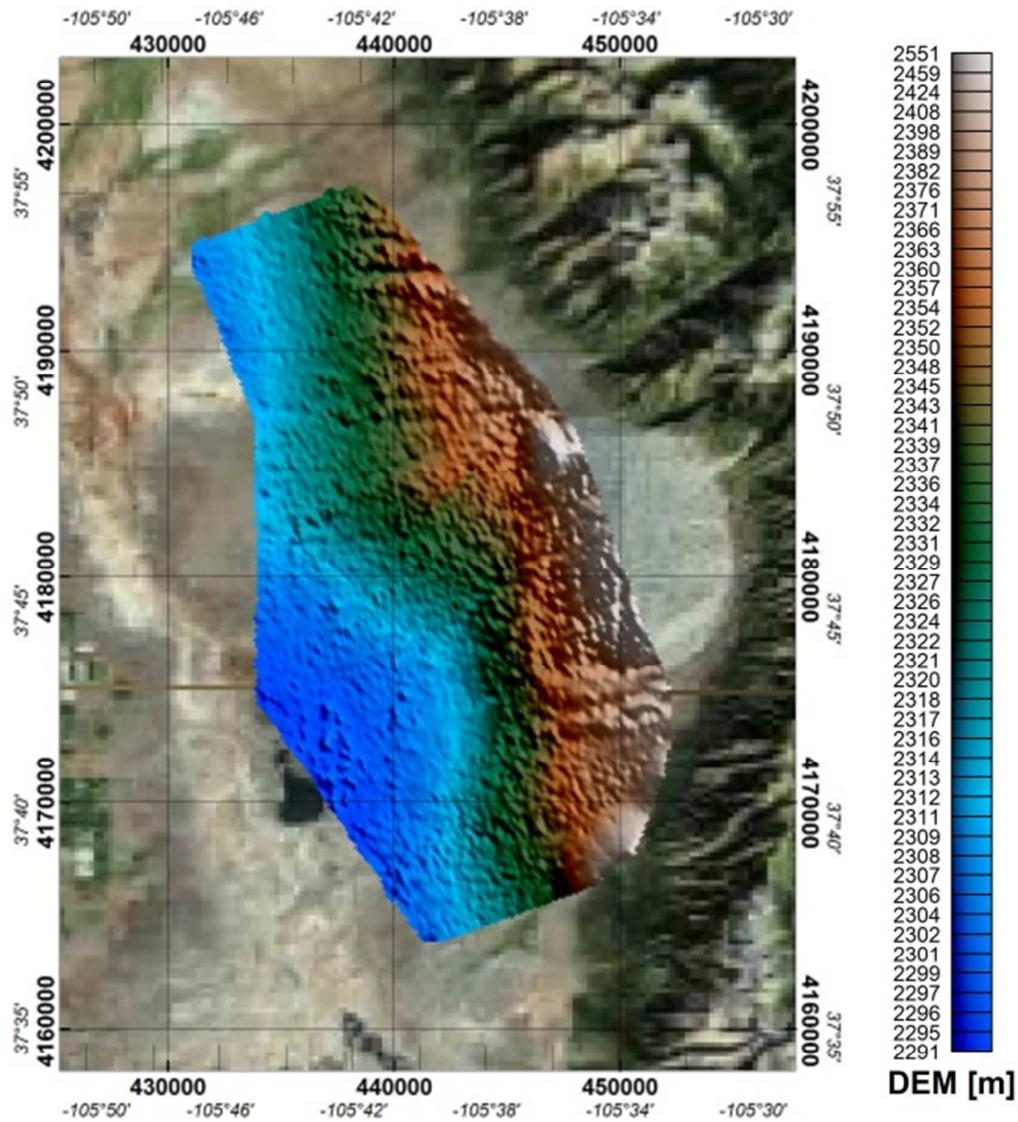


Figure 10 Digital Elevation Model of meters above sea level, cell size 100m UTM Zone 13N NAD83.

## EM GDB-files

The EM GDB files are the final result of the SkyTEM survey, containing all the collected and processed EM data and information used for the interpretation and inversion.

Data in the files are split at the beginning and end of each planned flight line.

The raw EM data and auxiliary data are filtered and processed as described above. All parameters in the GDB-file hence refer to the origin of the frame.

The GDB can be used as input for further processing and gridding and as input to inversion and interpretation software.

The projection of the GDB is given as Latitude/longitude, WGS84 and UTM Zone 12N (Paradox) / 13N (San Luis) NAD83.

The header of the EM GDB-file gives the following information:

Parameter	Explanation	Unit
Fid	Unique Fiducial number	seconds
Line	Line number	LLLLLL
Flight	Name of flight	yyyymmdd.ff
DateTime	DateTime format	Decimal days
Date	Date	yyyymmdd
Time	Time	hhmmss.zzz
AngleX	Angle in flight direction	Degrees
AngleY	Angle perpendicular to flight direction	Degrees
Height	Filtered height measurement	Meters
DEM	Digital Elevation Model	Meters above mean sea level
Lon	Latitude/longitude, WGS84	Decimal degrees
Lat	Latitude/longitude, WGS84	Decimal degrees
E	UTM Zone 12N (Paradox) / 13N (San Luis) NAD83	Meter
N	UTM Zone 12N (Paradox) / 13N (San Luis) NAD83	Meter
Alt	DGPS Altitude	Meters above mean sea level
GdSpeed	Ground Speed	[km/h]
Curr_1	Current, high moment	Amps
Curr_2	Current, low moment	Amps
LM_Z_G5[xx]	Normalized LM Z-coil value: gate 5-26. [xx] refer to Geosoft array channel number*	pV/(m4*A)
HM_Z_G18 [xx]**	Normalized HM Z-coil value: gate 16-34. [xx] refer to Geosoft array channel number*	pV/(m4*A)
LM_X_G5[xx]	Normalized LM X-coil value: gate 10-26. [xx] refer to Geosoft array channel number*	pV/(m4*A)
HM_X_G18[xx]**	Normalized HM Z-coil value: gate 18-34. [xx] refer to Geosoft array channel number*	pV/(m4*A)

\*) If Geosoft array channels are exported, the numbers in the brackets starts from [0]. I.e.

LM\_Z\_G5[4] corresponds to LM Z gate 9. The grids are named after the actual gate number I.e.

InnerBoxHM\_Z\_G21\_Mask.grd.gi is Inner Box, high moment Z, gate 21 (Gate21=Z[20])of the EM channels.

## Presentation of GDB-files

High and low moment z coil gates from the GDB-file have been exported as Geosoft .grd files. The files are included in the data delivery catalogue. Figure 11 shows an example of the HM data.

Please note that no height correction has been applied to the raw EM data. This can cause striations in the data set when looking at the grids. This is due to the fact that variations in height will change the magnitude of the EM signal.

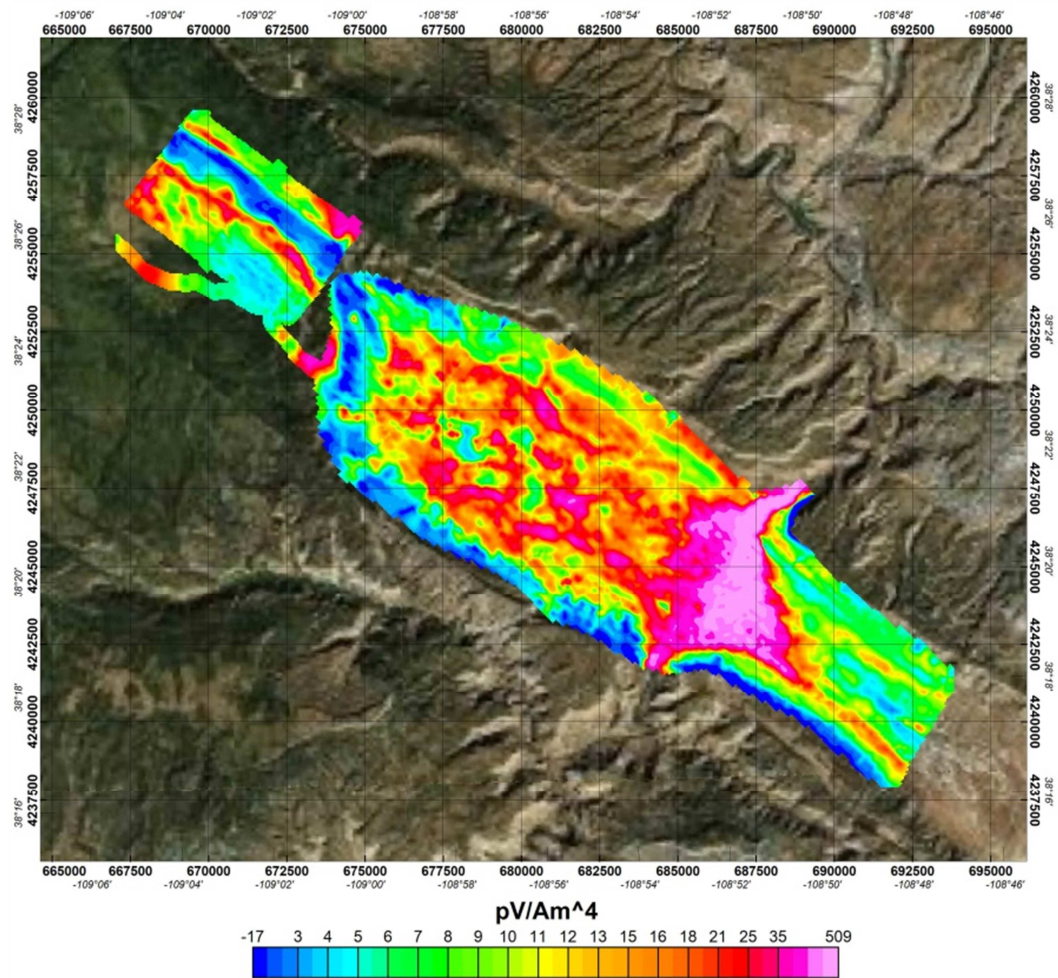


Figure 11 Plot of raw HM Z coil data from Gate 21 of the Outer Box. Gate plots can be found as Geosoft Montaj .grd files in the data delivery catalogue. Warm colors (red) represent high signal and cold colors (blue) represent low signal. UTM Zone 12N NAD83.

## Mag processing

Final processing of the magnetic data involved the application of traditional corrections to compensate for diurnal variation and heading effects prior to gridding. Advanced full processing of magnetic data was implemented in Geosoft's Oasis Montaj software as follows:

- Processing of static magnetic data acquired on magnetic base station
- Pre-processing of airborne magnetic data
  - Stacking of data from 60 Hz to 10 Hz in SkyPro.
  - Moving positions to the center of the sensor in SkyPro.
  - Adapting auxiliary data channels from EM GDB (processed height, Angles, Speed and DEM)
- Processing and filtering of airborne magnetic data
- Standard corrections to compensate the diurnal variation and heading effect
- IGRF correction
- Levelling
- Gridding

## Processing of base station magnetic data

The base station magnetometer data was transferred into the base station Geosoft GDB database on a daily basis for further processing. A non-linear filter was applied to remove spikes and a low-pass filter used to smooth the magnetic data.

IGRF was calculated and subtracted from TMI data to obtain residual magnetic field and remove secular variation.

Diurnal variation was calculated from residual magnetic field by subtracting the mean value averaged from all observations received on magnetic base station in course of the survey.

## Processing and Filtering of airborne magnetic data

No spikes or data out of range was observed on airborne TMI data therefore no manual editing or non-linear filtering of the data was required. TMI data was filtered and interpolated as follows:

- Adjacent record at the beginning and end of each 0.3 sec gap in magnetic data not measured during low moment TEM data acquisition was deleted. These records may still be influenced by B-field generated during low moment TEM data acquisition.
- Bi-cubic spline (tension of 1.0 and smoothness of 0.6 was applied as low-pass filter – this filter also interpolates the gaps in magnetic data not acquired during low moment TEM data acquisition (0.3 sec gaps)

## Corrections to the magnetic data

The processing of the data involved the application of the following corrections:

- Airborne magnetometer data was corrected for diurnal variations. Calculated diurnal variation was subtracted from the filtered airborne magnetic data.

- No time lag correction is necessary since the positions are shifted to the sensor location to account for the distance between the GPS position and the position of the magnetic sensor.

The heading correction test flown during the survey shows the heading errors as indicated in the following table.

Direction	Heading Correction
0 deg	-0.294
90 deg	-0.613
180 deg	0.128
270 deg	0.779

The coefficients listed above were so low that no heading correction was applied to the data.

### IGRF correction

The International Geomagnetic Reference Field (IGRF) is a long-wavelength regional magnetic field calculated from permanent observatory data collected around the world. The IGRF is updated and determined by an international committee of geophysicists every 5 years. Secular variations in the Earth's magnetic field are incorporated into the determination of the IGRF. The IGRF model for all blocks was calculated before levelling using the following parameters for the survey area:

IGRF model year: IGRF 11th generation

Date: variable according to date channel in database

Position: variable according to GPS WGS84 longitude and latitude

Elevation: variable according to magnetic sensor altitude derived from DGPS data

### Tie-line levelling and micro-levelling of magnetic data

After applying the above corrections to the profile data, statistical levelling of control lines followed by full levelling of traverse lines and micro-levelling is usually applied as a standard procedure. The following steps were adapted on the data:

- Statistical levelling on control lines applied
- Statistical levelling on trend lines applied
- Full levelling on traverse lines applied
- Micro levelling applied on traverse lines
  - Decorrugation cutoff wavelength:  
3600 m / 1200 m / 700 m (San Luis/Paradox / Buckley)
  - Max amplitude limit:  
2 nT / 1.5 nT / 1.0 nT (San Luis/Paradox / Buckley)
  - Naudy filter:

800 / 300 / 300 (San Luis / Paradox / Buckley)

The corrected data were then used to generate the final grids free of line directional noise.

### **TMI recalculation**

Residual magnetic field (RMF) was the outcome of processed magnetic data after all corrections and levelling was applied. Total magnetic intensity was recalculated to add back the IGRF using the following parameters.

IGRF model year: IGRF 11th generation

Date: variable as flown

Position: variable according to GPS WGS84 longitude and latitude

Elevation: variable according to magnetic sensor altitude derived from DGPS data

## MAG GDB-files

The GDB files are the main result of the magnetic survey, containing all the processed magnetic data and information for the interpretation and gridding. The projection of the GDB-files are in NAD83, UTM Zone 12N (Paradox) / 13N (San Luis) NAD83. The header of the magnetic GDB-file gives the following information:

Channel Name	Description	Units
Line	Line number	LLLLLS
Flight	Flight number	YYYYMMDD.FF
Date	UTC date	YYYYMMDD
Time	UTC time	HH:MM:SS.S
Lon	Longitude using WGS84 datum	Decimal-deg.
Lat	Latitude using WGS84 datum	Decimal-deg.
E	Easting in UTM Zone 12N (Paradox) / 13N (San Luis) NAD83	Meter
N	Northing in UTM Zone 12N (Paradox) / 13N (San Luis) NAD83	Meter
Alt	Mag sensor GPS altitude – mean sea level altitude – geoid EGM96	Meter
Height	Processed laser altimetry – mag sensor above ground level	Meter
DEM	Calculated digital elevation model – mean sea level	Meter
IGRF_TMI	calculated IGRF-11 - total magnetic intensity	nT
IGRF_Inc	calculated IGRF-11 - magnetic inclination	Degrees
IGRF_Dec	calculated IGRF-11 - magnetic declination	Degrees
Bmag_TMI	Total Magnetic Intensity – raw magnetic data – magnetic base station	nT
Bmag_diur	Diurnal variation– magnetic base station data	nT
mag_raw	raw magnetic data – total magnetic intensity - despiked	nT
Mag_cor	residual magnetic field - corrected for diurnal, lag, heading and IGRF-11	nT
RMF	Residual magnetic field – IGRF removed - final corrected and levelled magnetic data	nT
TMI	Total magnetic intensity – final corrected and levelled magnetic data; IGRF recalculated.	nT

## Gridding of magnetic data

The corrected data was used to generate the Residual Magnetic Field (RMF) and Total Magnetic Intensity (TMI) grid. Corrected magnetic line data was interpolated between survey lines using a minimum curvature gridding algorithm to yield x-y grid values for a standard grid cell size of 50/100 . A Hanning filter was used to remove residual noise.

Figure 12 (Paradox) and Figure 13 (San Luis) both show gridded data after processing data from the magnetometer. All grids from the areas (RMF and TMI) can be found in the data delivery folder.

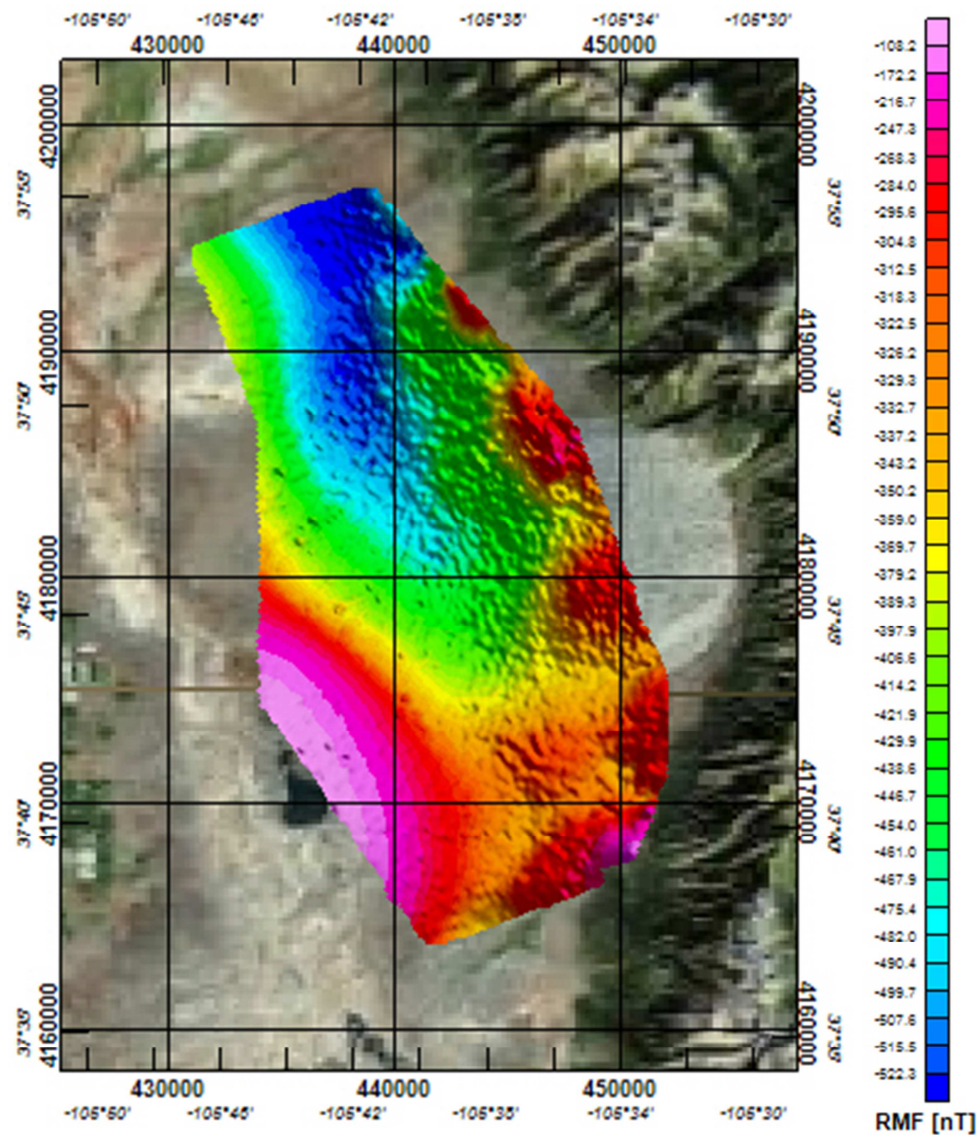


Figure 12 RMF grid of San Luis, cell size 100m. UTM Zone 13N NAD83.

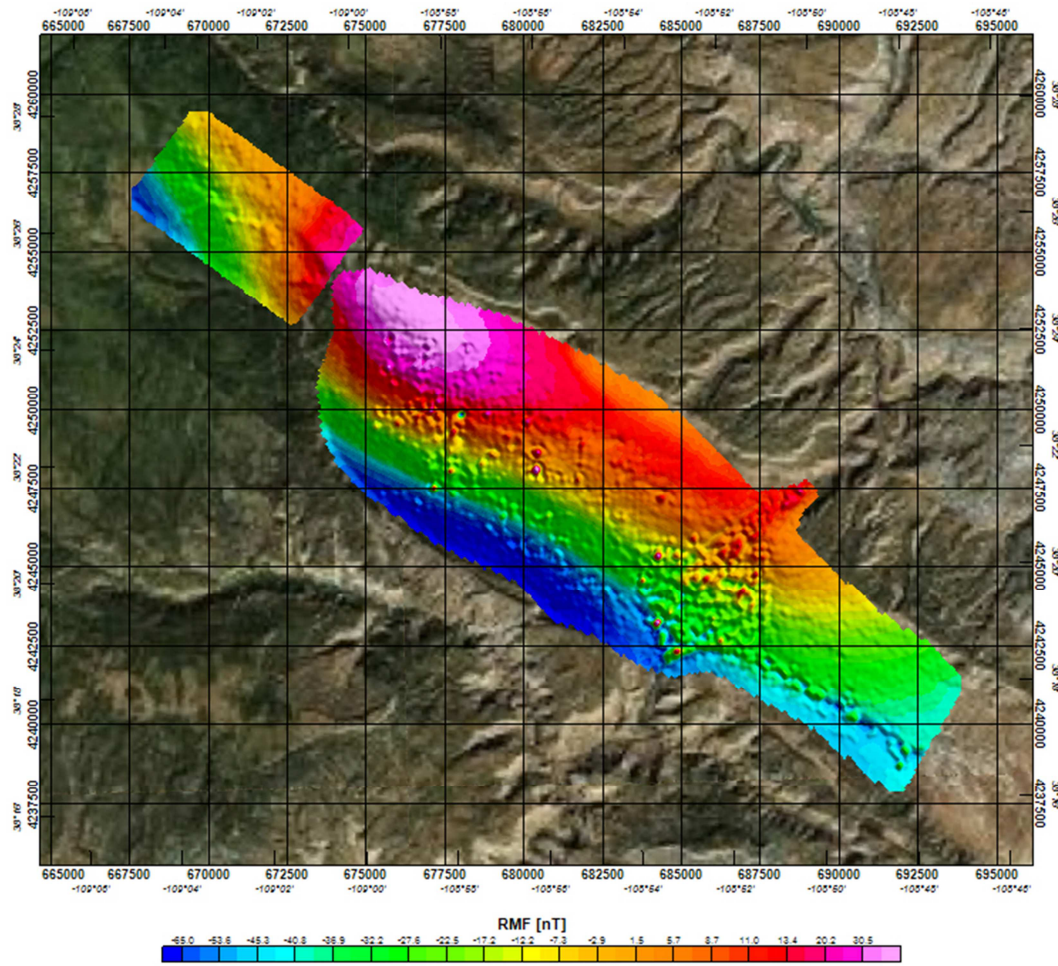


Figure 13 RMF grid of Paradox, cell size 50 m. UTM Zone 12N NAD83.

## Additional EM processing

### 30Hz Noise Investigation

During the inspection of the acquired data, an anomalous and detrimental signal behavior was identified in the high moment TEM data of both the Paradox and San Luis target areas. A thorough investigation was carried out in order to identify the cause of this problem and to assess the options for removing it through post processing. In the following, data from the flight 20111022.02 measured in the Paradox survey area are used for the presented examples. The reason for choosing this specific dataset for presentation is that it contains the most anomalous signal behavior in the entire Paradox area.

### Identifying the problem

Figure 14 displays an interval of high moment data with low signal levels, which has been smoothed along every gate by a spline interpolator. All of the presented gates display an oscillatory behavior with a variable period ranging from just a few to several seconds. These oscillations are related neither to geological variability nor carrier height and angle variations. Furthermore, the oscillations are clearly correlated between gates, and they are especially evident in the latest gates which contain little to no earth response. Regular low pass filtering of the data is unsuited to remove these oscillations due to their low frequency character. Such averaging filters would necessarily be very wide and thereby significantly distort the features of the target earth response.

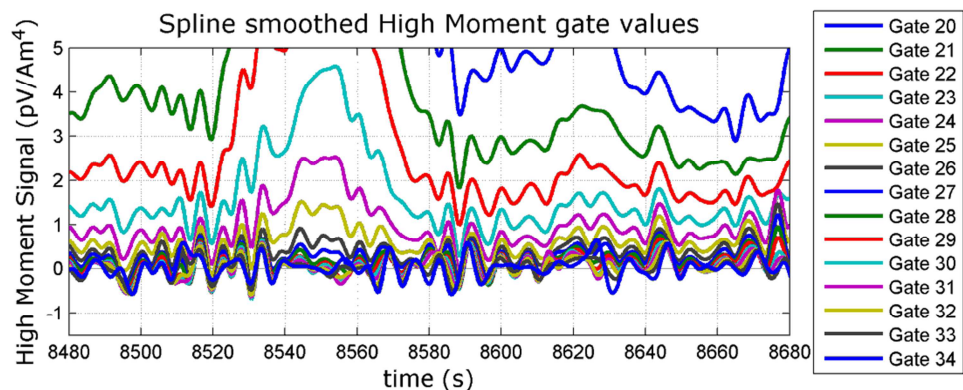


Figure 14 An example of the oscillatory signal behaviour. Many of the initial inversions exhibited numerous narrow "conductive" and "resistive" artefacts due to this.

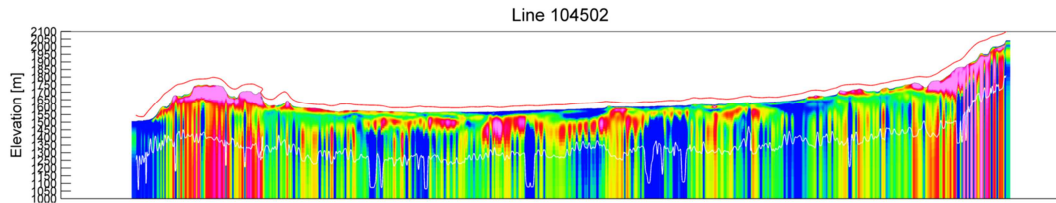


Figure 15 HyTEM inversion result of affected data on line 104502 illustrating the general way in which these oscillations effect the inversion result introducing narrow "conductive" and "resistive" artefacts.

## Noise signal characteristics

A spectral analysis tool applied to the latest gate (gate 26) of the acquired low moment Z data was developed in order to obtain an image of the frequency content of the noise signal and its temporal variations. The low moment measurements have been performed in blocks of 120 consecutive measurements, effectively setting an upper limit on the achievable frequency resolution. The period between transmitter pulses was 2.083 ms yielding a sampling frequency of 480Hz. The resulting Nyquist frequency allows us to resolve frequencies from 0 to 240 Hz, however, aliasing phenomena may occur as the dominant low-pass filtering effect is due to the gate integration (the gate width is 258.6  $\mu$ s for gate 26) which is insufficient to avoid aliasing. The low moment data were acquired using a sign pattern of [+ + - -] meaning that the earth response appears as a signal component at 120 Hz in the resulting spectrograms. Figure 16 displays a time interval of a typical spectrogram where the power line noise at 60 and 180 Hz is clearly visible, while a spurious and persistent noise component is visible at, or near, 30 Hz which appears to be correlated with the 60 Hz signal.

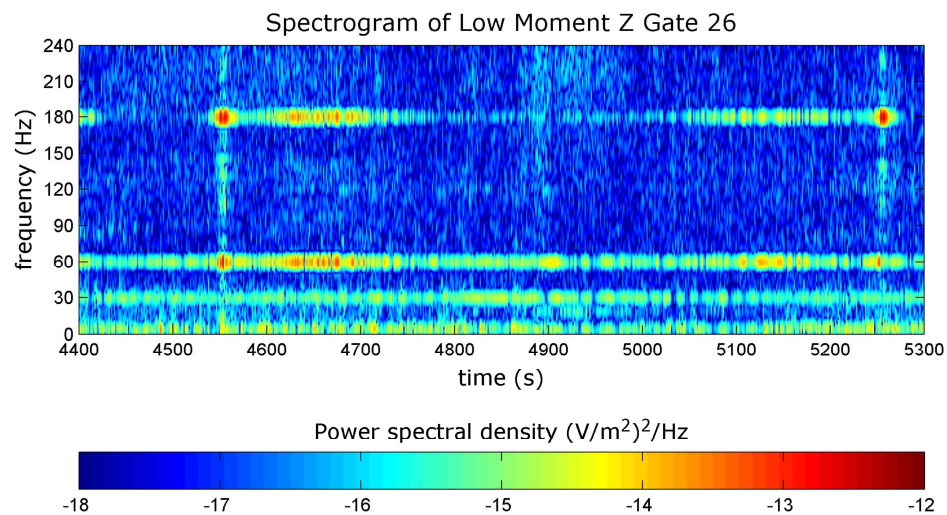


Figure 16 A typical spectrogram over a 900 second interval of survey flying. The power line noise at 60 and 180 Hz is clearly visible, while a spurious and persistent noise component is visible at, or near, 30 Hz which appears to be correlated with the 60 Hz signal.

The averaged low moment measurements are unaffected by the 30 Hz signal because all signal components away from 120 Hz are heavily attenuated by the applied synchronous stacking.

Unfortunately, the high moment measurements are performed using a sign pattern of [+ -] and a period between transmitter pulses of 16.67 ms yielding a sampling frequency of 60 Hz. The signal is therefore located at the Nyquist frequency of 30 Hz, which is deliberately done in order to maximize power line noise immunity. As indicated by Figure 17 synchronous stacking of the high moment data in the presence of a 30 Hz noise signal will introduce a constant offset of each gate with an amplitude that depends on the relative phase between the sampling pattern and the noise signal.

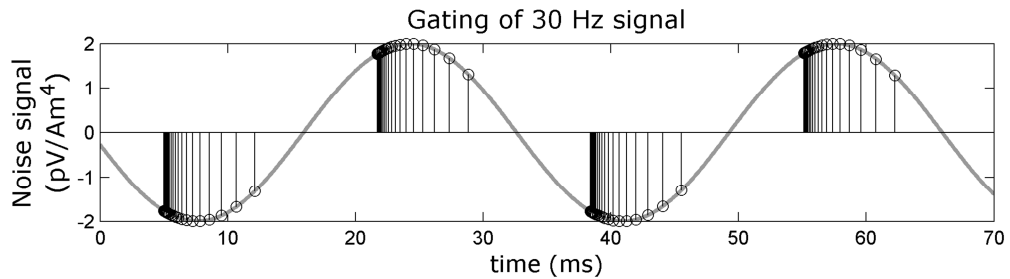


Figure 17 HM gate centre times plotted on a sinusoid wave of 30 Hz.

If the amplitude, frequency or phase of the noise signal changes slowly in time, these offset levels will likewise vary and a situation similar to that observed in Figure 14 may occur.

## Suppressing the noise signal

In an effort to determine and subtract the time varying, noise-generated gate offsets, an automated sinusoid fitting and subtraction tool was introduced and applied to the individual soundings prior to stacking. Assuming a constant noise frequency of 30 Hz, while using only the last four gates to calculate a least squares fit (in terms of amplitude and phase), it was possible to remove a significant part of the problematic oscillations. The most important prerequisite for the successful application of this noise compensation technique is that the 30 Hz noise signal must be the dominating signal contribution for the last 4 gates. This requires that the earth response is negligible in order for the sinusoid fit to be unbiased, while unrelated noise contributions will likewise tend to worsen the fit. Examples of fits and resulting compensated soundings are demonstrated in Figure 18.

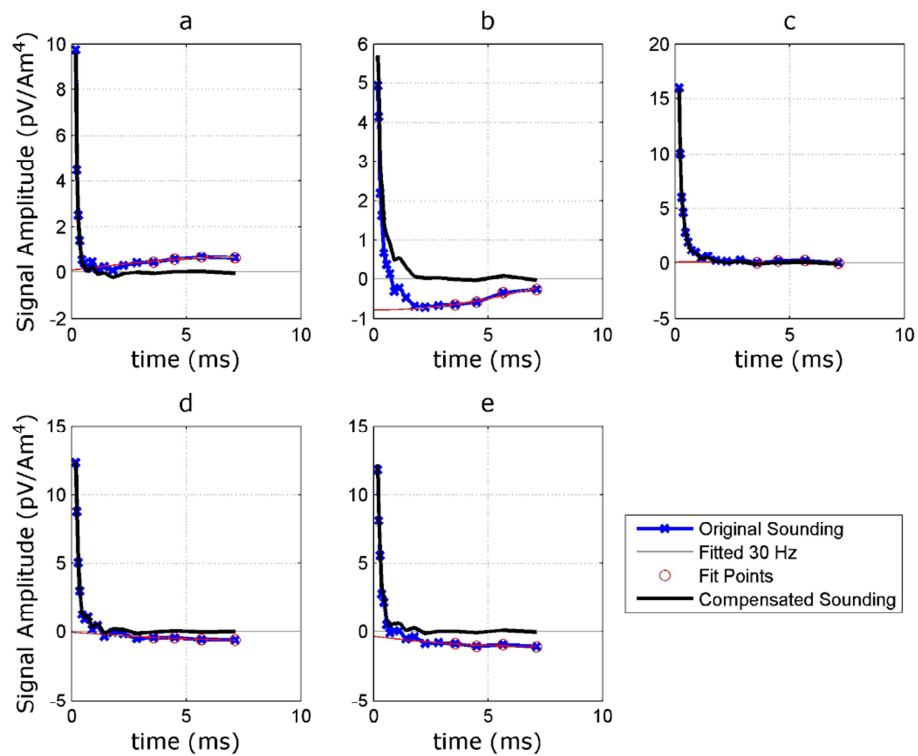


Figure 18 Examples of random decays displaying original and compensated soundings after the 30 Hz signal removal.

In order to avoid removing the earth response in regions with signal in the last four gates, a check on the fitted sinusoid amplitude was made and the compensation was "turned off" if the sinusoidal amplitude exceeded a certain threshold.

## Results and potential issues

Figure 19 shows a "before and after" noise compensation plot of the high moment Z data prior to stacking of the principal measurements (a principal measurement being the difference between a plus and the subsequent minus measurement). It is clear that a large part of the oscillatory noise phenomena has been removed in the lower plot.

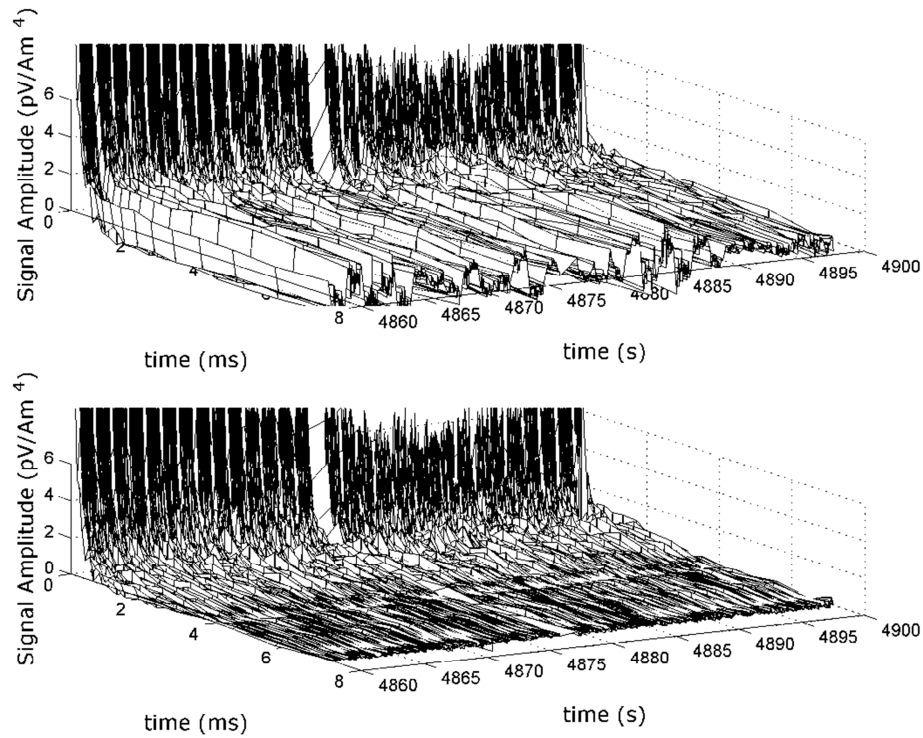


Figure 19 3D illustration of HM Z data before and after compensation (upper and lower plots respectively). Each decay is referenced to single point in time based on the turnoff for that sounding and is used to plot the data along the x axis 'time(s)'. The centre time for each gate determines the position on the x axis 'time(ms)' and the amplitude of the gate value is represented by the z axis 'signal amplitude(pV/Am<sup>4</sup>)'.

An example of the resulting improvement in inversion results is shown in Figure 20.

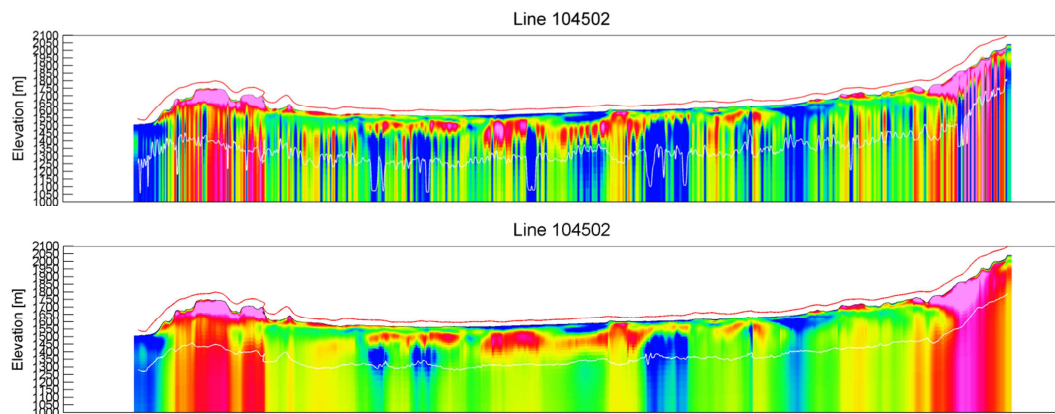


Figure 20 This image displays the improvement in the inversion result achieved through the use of the sinusoid compensation. The upper profile was generated from uncompensated data while the lower profile displays the improved results after compensation. Both images have the same colour scale applied.

The main concern in using the sinusoid fitting and subtraction procedure is the unavoidable small-scale distortion of late gates in conductive areas. The sinusoid fitting procedure will inevitably start to fit the earth response and remove it for very small levels of earth response before the threshold level is reached, yielding slight

distortions at the onset and trailing edge of isolated conductive areas. Nevertheless, it is found that the data improvement offered by the presented noise compensation scheme to significantly outweigh the mentioned drawbacks.

## Inversion of SkyTEM data

In this section, the particulars of modeling and inversion of SkyTEM data from Colorado, USA will be described with reference to the more general material found in Appendix 5. The inversion code is named SELMA, ref /2/ and /3/. However, recent developments including the lateral parameter correlation, not yet published, have enhanced the accuracy of the code.

### Initial model and optimization norm

The inversion is performed as a regularized, damped, least-squares inversion on individual sounding data along the profiles with a one-dimensional (1D), multi-layer model (MLM) with 30 layers. In the inversion, the thickness of the layers are kept constant and only the layer resistivities are allowed to vary in order to let the model fit the measured data.

To obtain laterally smooth model sections, the Lateral Parameter Correlation (LPC) procedure is used (/3/ and /4/).

In the inversion the thickness of the first layer is 5 m and the depth to the deepest layer boundary is 500 m. Thicknesses and depths to top of layers for all layers are stated in the table below. In the top of the model, the layer thickness increases slowly, giving a linear sampling of the subsurface, while layer thickness increases exponentially at the deeper parts of the model.

The input data to the inversion is the z-component of the EM-data described in the chapter 'Processed data'.

In the Colorado survey the resistivity of the initial model for the inversion is set to 500  $\Omega\text{m}$ . Resistivities are allowed to vary within the interval of 0.1 to 10000  $\Omega\text{m}$ . Optimization is performed using the L2-norm.

In the Colorado area the inversions are based on a 3 Hz input file giving a model for approx. every 4 m.

Layer #	Layer Thickness [m]	Layer depth [m]
1	5.00	0.00
2	5.06	5.00
3	5.17	10.06
4	5.34	15.22
5	5.56	20.56
6	5.85	26.12
7	6.21	31.97
8	6.63	38.18
9	7.13	44.81
10	7.70	51.93
11	8.36	59.63
12	9.11	67.99
13	9.97	77.11
14	10.93	87.08
15	12.02	98.01
16	13.24	110.03
17	14.60	123.26
18	16.13	137.86
19	17.83	153.99
20	19.74	171.82
21	21.86	191.56
22	24.22	213.41
23	26.85	237.64
24	29.78	264.49
25	33.04	294.27
26	36.66	327.31
27	40.70	363.97
28	45.18	404.67
29	50.16	449.84
30	N/A	500.00

## Regularization

A statistical broadband approach is used in the regularization of the multi-layer model. Nine different correlation lengths with a maximum of 10 000 km and a standard deviation of 1 were used to define the correlation matrix. (See Appendix 5 for more detail).

## Noise model

In the Colorado survey, the noise parameters for both inversions were chosen as:

Low moment

$V_0 = 2.5e-12$  in field units normalized with Tx moment

$t_0 = 1$  ms

slope = -0.5

High Moment

$V_0 = 2.5e-13$  in field units normalized with Tx moment

$t_0 = 1$  ms

slope = -0.5

Negative data values caused by e.g. capacitive coupling and values lower than  $0.01 * \text{noise level}$ , were excluded in the inversion.

## Inversion results

The results of the inversion are presented in a GDB file included in the data delivery catalogue. The file contains the resistivities for each layer in the model. The header of the GDB file is described in the table below (also see Appendix 6 for more detail).

Parameter	Explanation	Unit
FID	Fiducial number	
LINE	Line number	
E	UTM Zone 12N (Paradox) / 13N (San Luis) NAD83	Meter
N	UTM Zone 12N (Paradox) / 13N (San Luis) NAD83	Meter
DTM	Digital Elevation Model	Meters above mean sea level
ResI1	Residual of data	-
ResI4	Residual total	-
Height	Height above ground	Meter
Layer	Number of layers in model	-
DOI	Depth of Investigation	Meter
Elev[xx]	Elevation of top of layer. [xx] refer to Geosoft channel number.	Meter
Res[xx]	Resistivity of layer. [xx] refer to Geosoft channel number.	$\Omega$ meter
RUnc[xx]	Relative uncertainty of layer. [xx] refer to Geosoft channel number.	-

## Presentations - Model sections and grids

The models resulting from the inversion are presented as model sections/profiles including analytic sections that display the normalized standard deviation of the resistivity sections along with the DOI (Figure 23) and as grids of resistivity in each model layer for Inner Box (Figure 21) and Outer Box (Figure 22).

The model sections and grids are enclosed in digital form. A brief description is given in Appendix 6.

The model sections have a large vertical exaggeration which will make the structures look more vertical than they are.

## Residuals

The quality of the inversion results can be evaluated by inspecting the residuals.

The data residual is calculated by comparing the measured data with the response of the resulting model after inversion. If the residual is in the range of 1, the misfit between the response of the final model and the data is, on average, equal to the noise. If the residual is high, it might be caused by data that are noisier than the noise model takes into account. This can be seen where resistivities are very high and the signal consequently very low. A high data residual can also be due to the inconsistency between the model assumed in the inversion and the 2D/3D character of the real world. These are found primarily at the edges of sharp lateral conductivity contrasts. Finally, coupling effects due to power lines and other manmade conductors can also be a source of a high residual.

The total residual is a weighted sum of the data residual and the model residual, where the latter is a measure of the roughness of the model, i.e. the deviation of the final model from the initial homogeneous half space model.

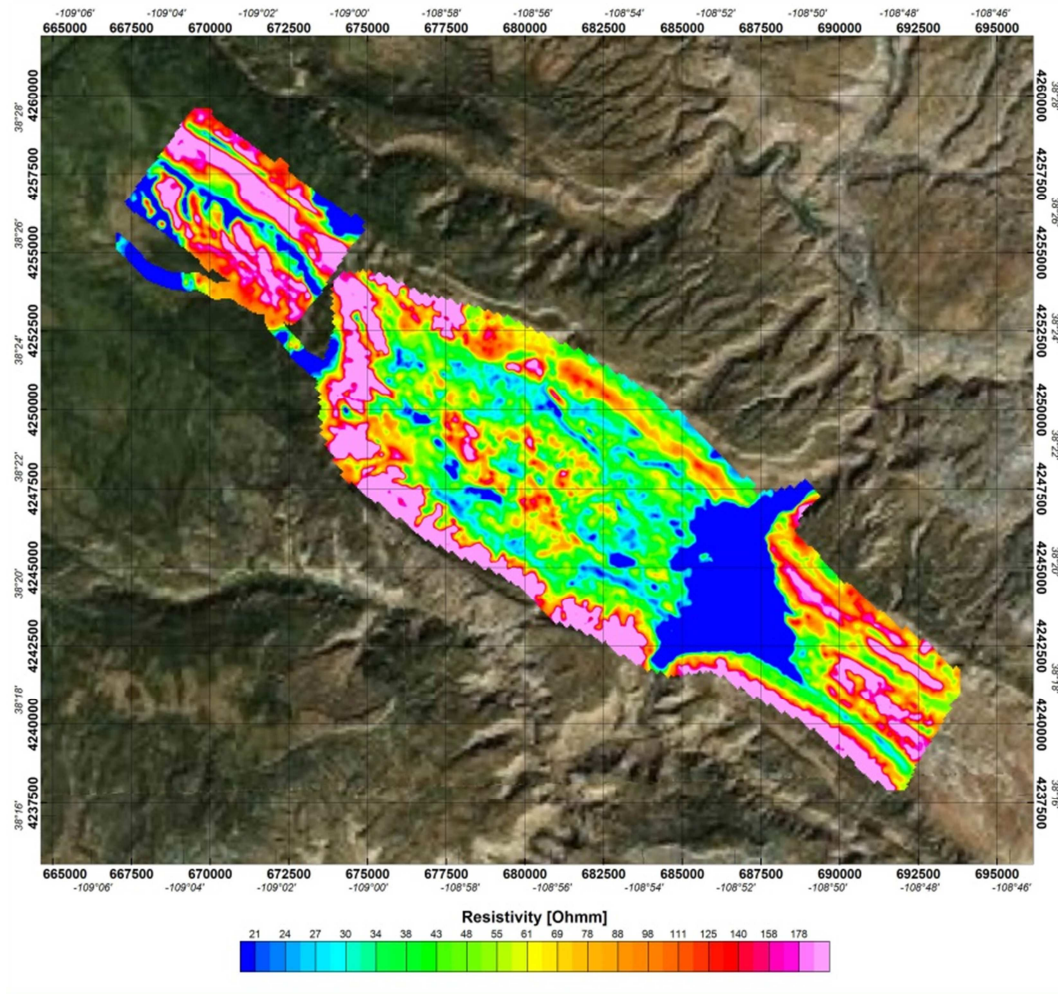


Figure 21 The image above is a low resolution example of the enclosed PDF maps displaying the inversion results for the Paradox survey area for layer 7 (32.0-38.2m, cell size 50m) UTM Zone 12N NAD83. Geosoft grids are found in the data delivery folder.

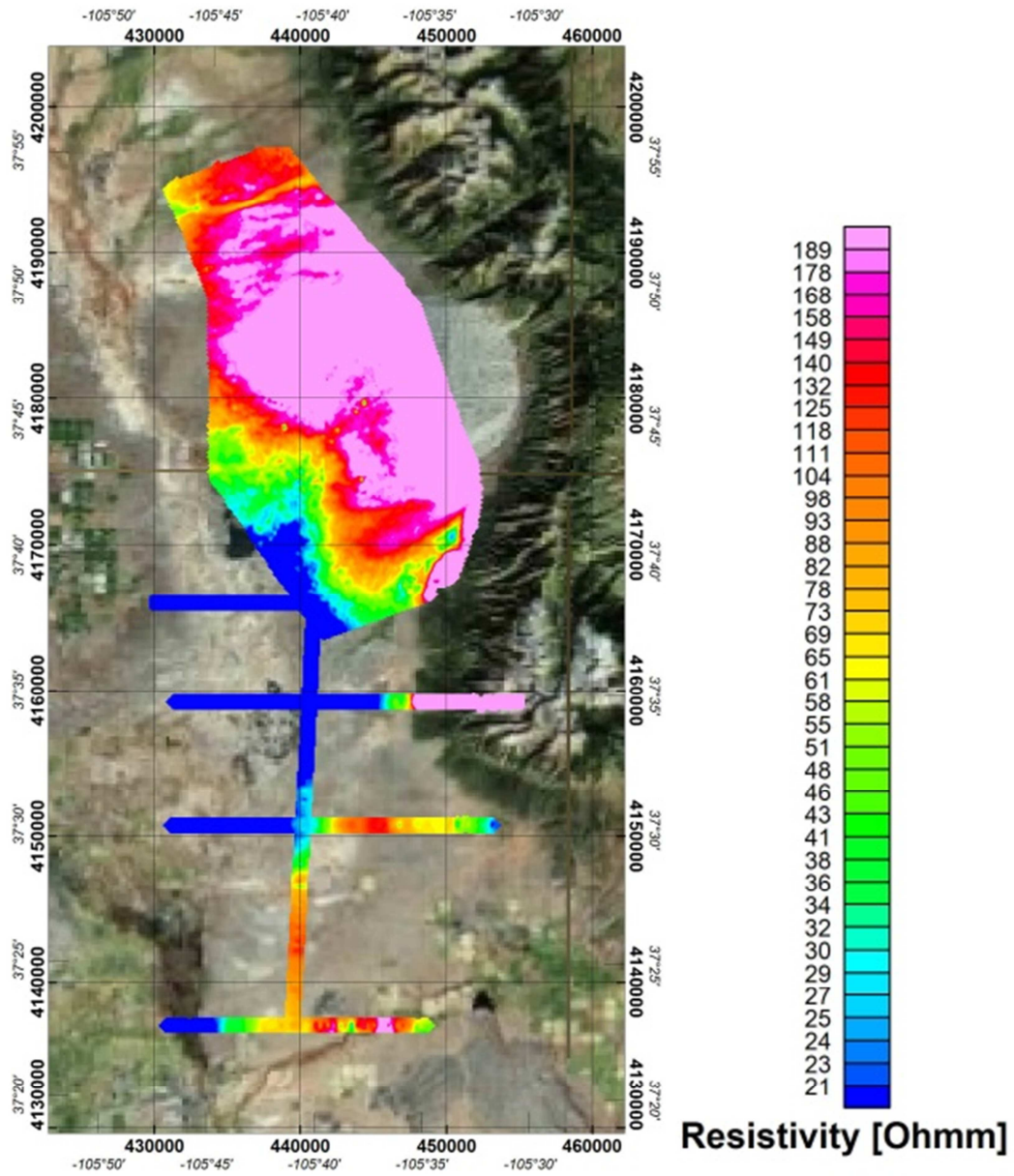


Figure 22 The image above is a low resolution example of the enclosed PDF maps displaying the inversion results for the San Luis survey area layer 7 (32.0-38.2m, cell size 100m) UTM Zone 13N NAD83. Geosoft grids and PDF's are found in the data delivery folder.

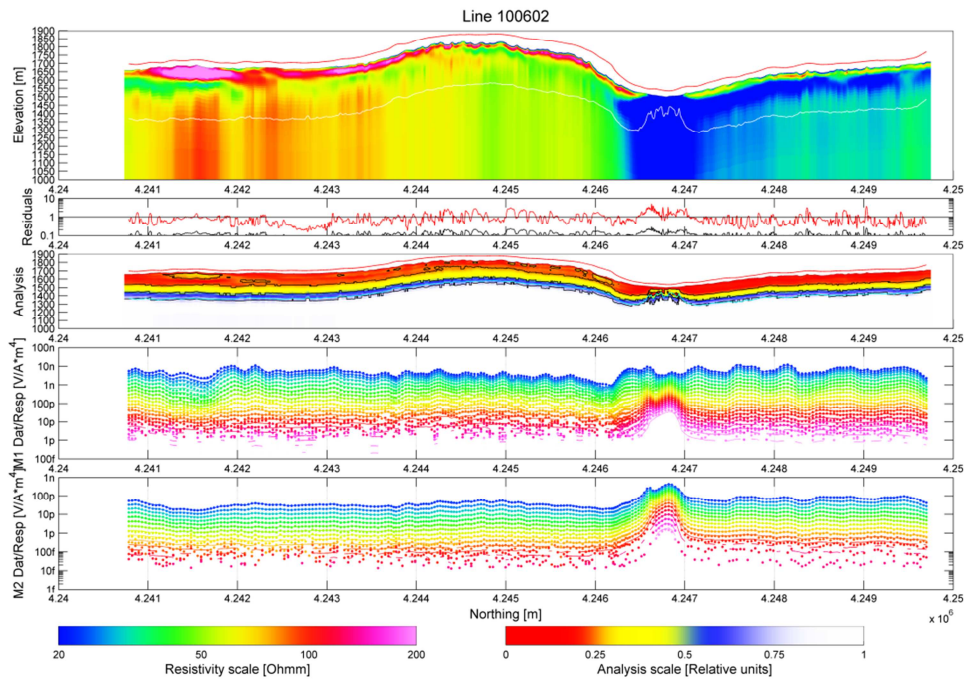


Figure 23 Sample of the model section plots enclosed as PDF's. Top plot: Resistivity section with flight height (red) and depth of investigation (white line) indicated. Data and total residuals are displayed in the second plot. The third plot show the analysis section. The bottom plots are the low and high moment data (dots) and model response (full line). Profile section for flown lines are found as PDF's in the data delivery folder.

## References

- /1/ Sorensen, K. I. and Auken, E. (2004). SkyTEM - A new high-resolution helicopter transient electromagnetic system, *Exploration Geophysics*, 35, 191-199.
- /2/ Christensen, N. B. (2002). A generic 1-D imaging method for transient electromagnetic data. *Geophysics*, 67, 438-447.
- /3/ Christensen, N.B., Reid, J.E. and Halkjær, M. (2009). Fast, laterally smooth inversion of airborne time-domain electromagnetic data, *Near Surface Geophysics*, 7, 599-612
- /4/ Christensen N.B. and Tølbøll R.J. 2009, A lateral model parameter correlation procedure for one-dimensional inverse modeling. *Geophysical Prospecting* 57, 919-929. DOI: 10.1111/j.1365-2478.2008.00756.x

## Appendix list

Appendix 1: Instruments

Appendix 2: Time gates

Appendix 3: Calibration

Appendix 4: Control parameters

Appendix 5: Modeling and inversion of TEM data

Appendix 6: Inversion results

Appendix 7: Digital data

# Appendix 1: Instruments

# Instrument positions

The instrumentation involves a time domain electromagnetic system, two inclinometers, two altimeters and two DGPS'.

The measurements were carried out, using a setup as described below.

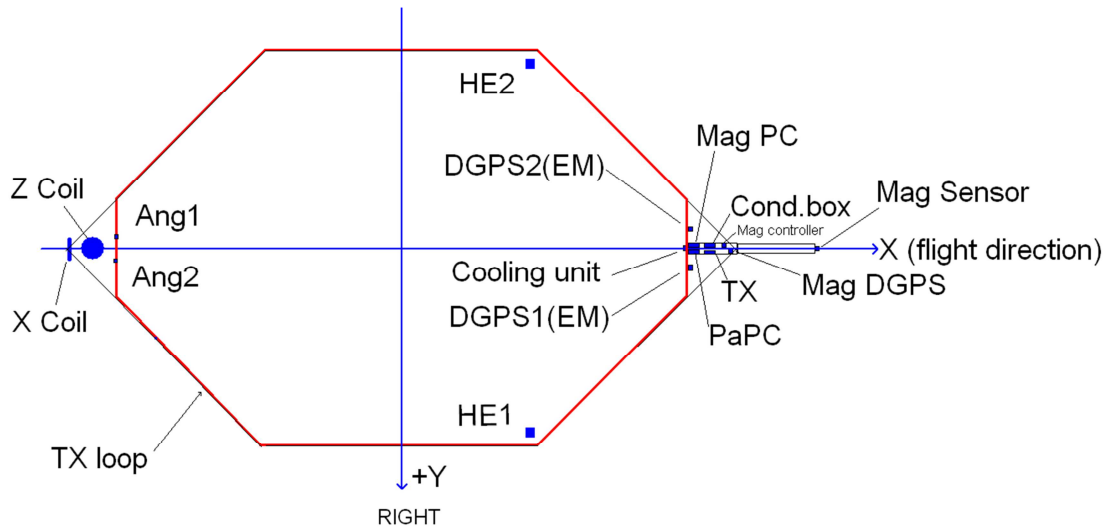


Figure 1 Sketch showing the frame and the position of the basic instruments. The red line defines the transmitter loop. The horizontal plane is defined by (x, y).

The location of instruments in respect to the frame is shown in Figure 1 and is given in (x, y, z) coordinates in the table below.

X and y define the horizontal plane. Z is perpendicular to (x, y). X is positive in the flight direction, y is positive to the right of the flight direction, and z is positive downwards.

The generator used for powering of the transmitter is 10 m below the helicopter.

Device	X	Y	Z
DGPS1 (EM)	11.85	1.01	-0.23
DGPS2 (EM)	11.85	-0.60	-0.23
HE1 (altim.)	5.15	7.72	0.02
HE2 (altim.)	5.15	-7.72	0.02
Inclinometer 1	-11.96	-0.50	-0.37
Inclinometer 2	-11.96	0.50	-0.37
RX (Z Coil)	-12.64	0.00	-2.10
RX (X Coil)	-13.8	0.00	0.00
TX (transmit.)	12.73	0.16	-0.74
Condensator	12.73	-0.16	-0.74

For the location of instruments see Figure 1.

## Transmitter

The time domain transmitter loop can be described as an octagon with the corners listed below:

X	Y
-11.87	-2.03
-5.68	-8.22
5.68	-8.22
11.87	-2.03
11.87	2.03
5.68	8.22
-5.68	8.22
-11.87	2.03

The total area of the transmitter coil defined by the corner points is 314 m<sup>2</sup> and 65.9 m in circumference.

The key parameters defining the transmitter set up are:

#### Low moment

Parameter	Value
Number of transmitter turns	1
Transmitter area	314 m <sup>2</sup>
Peak current	5
Peak moment	~3,140 NIA
Repetition frequency	240 Hz
On-time	800 μs
Off-time	1283 μs
Duty cycle	38 %
Wave form	Square
Turn on wave form exp. decay constant	44000 s <sup>-1</sup>
Turn off linear ramp	4.46e6 A/s
Turn off current end avalanche mode	1.5 A
Turn off free decay exp. decay constant	-3.00e6 s <sup>-1</sup>

#### High Moment

Parameter	Value
Number of transmitter turns	4
Transmitter area	314 m <sup>2</sup>
Peak current	114.1
Peak moment	~150,000 NIA
Repetition frequency	30 Hz
On-time	8000 μs
Off-time	8667 μs
Duty cycle	48 %
Wave form	Square
Turn on wave form exp. decay constant	410 s <sup>-1</sup>
Turn off linear ramp	2.38e6 A/s
Turn off current end avalanche mode	1.0 A
Turn off free decay exp. decay constant	-1.29e6 s <sup>-1</sup>

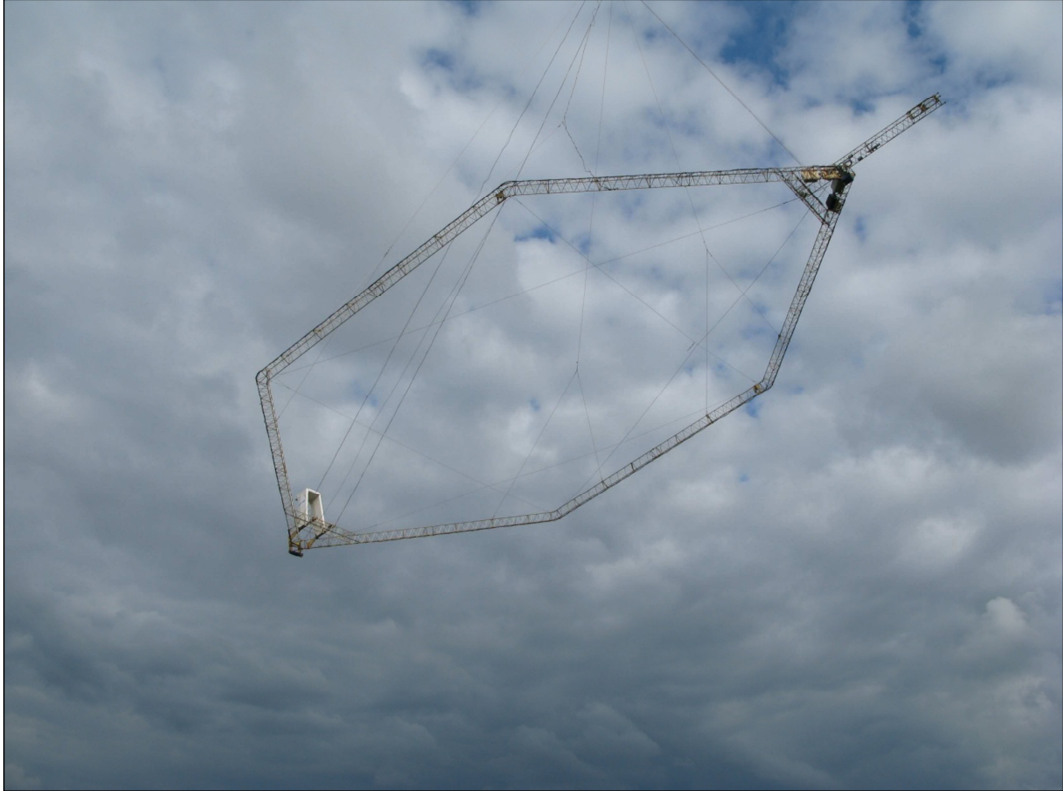


*Figure 2 The 314 m<sup>2</sup> frame in production mode.*

## Receiver system

The decay of the secondary magnetic field is measured using two independent active induction coils. The Z coil is the vertical component, and the X coil is the horizontal in-line component. Each coil has an effective receiver area of 105 m<sup>2</sup> .

The receiver coils are placed in a null-position:

Z coil  $(x, y, z) = (-12.80 \text{ m}, 0.0 \text{ m}, -2.22)$

X coil  $(x, y, z) = (-13.75 \text{ m}, 0.0 \text{ m}, 0.0 \text{ m})$

In the null-position, the primary field is damped with a factor of 0.01.



Figure 3 Rudder containing the Z coil located approximately in the top part of the tower.

The key parameters defining the receiver set up are:

Receiver parameters		
Sample rate		All decays are measured
Number of output gates		34 (HM) and 26 (LM)
Receiver coil low pass filter		450 kHz
Receiver instrument low pass filter		300 kHz
Repetition frequency	LM HM	240 Hz 30 Hz
Front gate	LM HM	0.0 $\mu$ s 60.0 $\mu$ s

Receiver gate times are measured from the start of the transmitter current turn-off. A complete list describing gate open, close and centre times are listed in Appendix 2.

# Inclination

Instrument type: Bjerre Technology

The inclination of the frame is measured with 2 independent inclinometers. The x and y angles are measured 2 times per second in both directions. The inclinometers are placed in the rear of the frame as close to the z coil as possible, see Figure 1.

The angle data are stored as x, y readings. X is parallel to the flight direction and positive when the front of the frame is above horizontal. Y is perpendicular to the flight direction and negative when the right side of the frame is above horizontal.

The angle is checked and calibrated manually within 1.0 degree by use of a level meter.

# DGPS airborne unit and base stations

Chipset: OEMV1-L1 14-channel rate.

Antenna: Trimble, Bullet III GPS Antenna

The differential GPS receiver is on top of the boom in front of the frame.

The DGPS delivers one dataset per second. The raw coordinates are given in Latitude/longitude, WGS84.

The uncertainty in the xyz-directions is  $\pm 1$  m after processing.

The processed DGPS data is combined with the EM data in the xyz-files, giving the precise position.

DGPS parameters	
Sample rate	1 Hz
Uncertainty	$\pm 1$ m

# Altimeter

Instrument type: MDL ILM300R

Two independent laser units mounted on each side of the frame measure the distance from the frame to the ground, see Figure 1.

Each laser delivers 30 measurements per second, and covers the interval from 1.5 m to approximately 130 m.

Dark surfaces including water surfaces will reduce the reflected signal. Consequently, it may occur that some measurements do not result in useful values.

The altimeter measurements are given in meters with two decimals. The uncertainty is 10 - 30 cm. The lasers are checked on a regular basis against well defined targets.

Laser parameters	
Sample rate	30 Hz
Uncertainty	10 - 30 cm
Min/ max range	1.5 m / 130 m

# Magnetometer airborne unit

Instrument type: Geometrics G822A sensor and Kroum KMAG4 counter.

The Geometrics G822A sensor and Kroum KMAG4 counter is a high sensitivity cesium magnetometer. The basic of the sensor is a self-oscillating split-beam Cesium Vapor (non-radioactive) Principle, which operates on principles similar to other alkali vapor magnetometers.

The sensitivity of the Geometrics G822A sensor and Kroum KMAG4 counter is stated as  $<0.0005 \text{ nT}/\sqrt{\text{Hz}}$  rms. Typically 0.002 nT P-P at a 0.1 second sample rate, combined with absolute accuracy of 3 nT over its full operating range.

The magnetometer is synchronized with the TEM system. When the TEM signal is on, the counter is closed. In the TEM off-time the magnetometer data is measured from 100 microseconds until the next TEM pulse is transmitted. The data are averaged and sampled as 60 Hz.

Parameter	Value
Sample frequency	60 Hz (in between each HM EM pulse)
Magnetometer on	HM Cycles
Magnetometer off	LM Cycles

# Magnetometer base station

Instrument type: GEM Overhauser.

The GEM Overhauser is a portable high-sensitivity precession magnetometer.

The GEM Overhauser is a secondary standard for measurement of the Earth's magnetic field with 0.01 nT resolutions, and 1 nT absolute accuracy over its full temperature range.

The base station data are sampled with 1 Hz frequency.

## Appendix 2: Time gates

Gate	GateOpen (μs)	Gatewidth (μs)	GateClose (μs)	Raw GateCenter (μs)	GateCenter Applied time shift calibration for HM and LM (μs)	Comment
1	0.390	5.610	6.000	3.195	2.095	Not used
2	6.390	1.610	8.000	7.195	6.095	Not used
3	8.390	1.610	10.000	9.195	8.095	Not used
4	10.390	1.610	12.000	11.195	10.095	Not used
5	12.390	1.610	14.000	13.195	12.095	LM only
6	14.390	1.610	16.000	15.195	14.095	LM only
7	16.390	1.610	18.000	17.195	16.095	LM only
8	18.390	3.610	22.000	20.195	19.095	LM only
9	22.390	4.610	27.000	24.695	23.595	LM only
10	27.390	6.610	34.000	30.695	29.595	LM only
11	34.390	7.610	42.000	38.195	37.095	LM only
12	42.390	9.610	52.000	47.195	46.095	LM only
13	52.390	12.610	65.000	58.695	57.595	LM only
14	65.390	15.610	81.000	73.195	72.095	LM only
15	81.390	20.610	102.000	91.695	90.595	LM only
16	102.390	25.610	128.000	115.195	114.095	LM only
17	128.390	31.610	160.000	144.195	143.095	LM only
18	160.390	41.610	202.000	181.195	180.095	LM & HM
19	202.390	50.610	253.000	227.695	226.595	LM & HM
20	253.390	64.610	318.000	285.695	284.595	LM & HM
21	318.390	81.610	400.000	359.195	358.095	LM & HM
22	400.390	102.610	503.000	451.695	450.595	LM & HM
23	503.390	129.610	633.000	568.195	567.095	LM & HM
24	633.390	162.610	796.000	714.695	713.595	LM & HM
25	796.390	205.610	1002.000	899.195	898.095	LM & HM
26	1002.390	258.610	1261.000	1131.695	1130.595	LM & HM
27	1261.390	325.610	1587.000	1424.195	1423.095	HM only
28	1587.390	409.610	1997.000	1792.195	1791.095	HM only
29	1997.390	516.610	2514.000	2255.695	2254.595	HM only
30	2514.390	649.610	3164.000	2839.195	2838.095	HM only
31	3164.390	818.610	3983.000	3573.695	3572.595	HM only
32	3983.390	1030.610	5014.000	4498.695	4497.595	HM only
33	5014.390	1297.610	6312.000	5663.195	5662.095	HM only
34	6312.390	1632.610	7945.000	7128.695	7127.595	HM only

Note: The first gates are not used in any of the moments in the present survey as it is in the transition zone.

SkyTEM inversion software (iTEM) handles time shift calibration during import of data.

If third party processing software is used the calibrated Gate centre times should be used.

## Appendix 3: Calibration of the TEM system

As described in the main document the system has been calibrated in a 50 Hz power supply grid setting (In Denmark), but the data was recorded in a 60 Hz environment (USA).

The wave form is measured with the 60 Hz script with a repetition frequency of 240 Hz for LM and with a repetition frequency of 30 Hz HM. Figure 1 to Figure 4 show the up and down ramp, respectively.

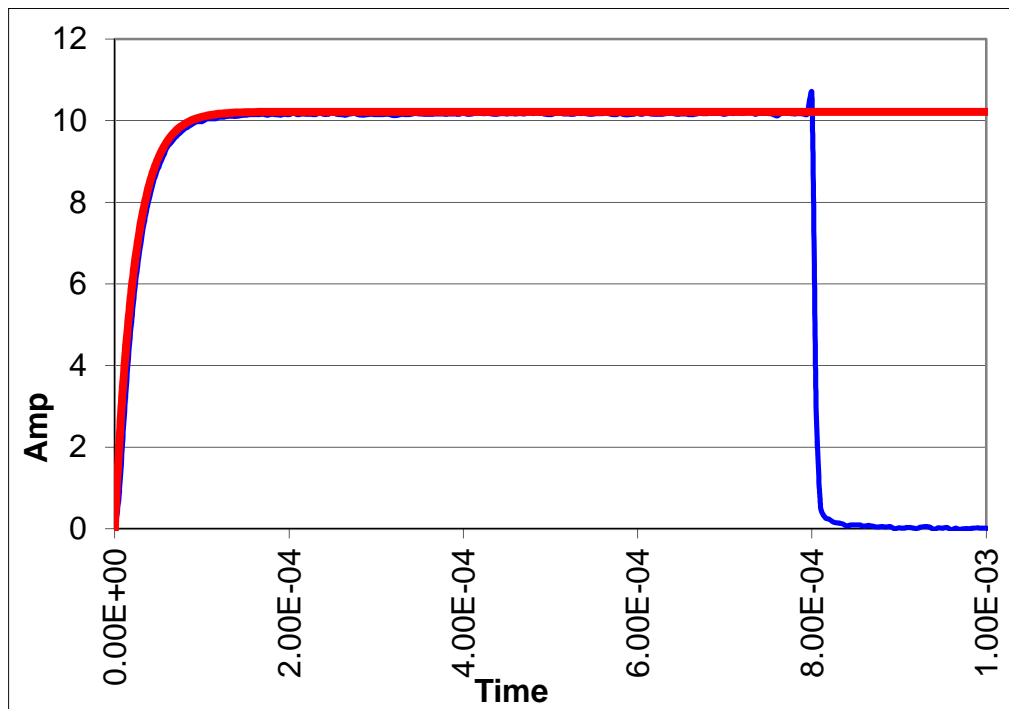


Figure 1 Ramp up at 240 Hz. Blue curve is the measured wave form. Red curve is the function that fits the data. The current is 10 A and the decay constant  $\tau = 44000 \text{ s}^{-1}$ .

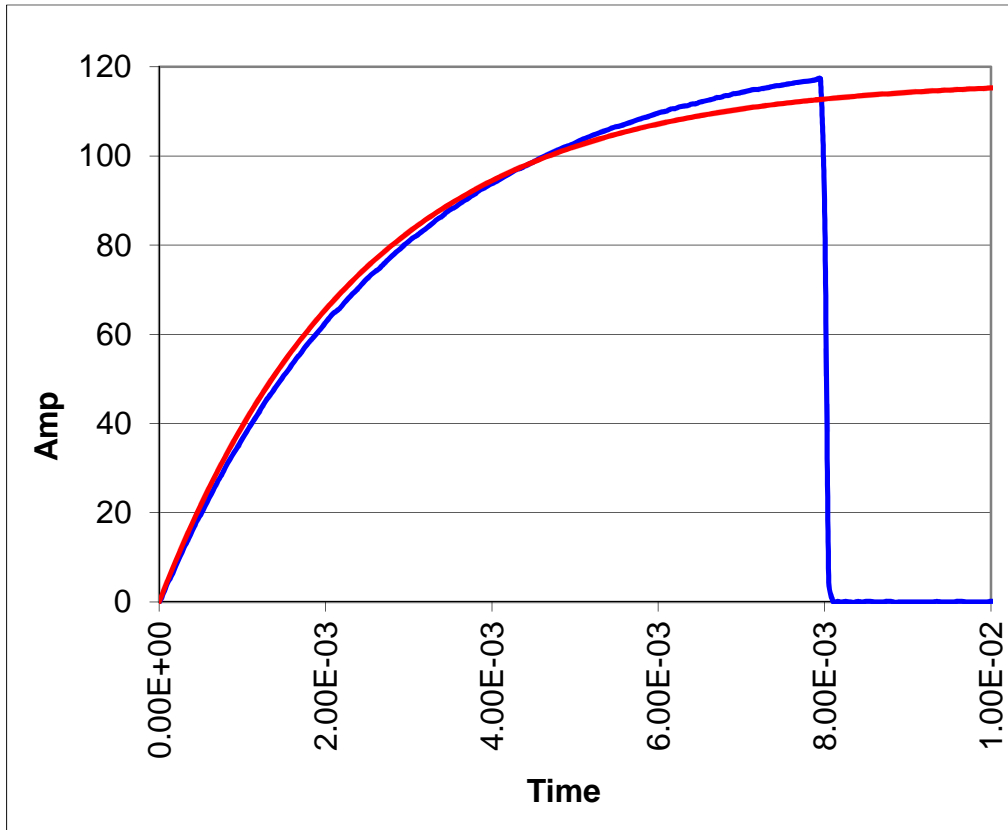


Figure 2 Ramp up at 30 Hz. Blue curve is the measured wave form. Red curve is the function that fits the data. The current is 117 A and the decay constant  $\tau = 410 \text{ s}^{-1}$ .

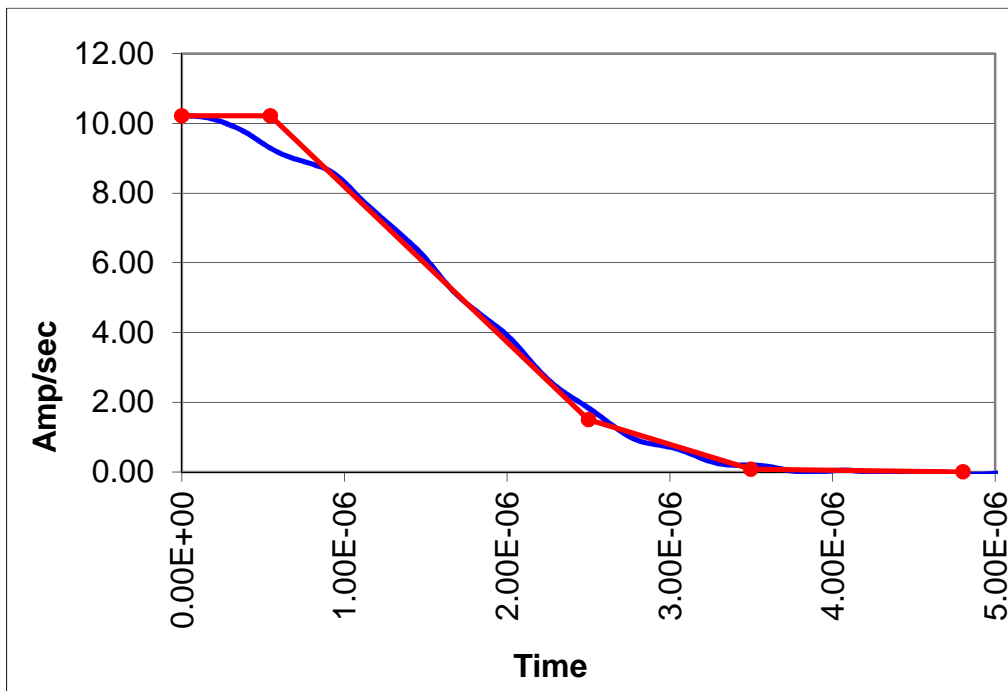


Figure 3 Ramp down at 240 Hz. Blue curve is the measured wave form. Red curve is the piecewise linear function that fits the data. Decay constant -  $3.00\text{e}6 \text{ s}^{-1}$ .

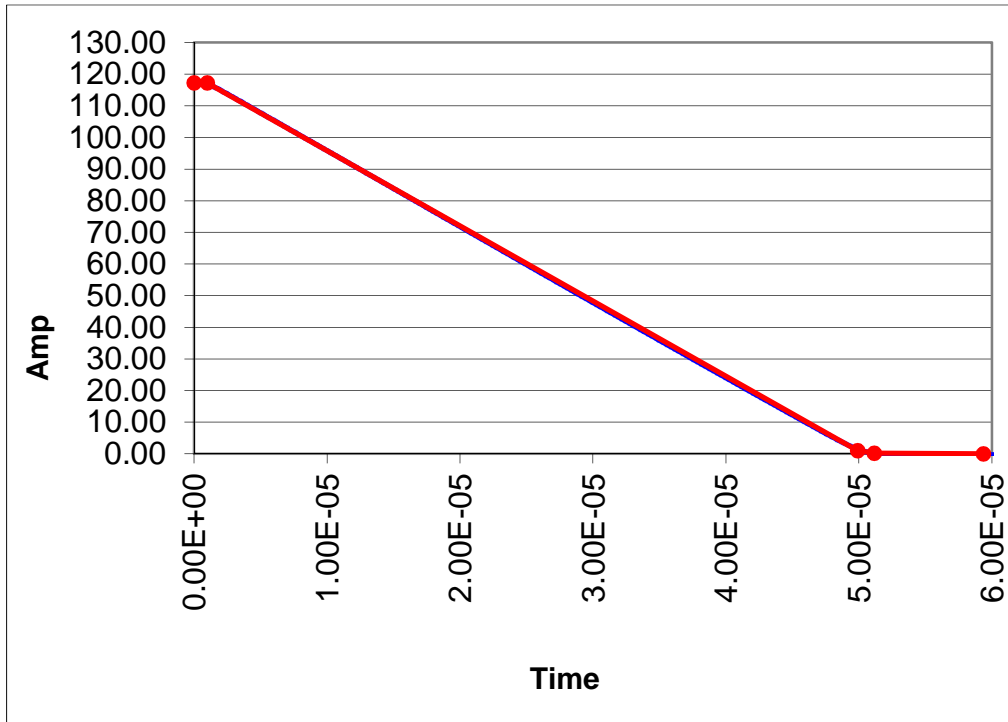


Figure 4 Ramp down at 30 Hz. Blue curve is the measured wave form. Red curve is the piecewise linear function that fits the data. Decay constant -  $1.29e6 \text{ s}^{-1}$ .

LM

	Parameter	Value
Ramp up	Repetition frequency	240 Hz
	Decay constant, $\tau$	44000 s <sup>-1</sup>
Ramp Down	Avalanche mode	1.96 $\mu$ s
	Linear ramp dI/dt	4.46e6 A/s
	End avalanche mode current	1.5 A
	Decay const exp mode, $\tau$	-3.00e6 s <sup>-1</sup>

HM

	Parameter	Value
Ramp up	Repetition frequency	30 Hz
	Decay constant, $\tau$	410 s <sup>-1</sup>
Ramp Down	Avalanche mode	48.9 $\mu$ s
	Linear ramp dI/dt	2.38e6 A/s
	End avalanche mode	1.0 A
	Decay const exp mode, $\tau$	-1.29e6 s <sup>-1</sup>

The complete SkyTEM equipment has been calibrated at the National Danish Reference Site. The following plots, Figure 5 to Figure 8, show the measured data as well as the expected response in altitudes 5 m, 10 m, 15 m, 20 m and 30 m.

The reference data for both LM and HM data are shown as blue curves and the measured data for LM and HM as red curves.

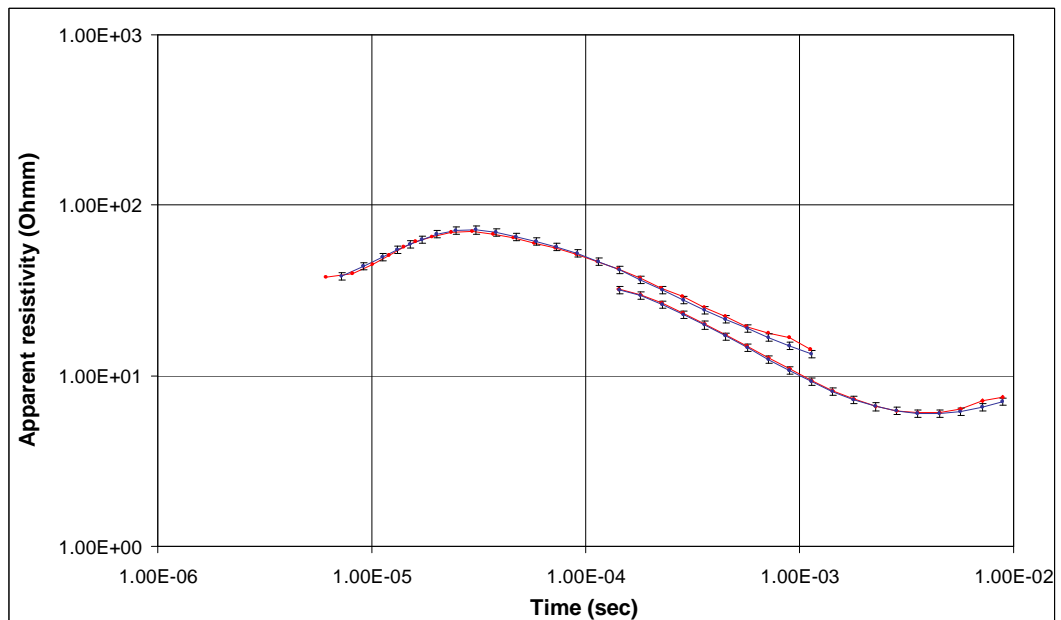


Figure 5 The frame is in 5 m altitude. Blue curves with 5% error bars are the expected response, and red curves are the actual measurements.

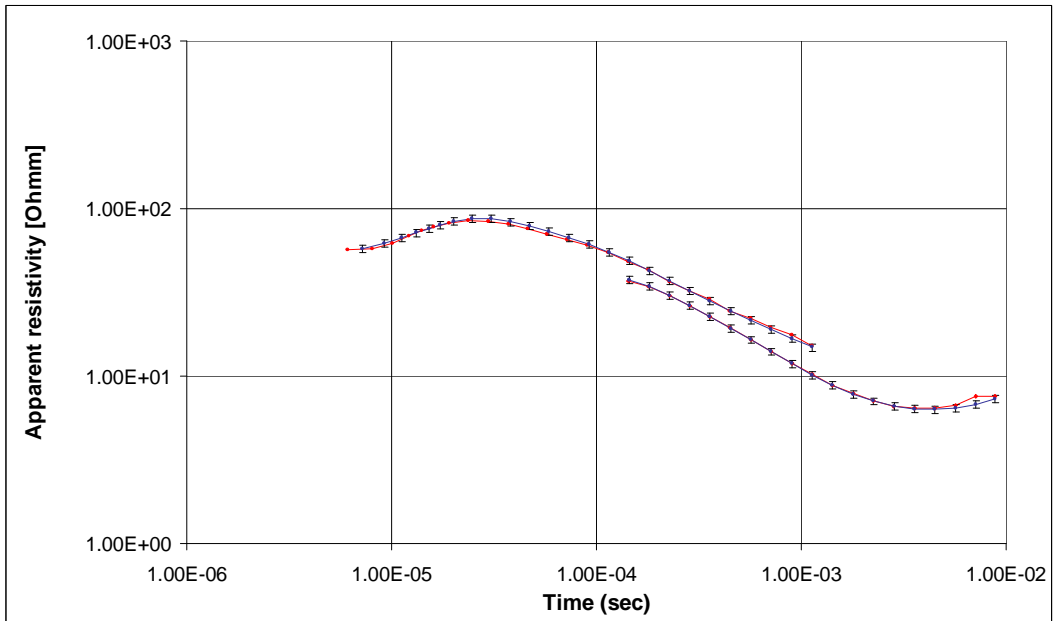


Figure 6 The frame is in 10 m altitude. Blue curves with 5% error bars are the expected response, and red curves are the actual measurements.

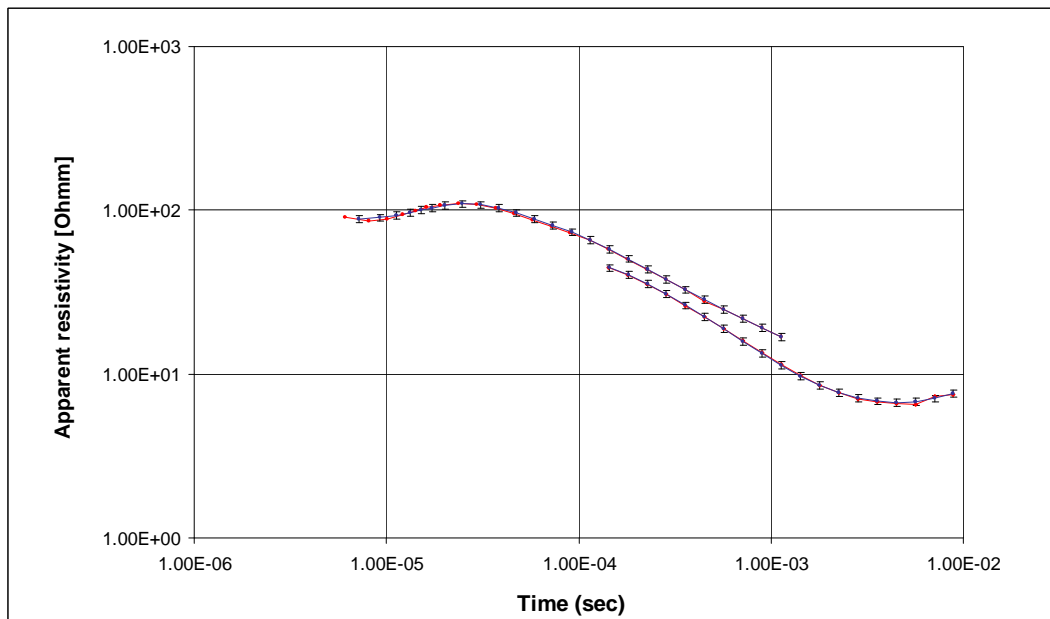


Figure 7 The frame is in 15 m altitude. Blue curves with 5% error bars are the expected response, and red curves are the actual measurements.

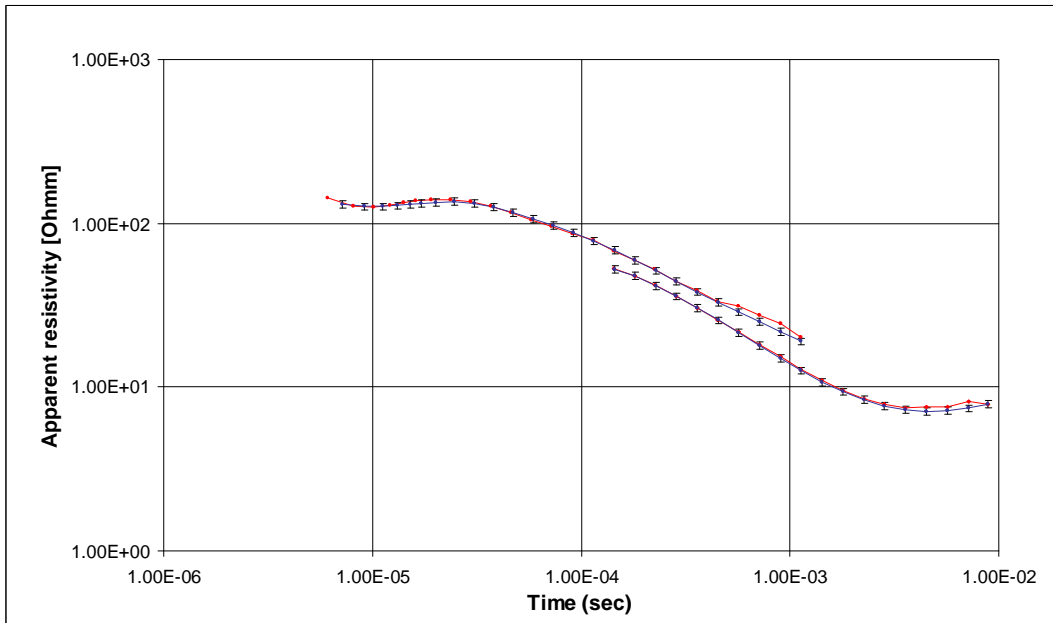


Figure 8 The frame is in 20 m altitude. Blue curves with 5% error bars are the expected response and red curves are the actual measurements.

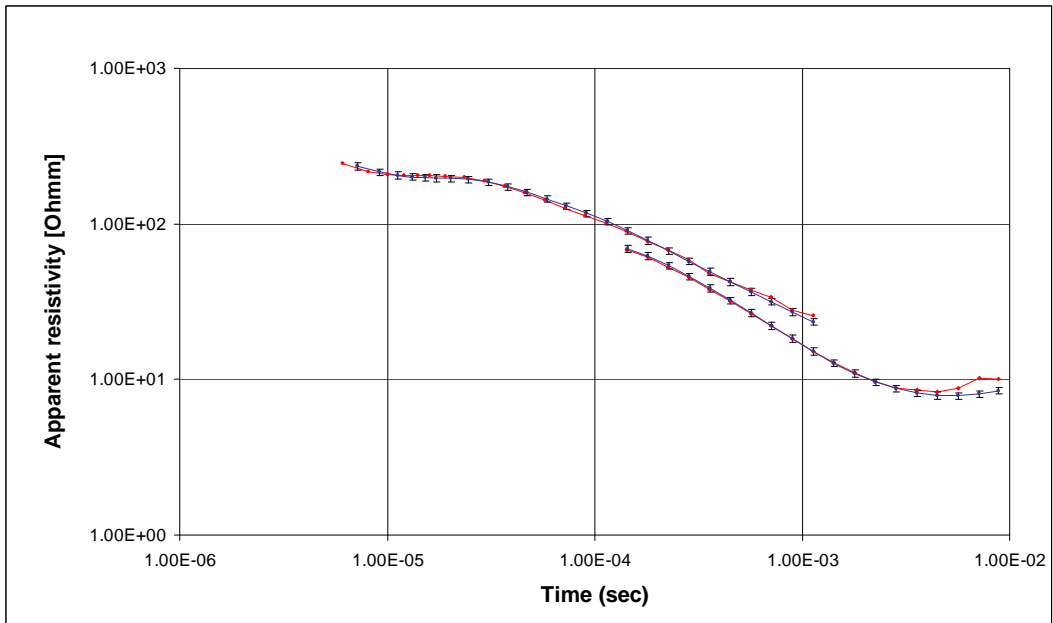


Figure 9 The frame is in 30 m altitude. Blue curves with 5% error bars are the expected response and red curves are the actual measurements

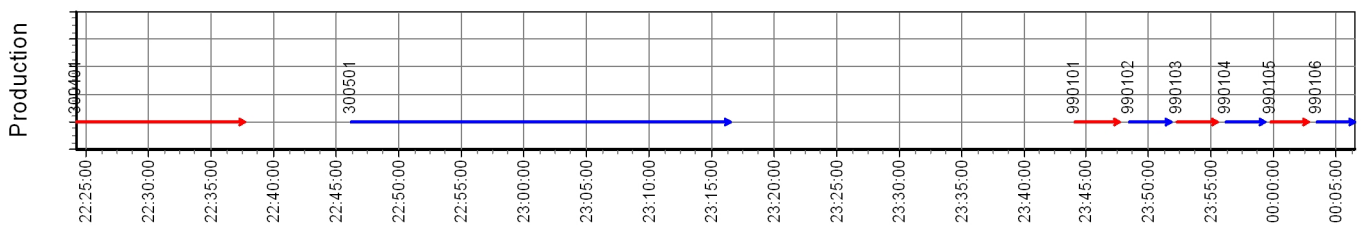
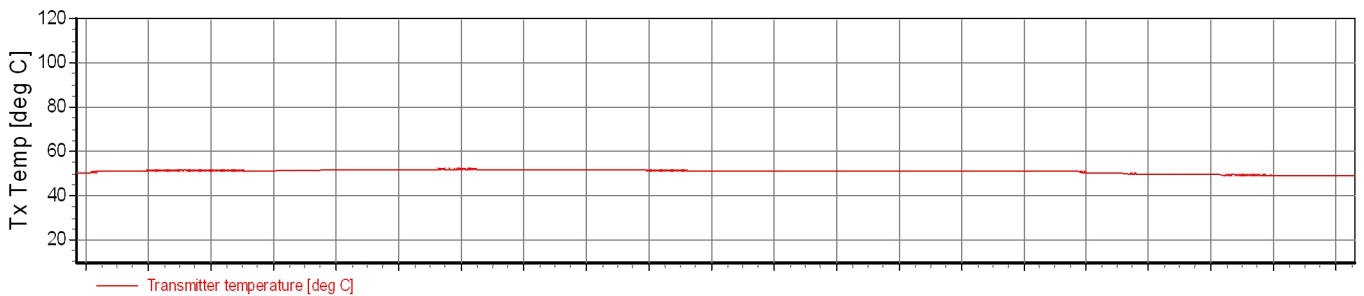
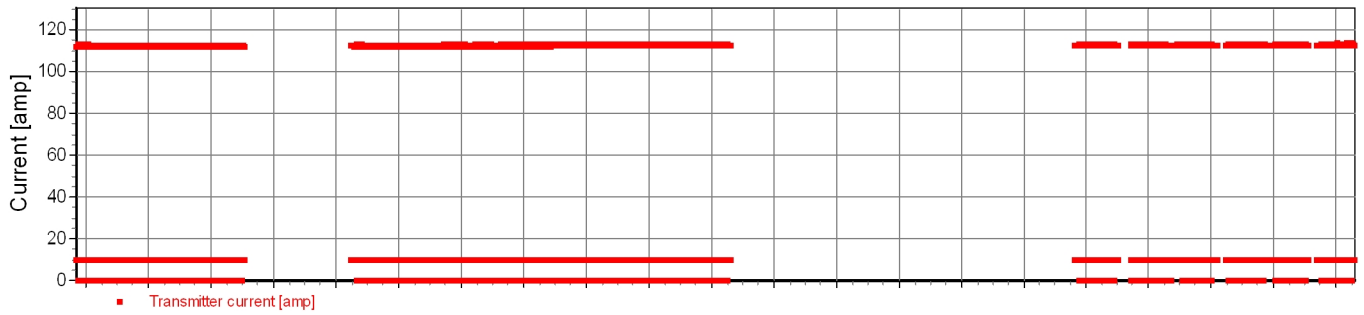
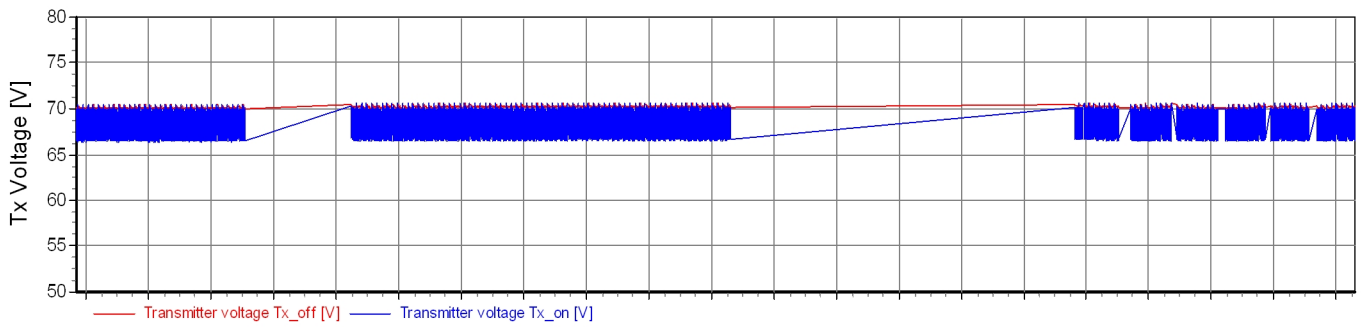
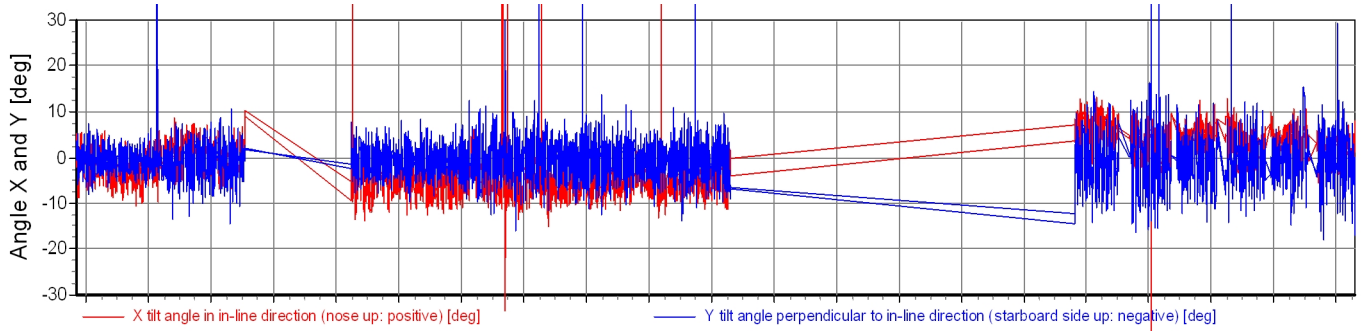
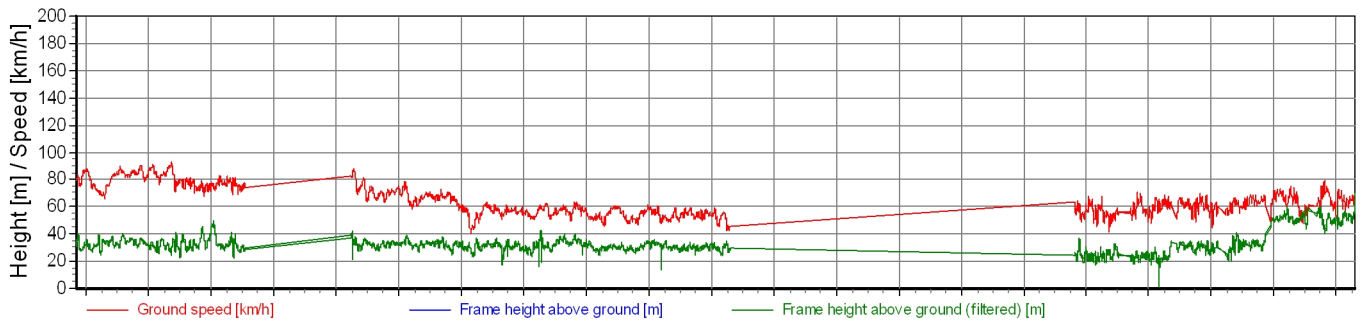
## Appendix 4: Control parameters

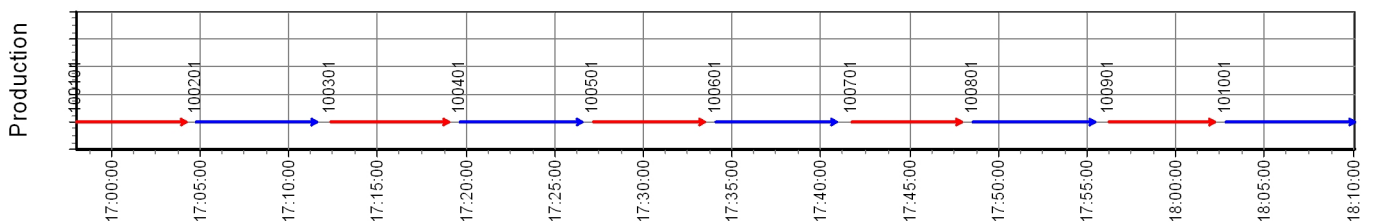
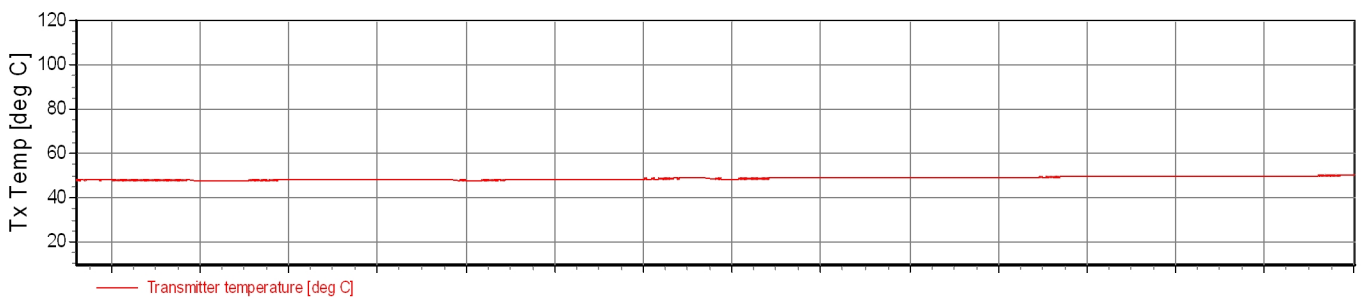
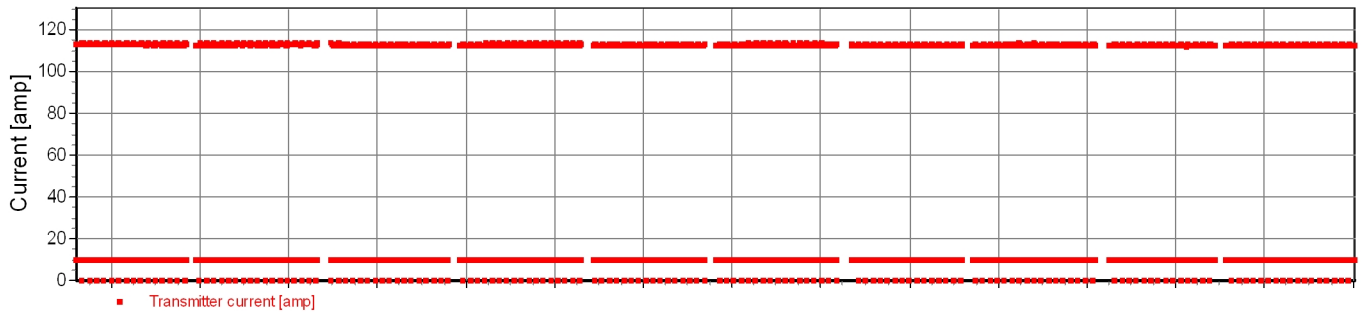
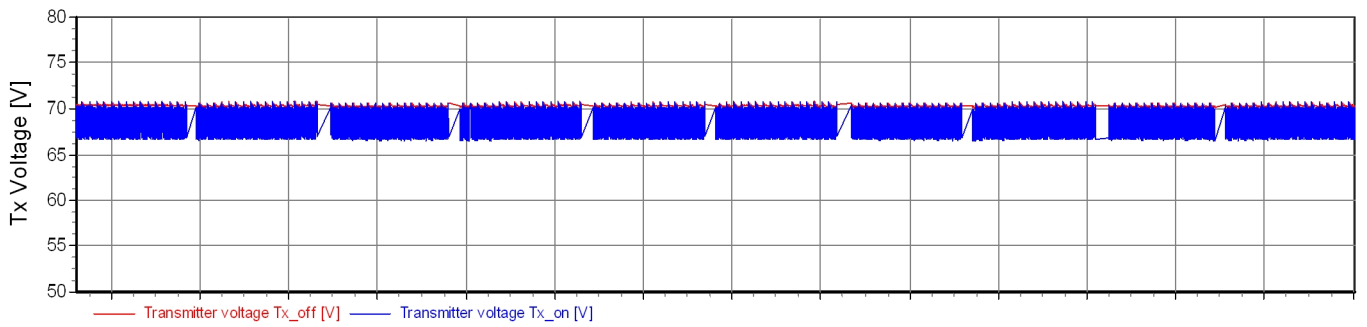
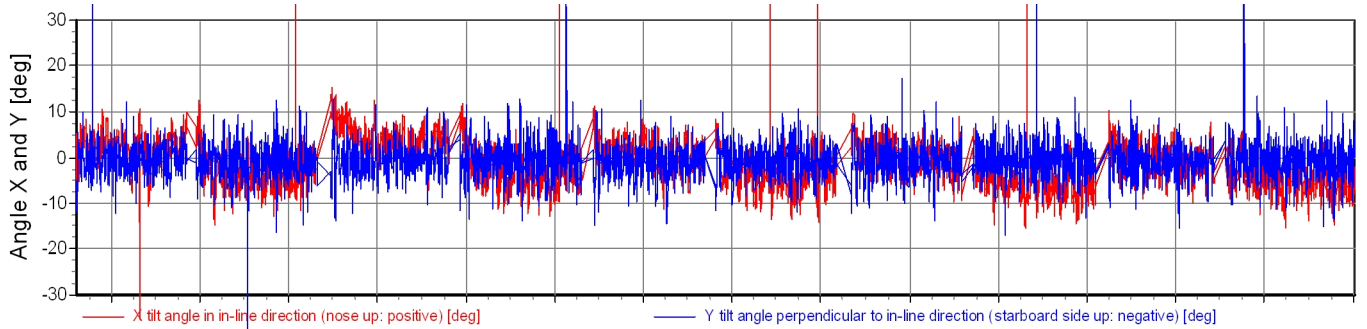
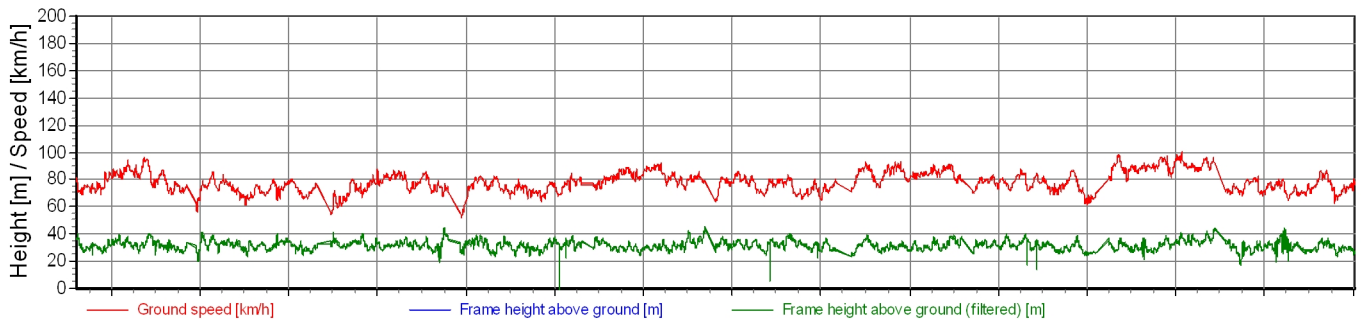
The following plots show the speed, altitude and the angle of the frame for every flight. Variations in the current, voltage on the transmitter and transmitter temperature are also shown.

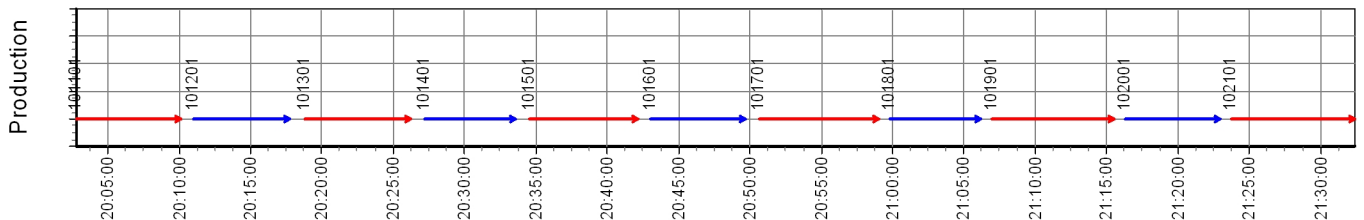
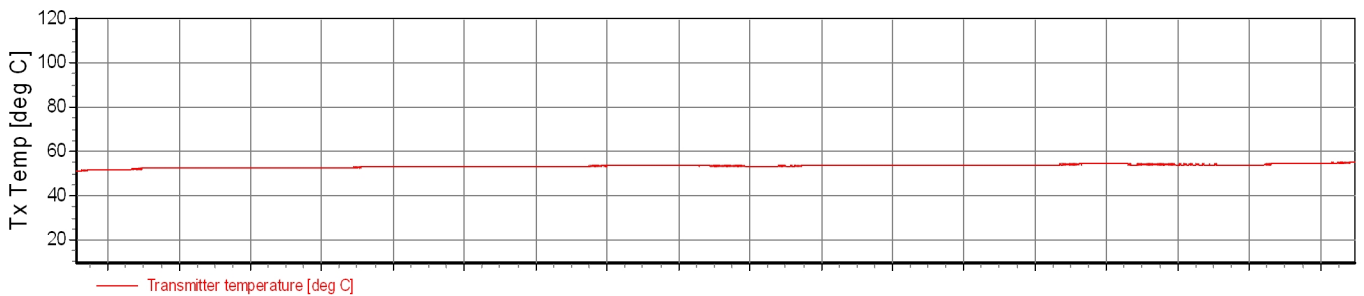
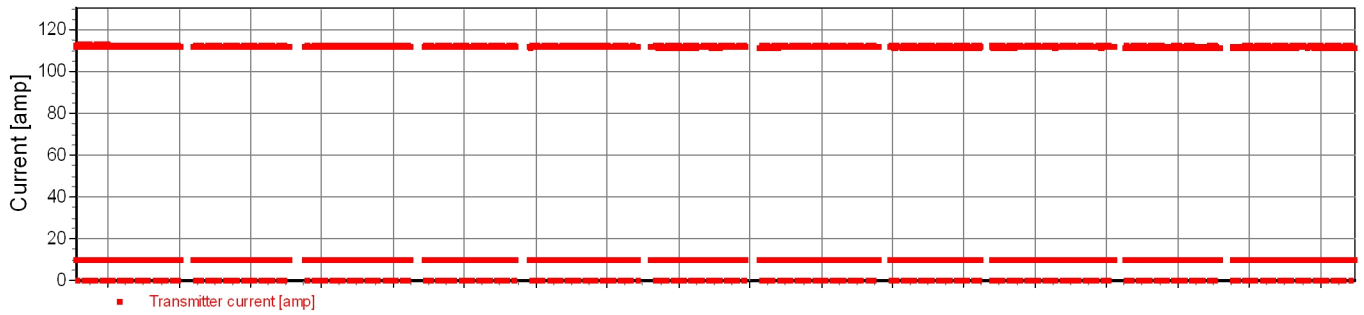
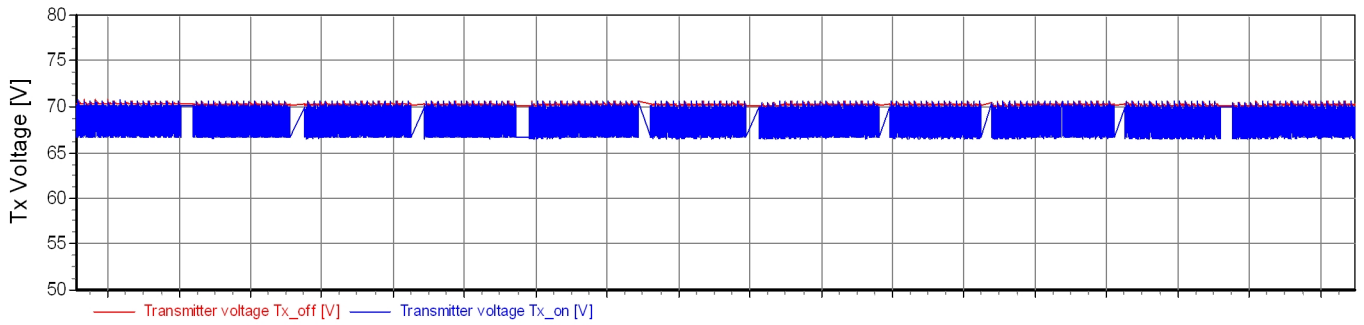
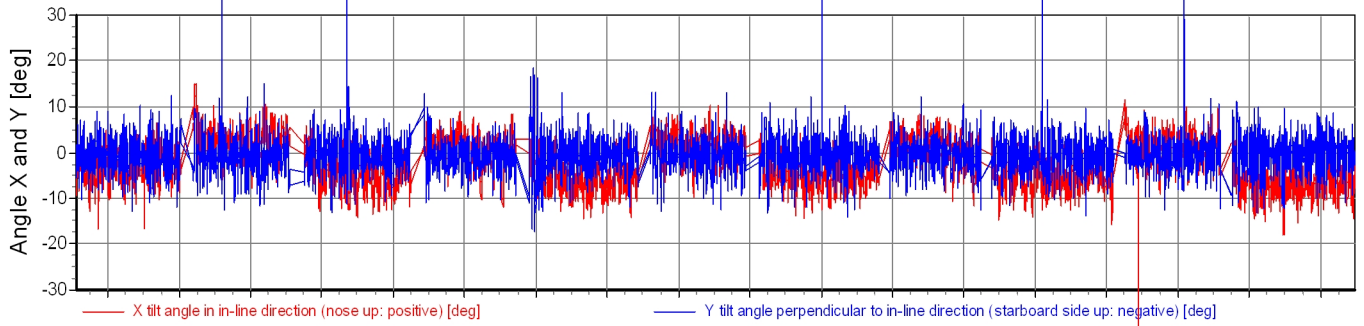
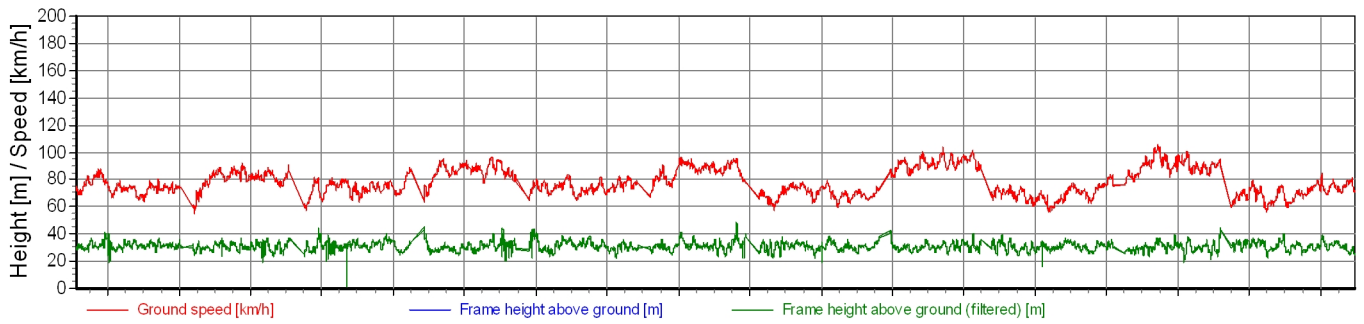
The green line, depicting processed frame height, shows the SkyPRO input from HE1 and HE2 after the frame has been corrected from deviations, away from the horizontal plane and any obstacles on the ground e.g. trees.

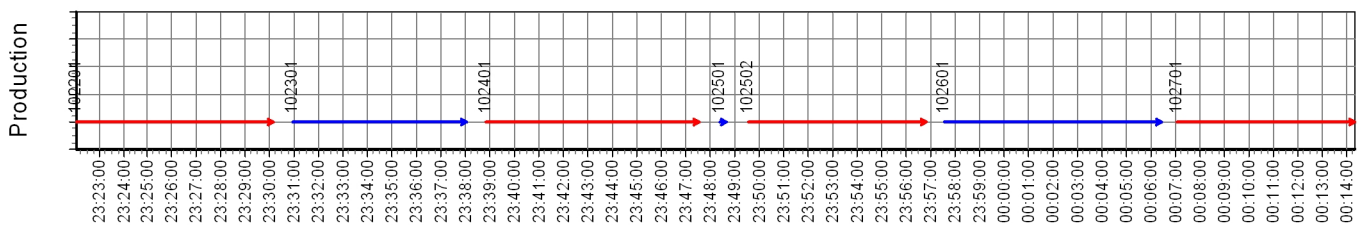
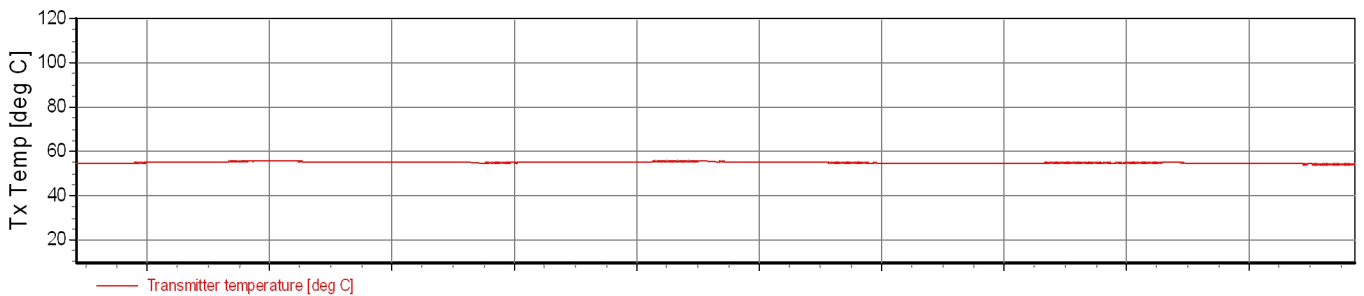
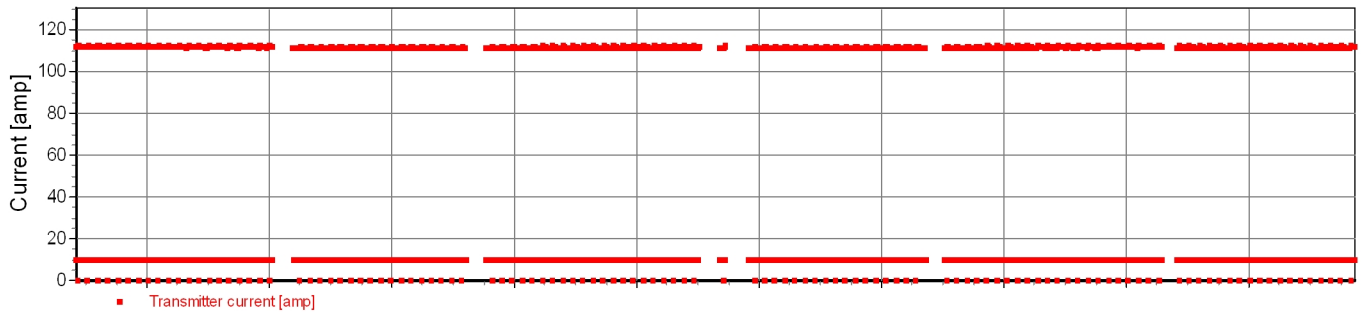
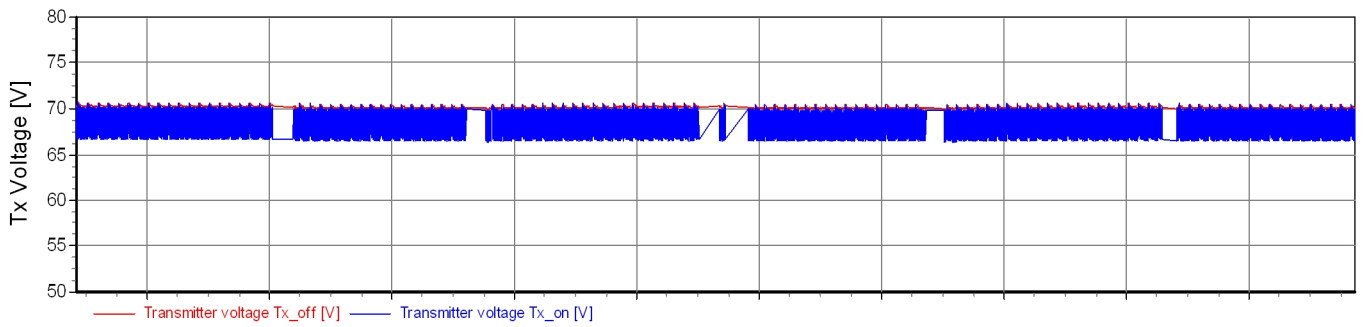
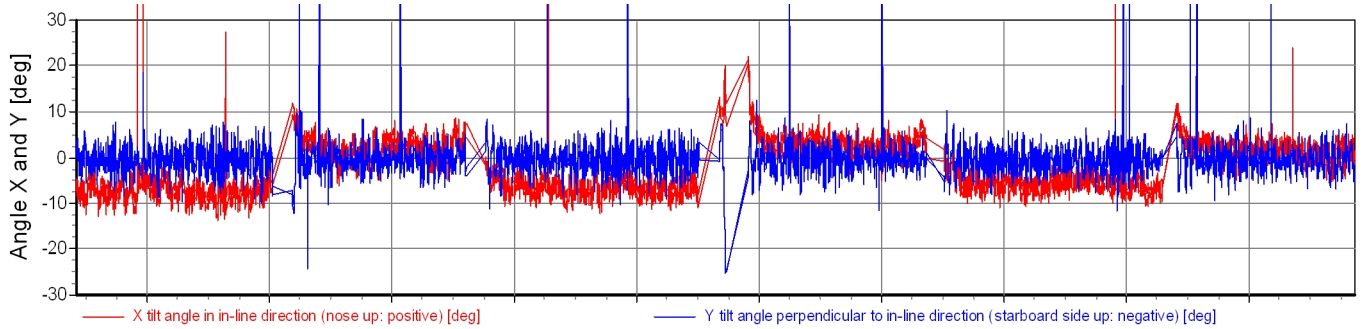
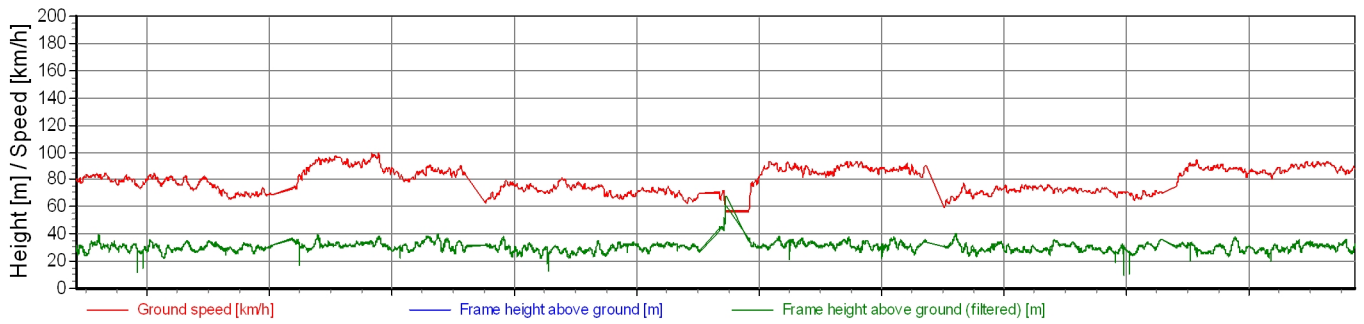
Turns at the end of flight lines and transport are shown as gaps in the bottom of the display.

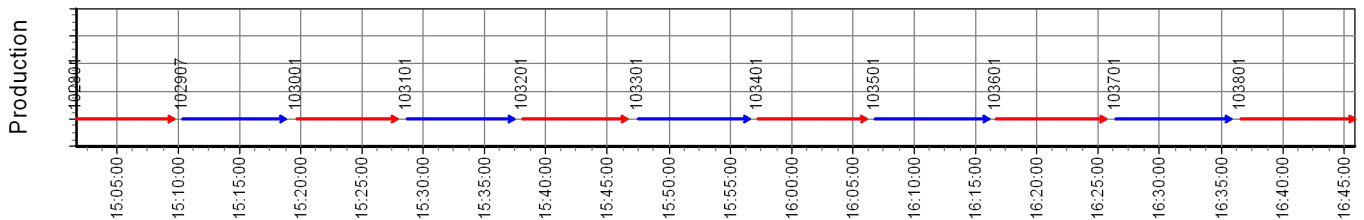
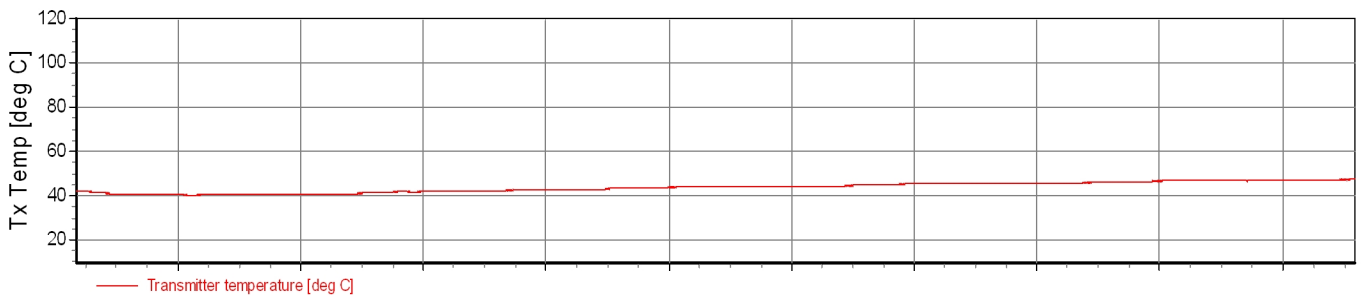
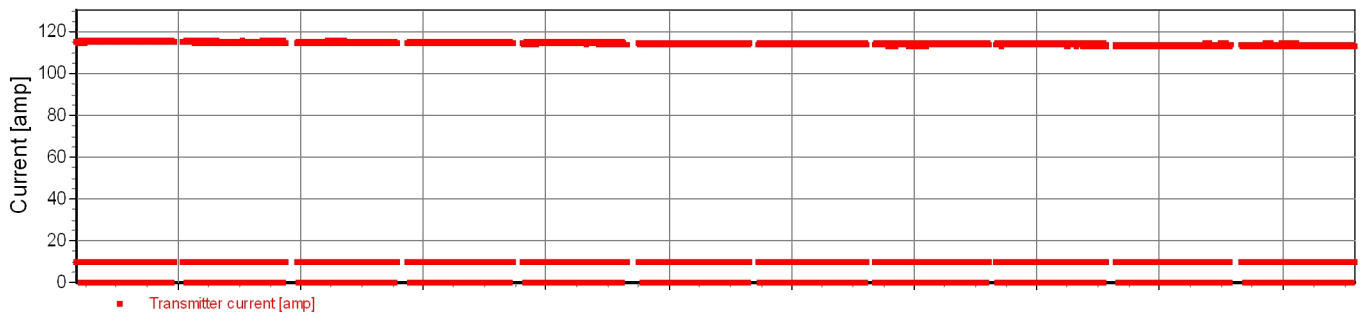
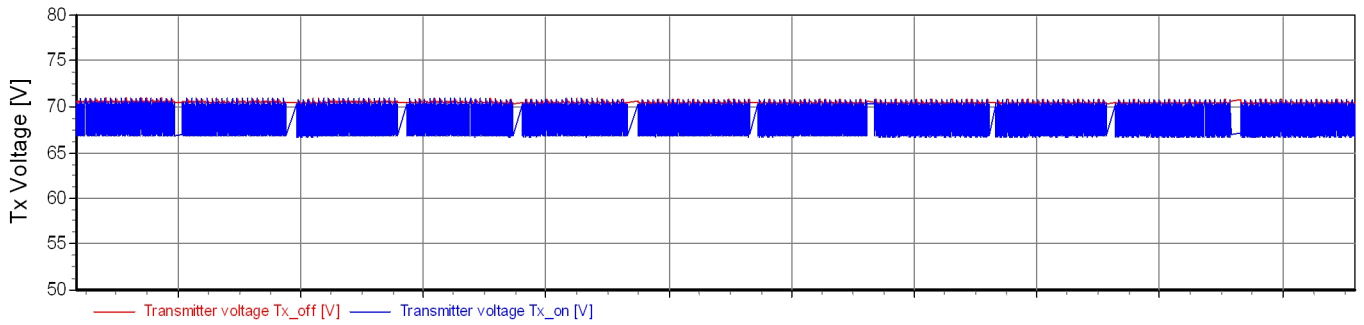
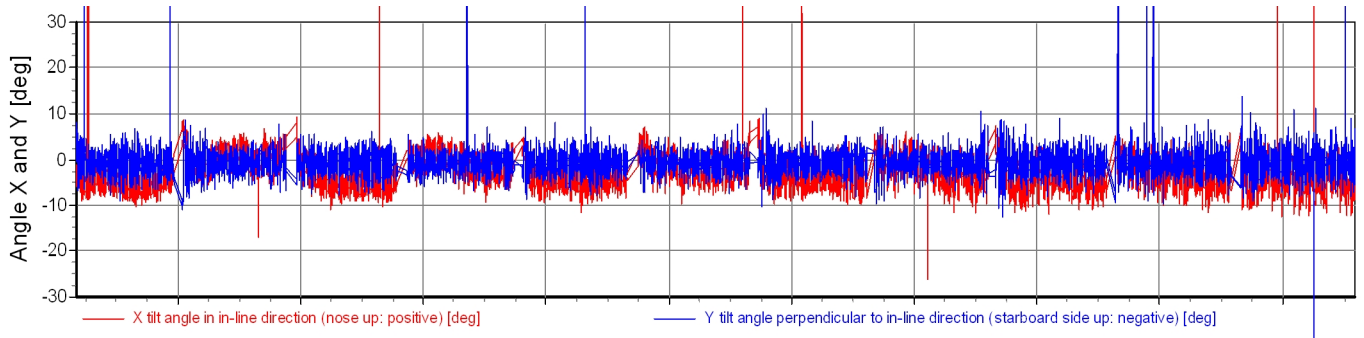
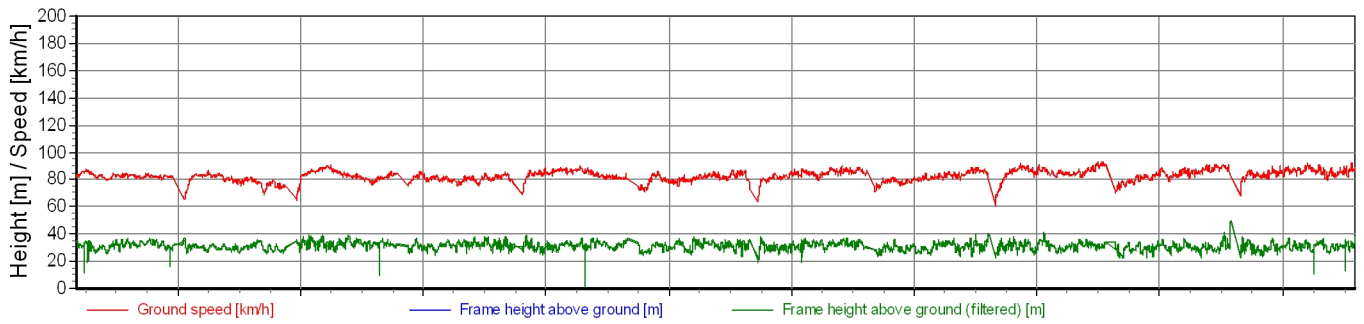
The ground speed in the uppermost window displays the signal from both gps GP1 and GP2.

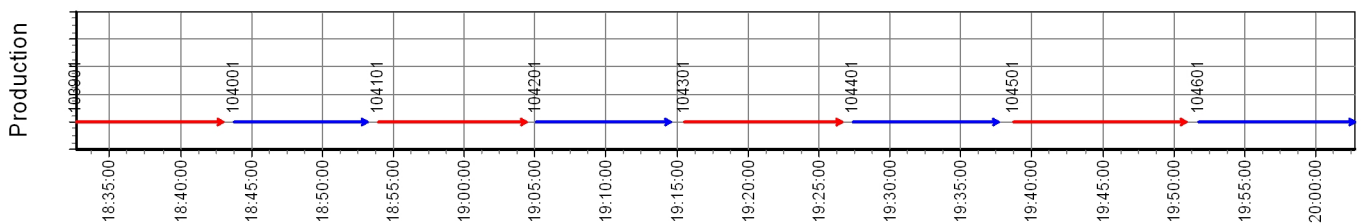
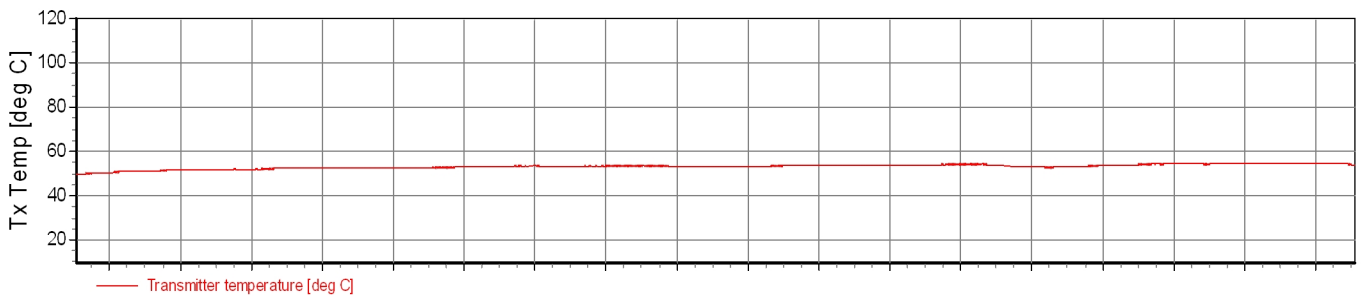
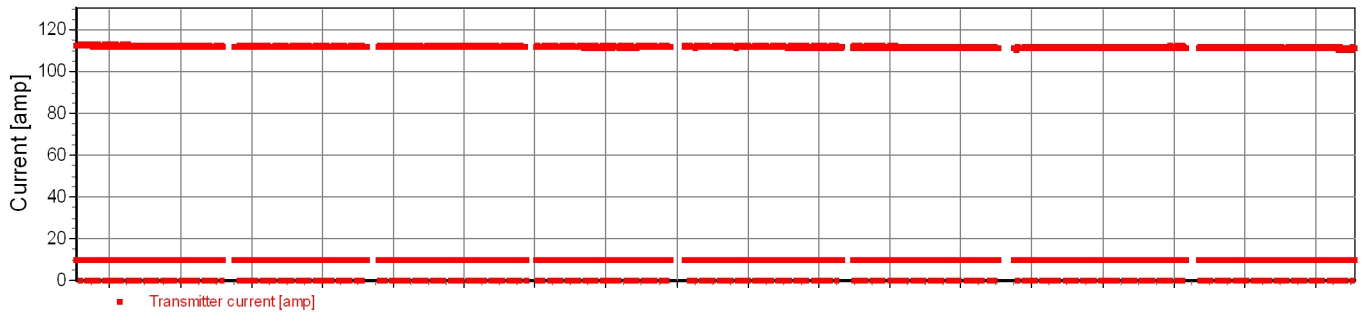
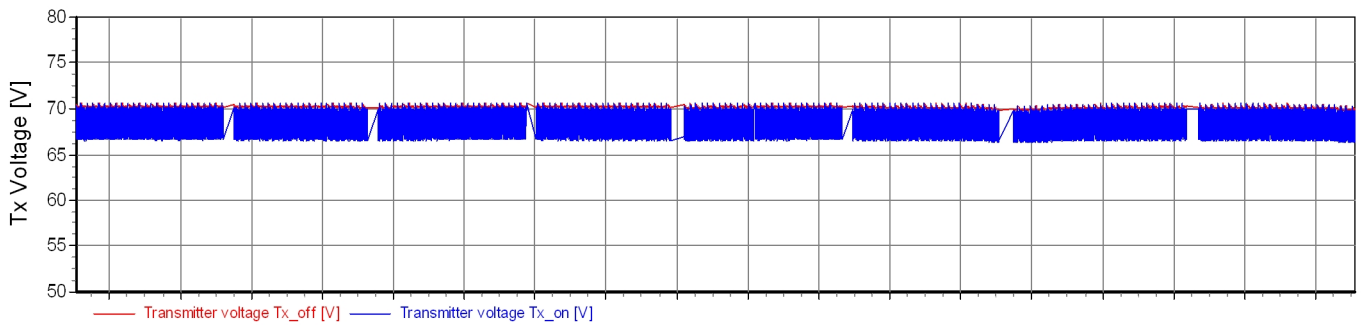
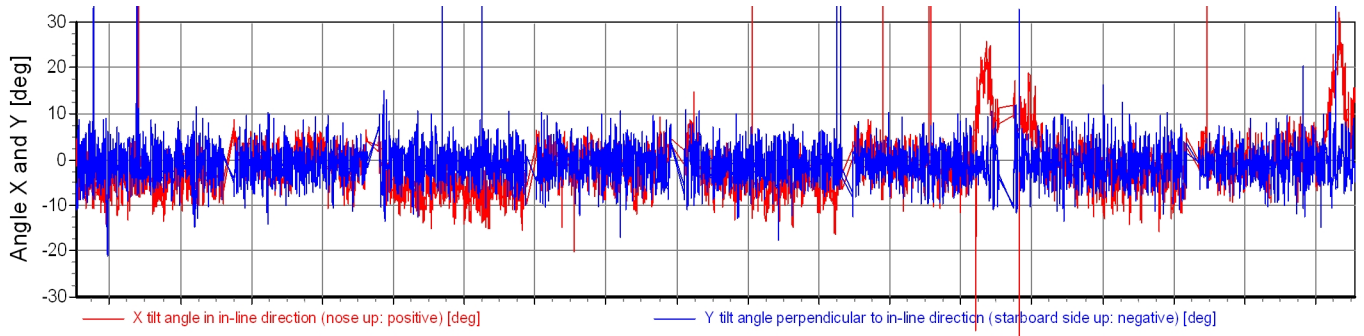
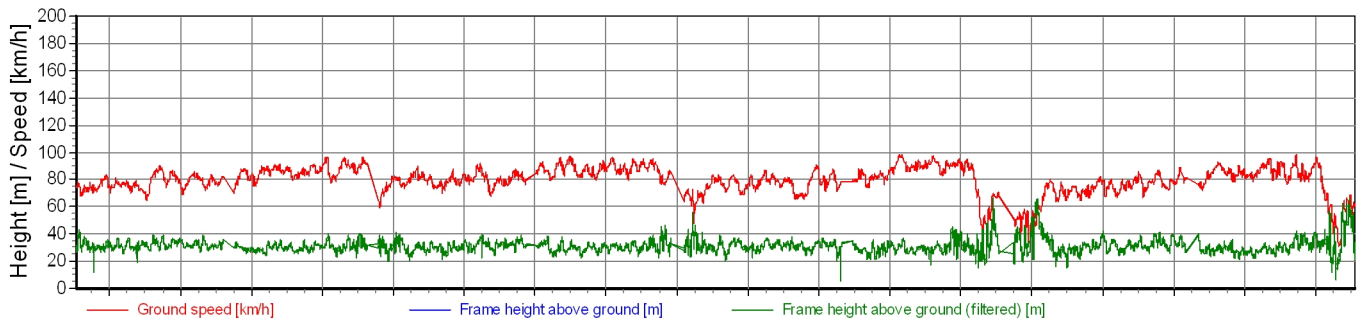


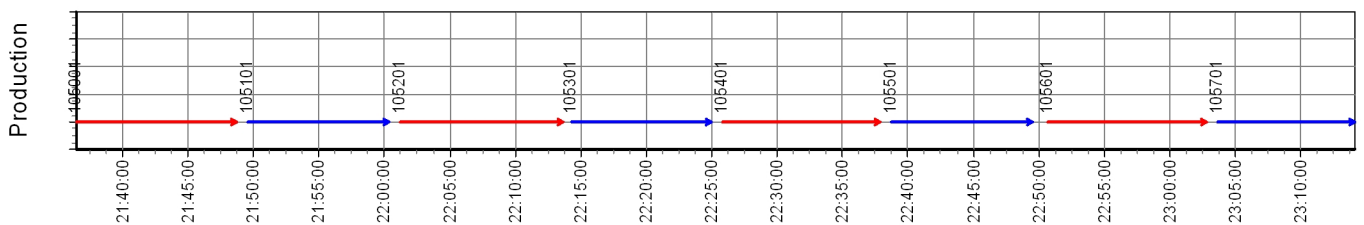
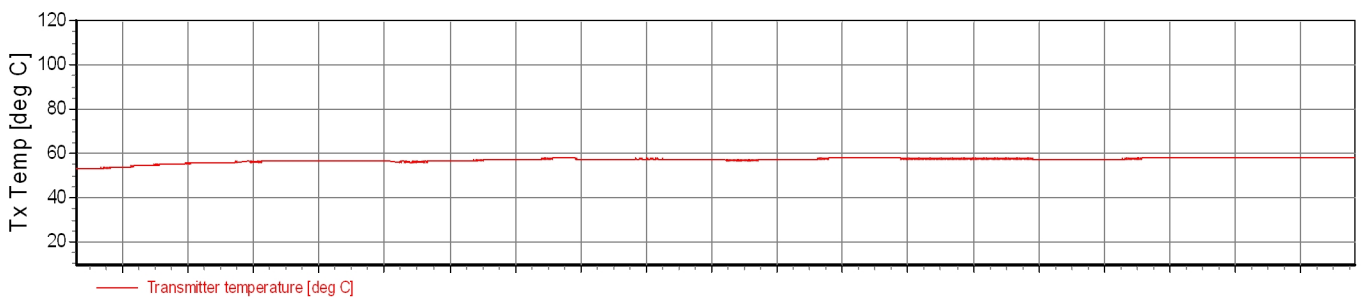
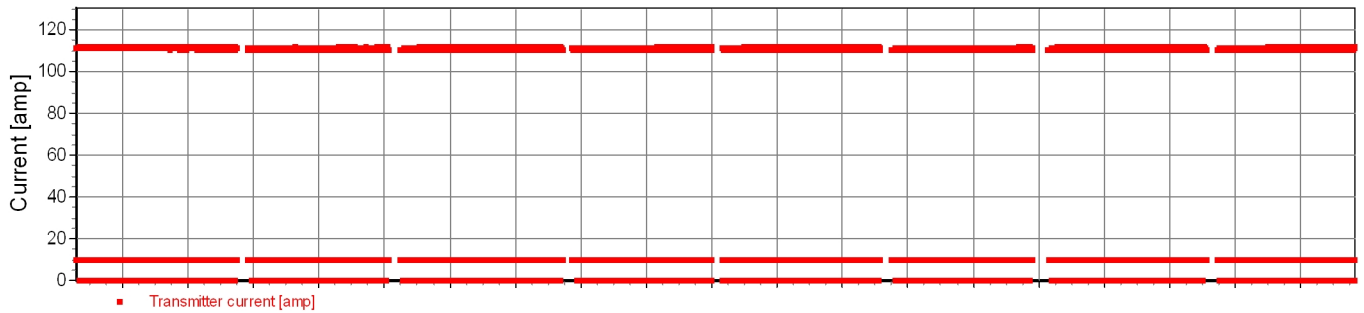
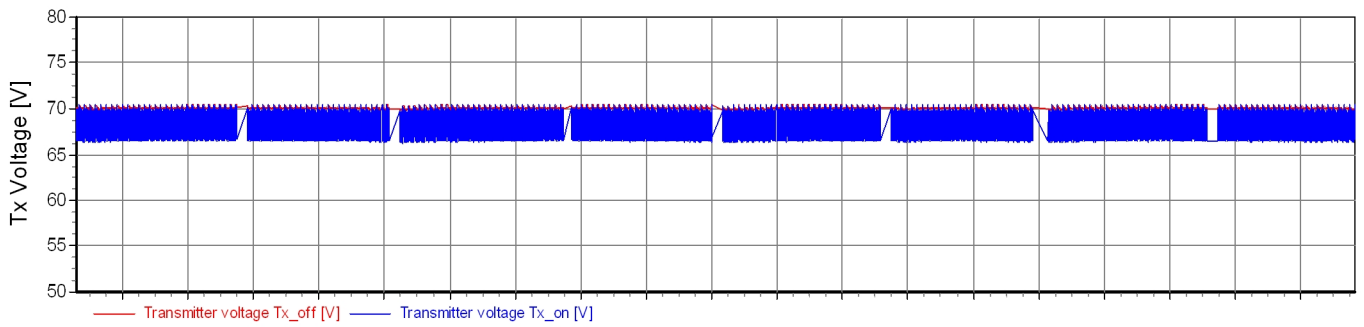
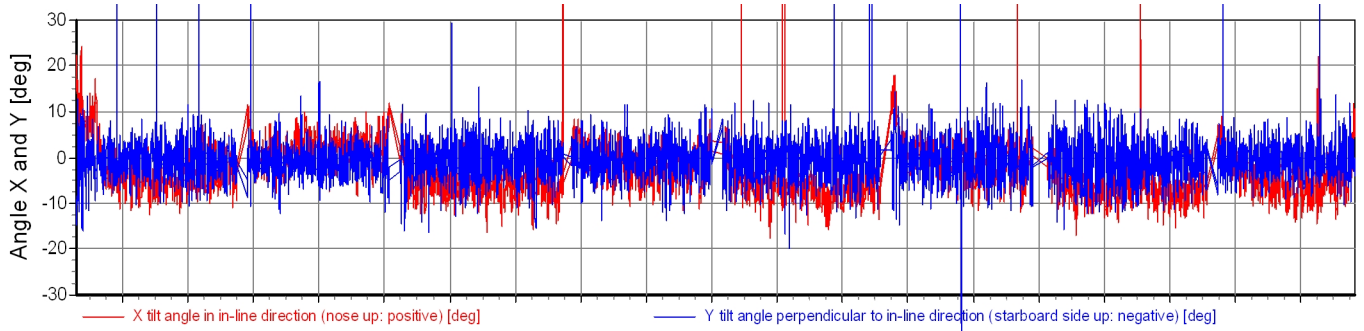
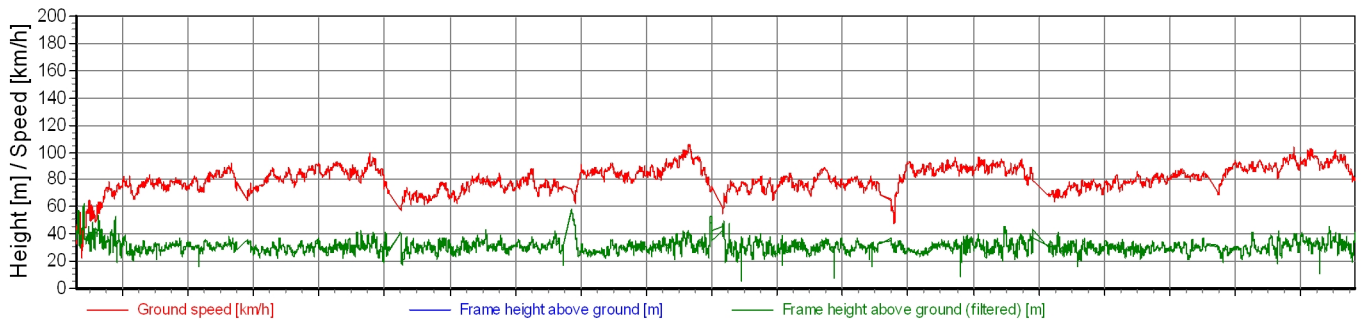


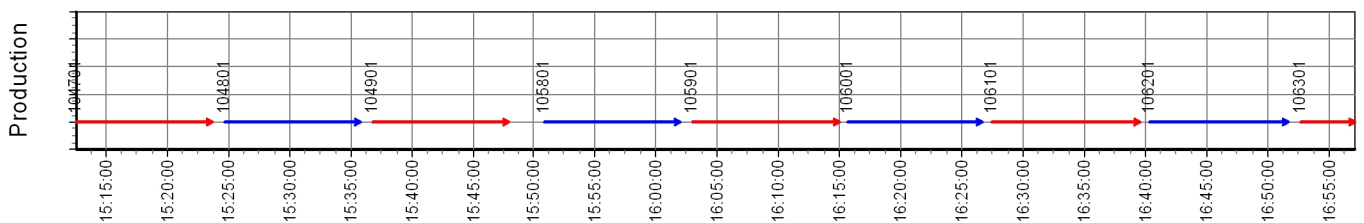
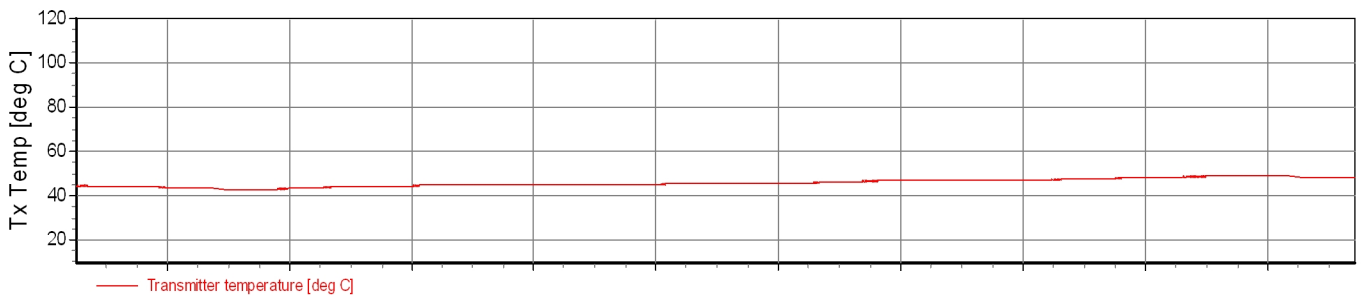
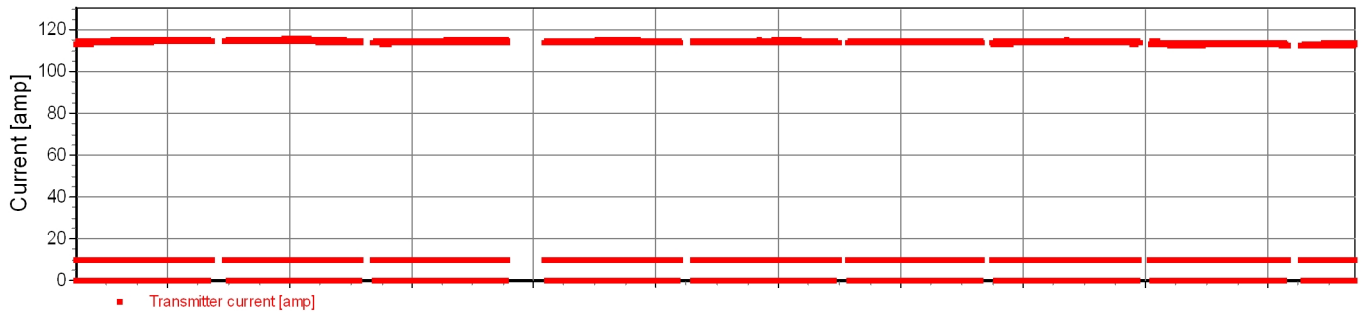
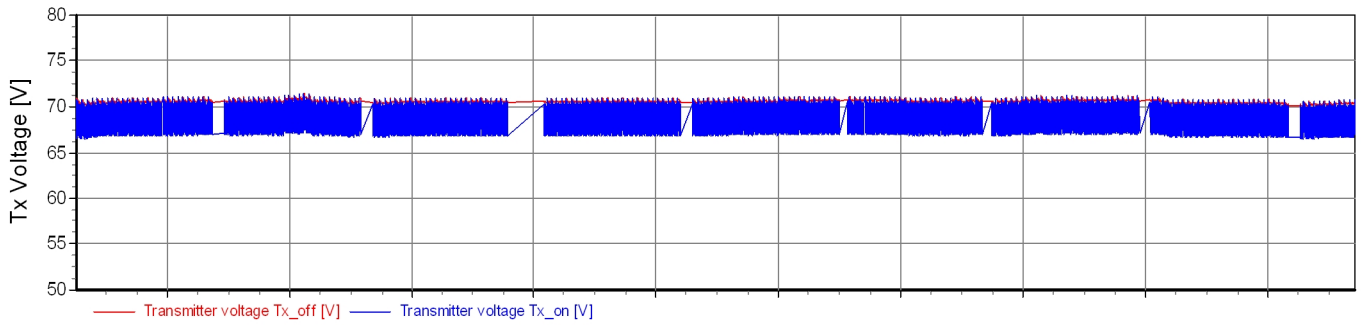
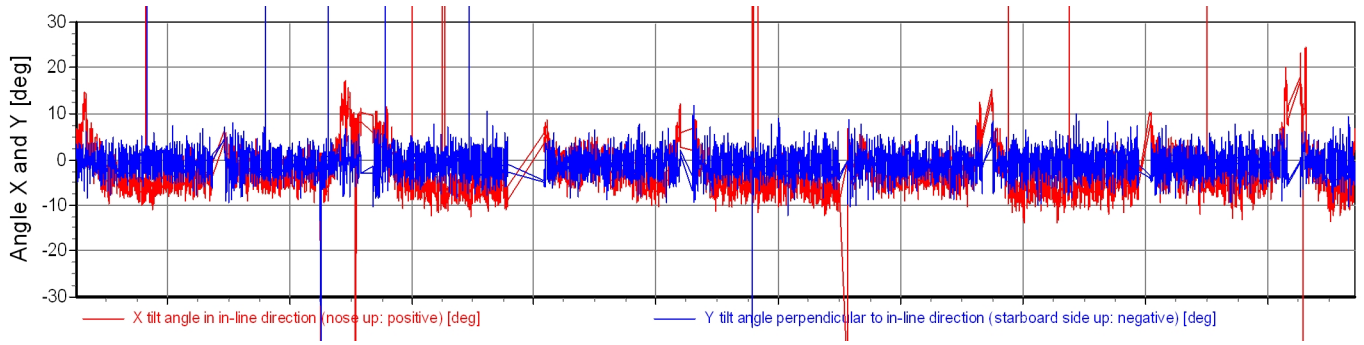
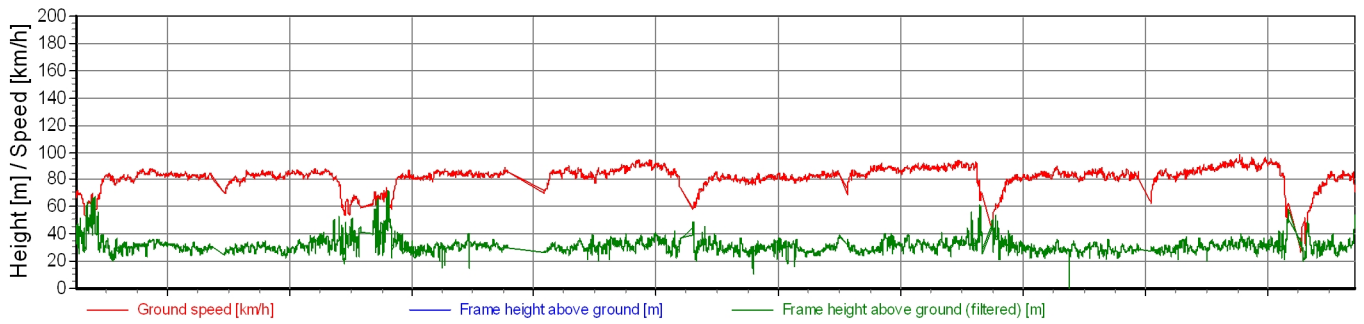


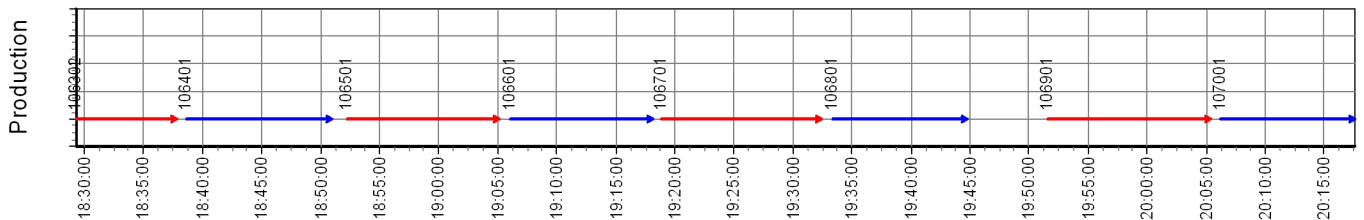
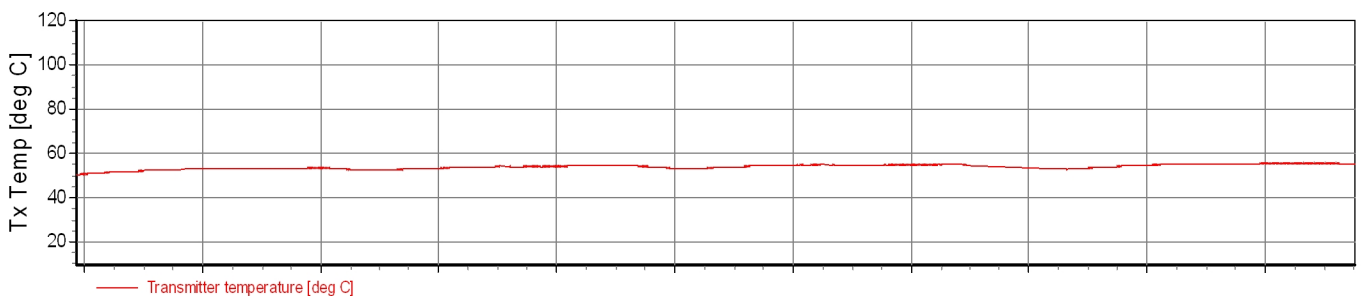
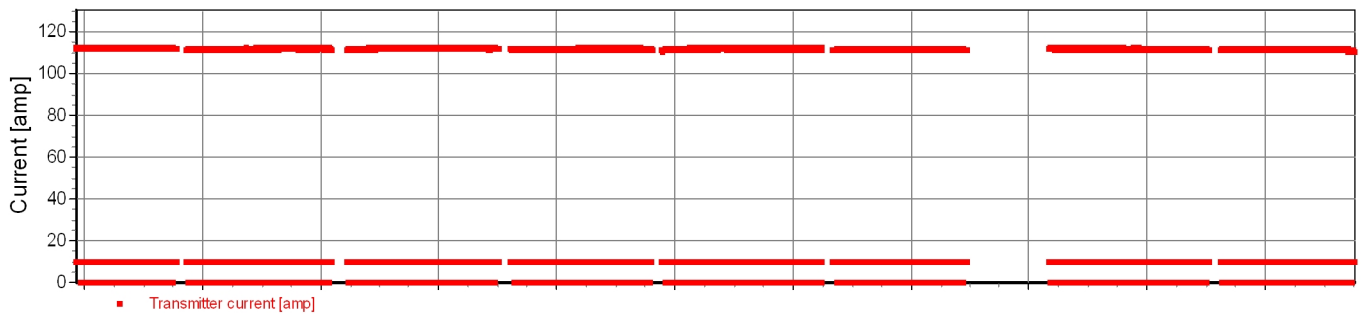
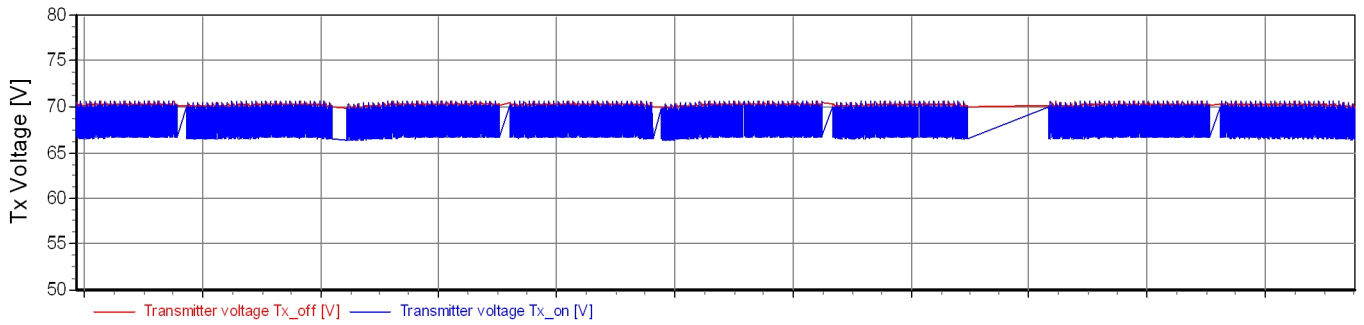
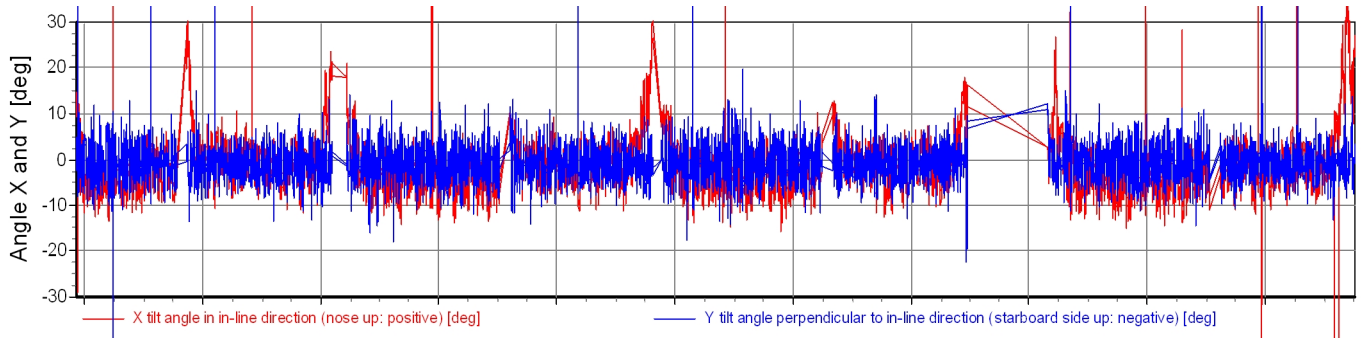
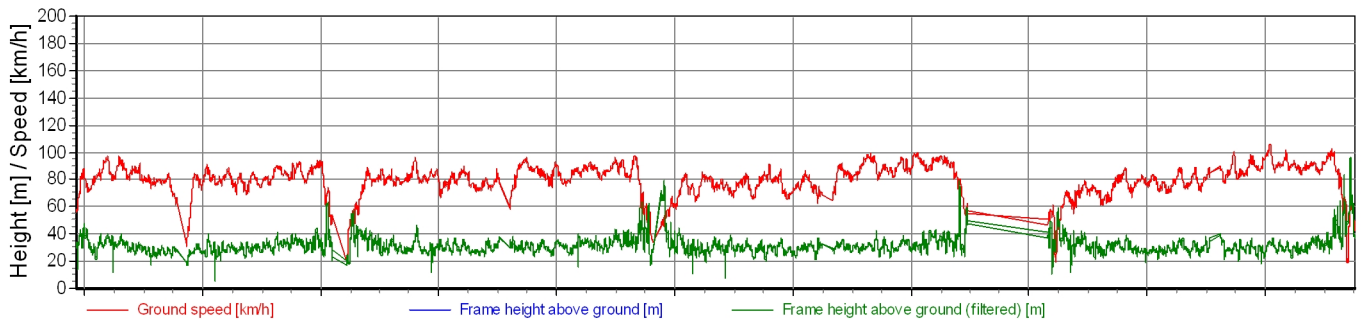


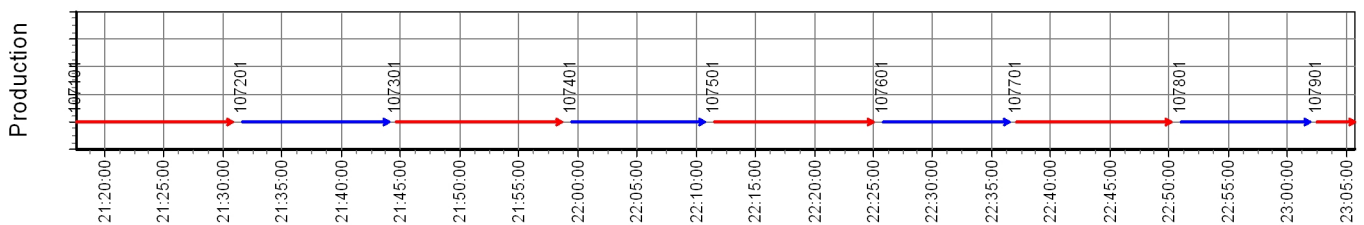
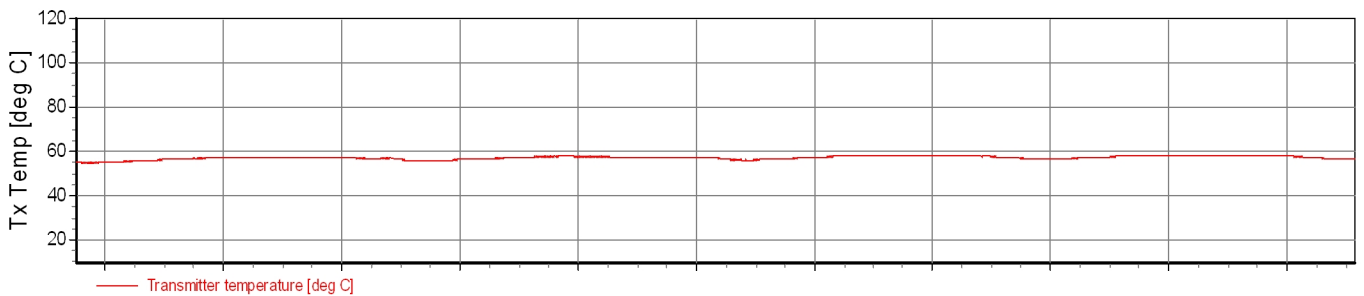
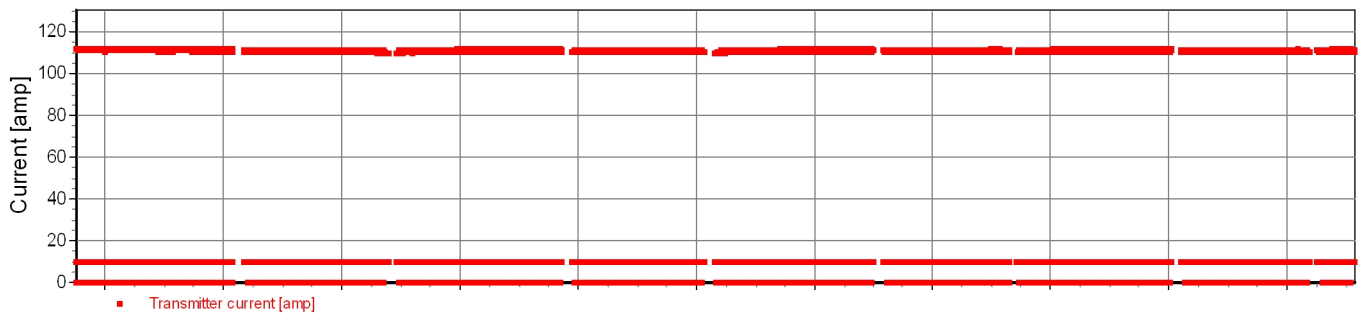
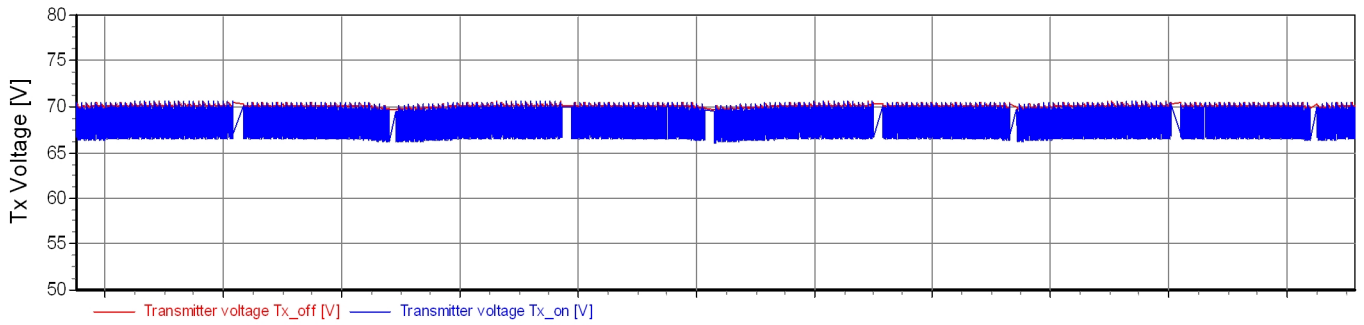
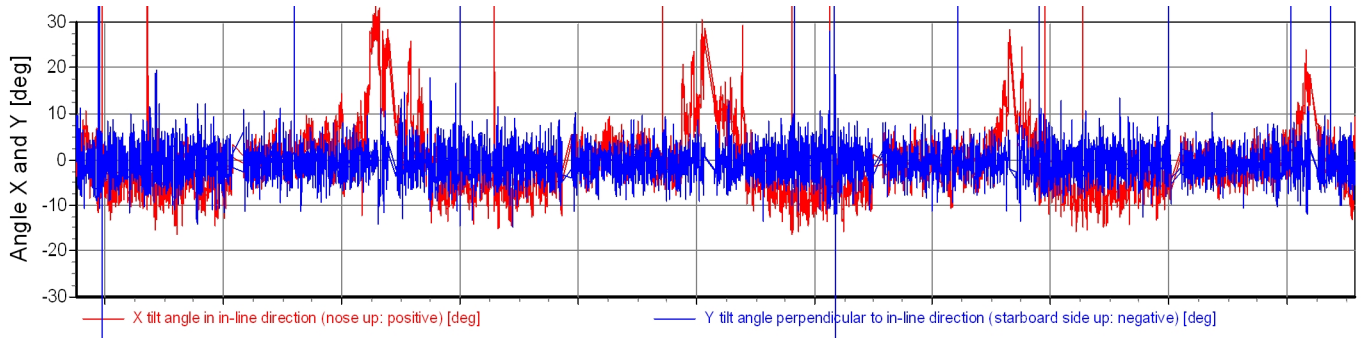
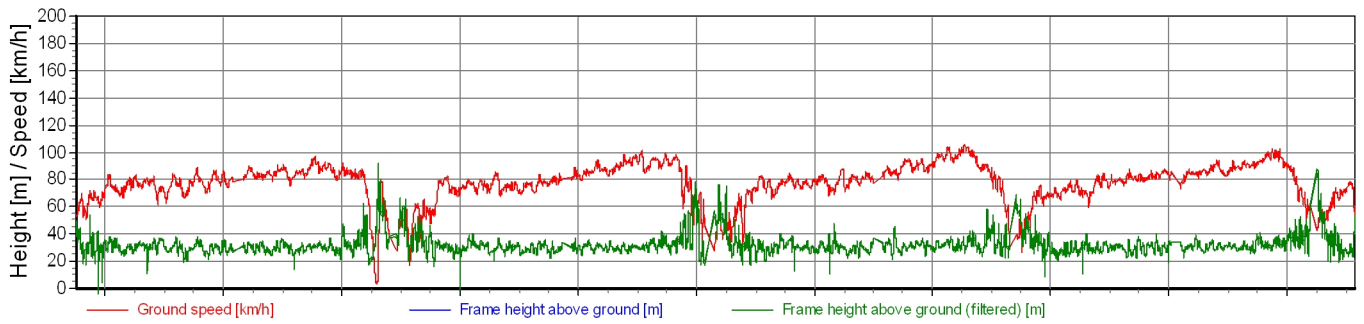


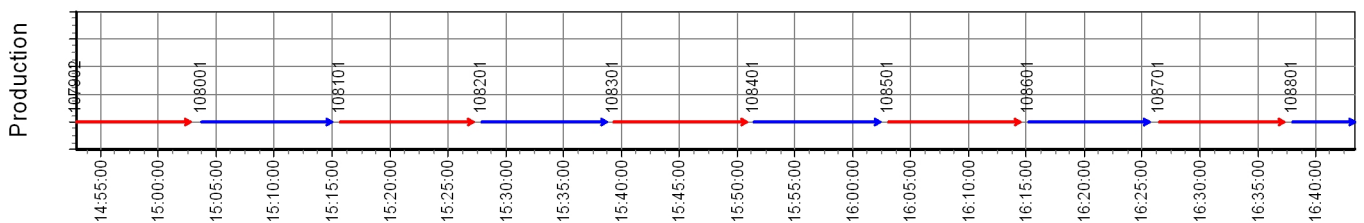
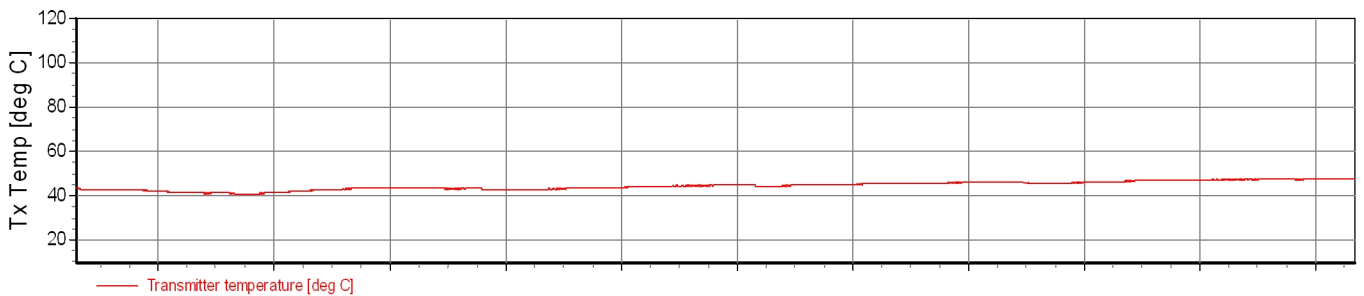
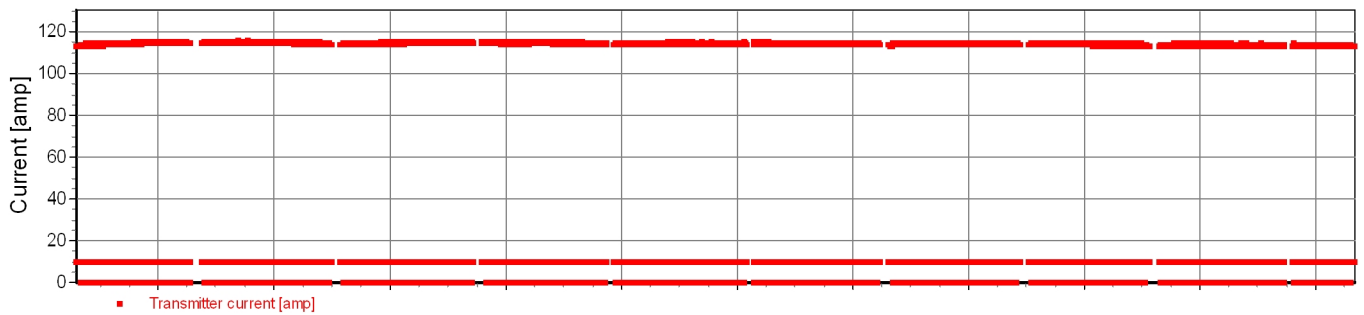
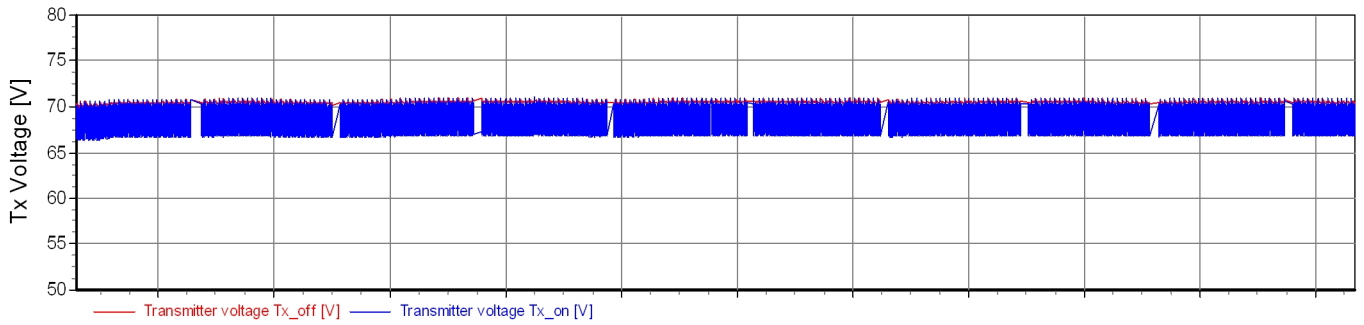
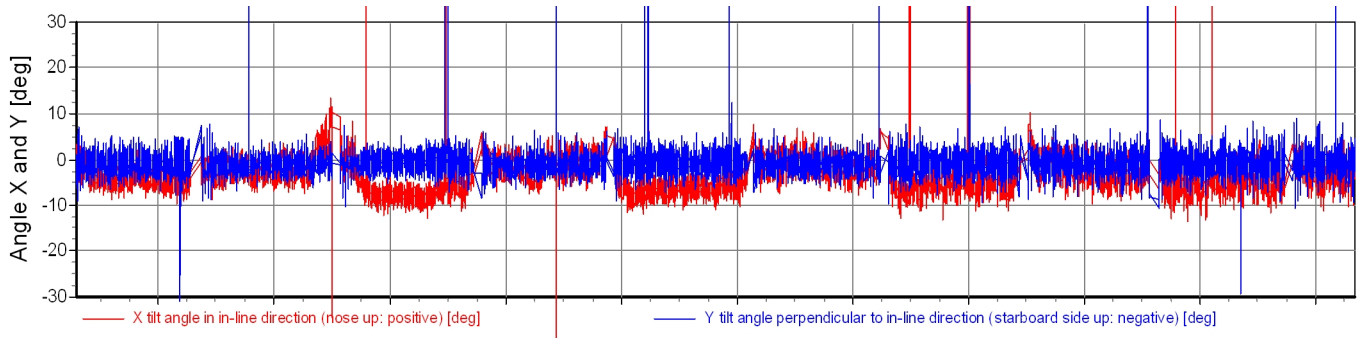
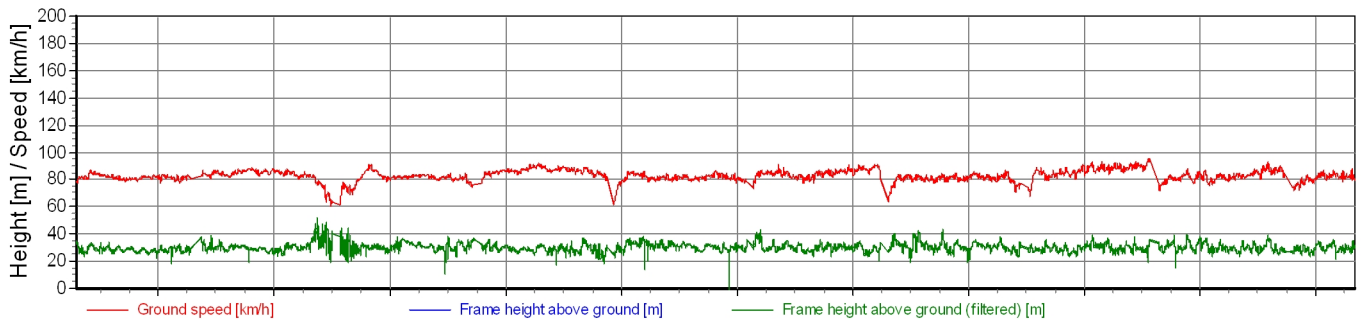


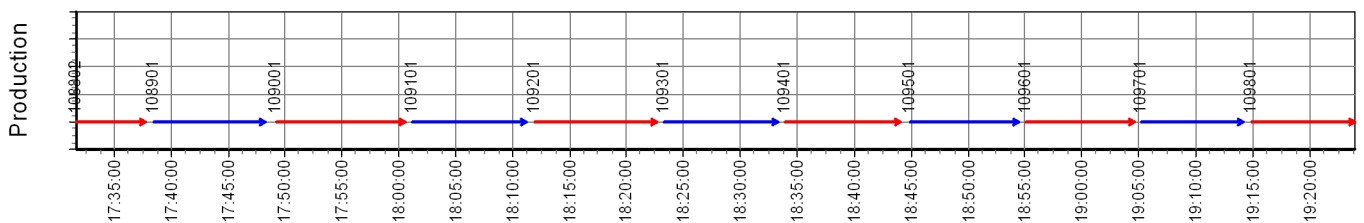
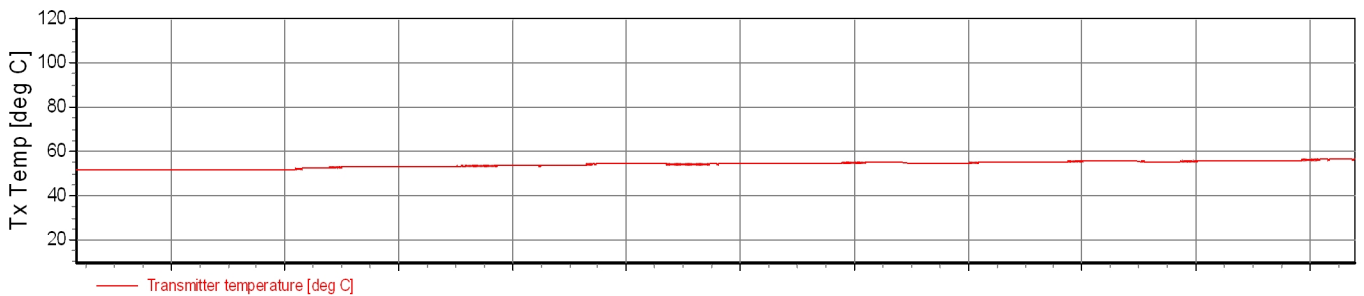
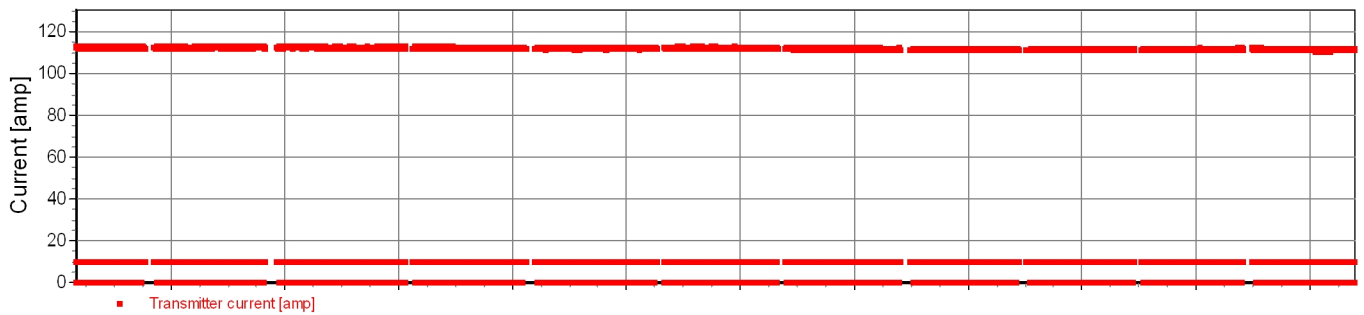
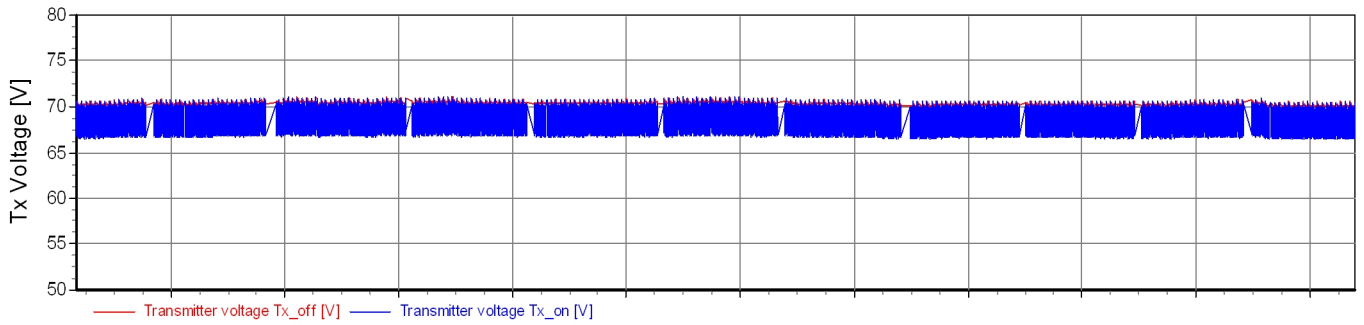
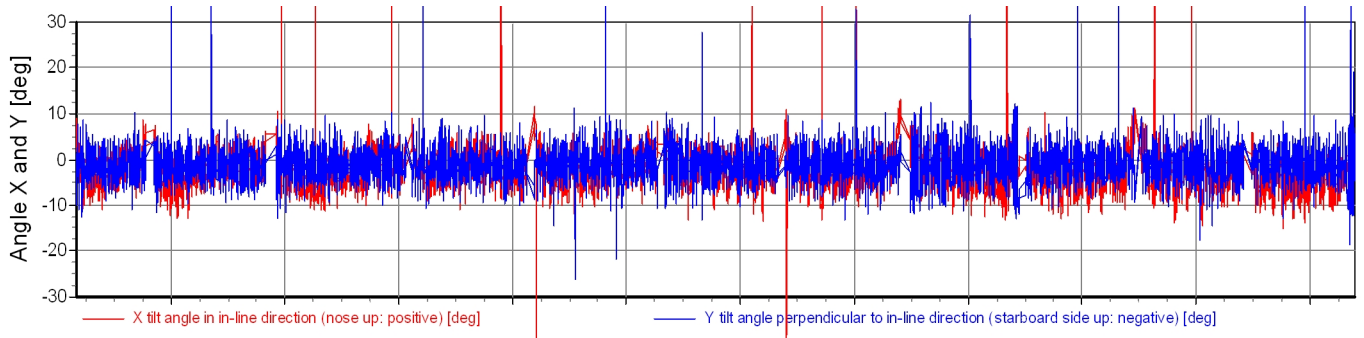
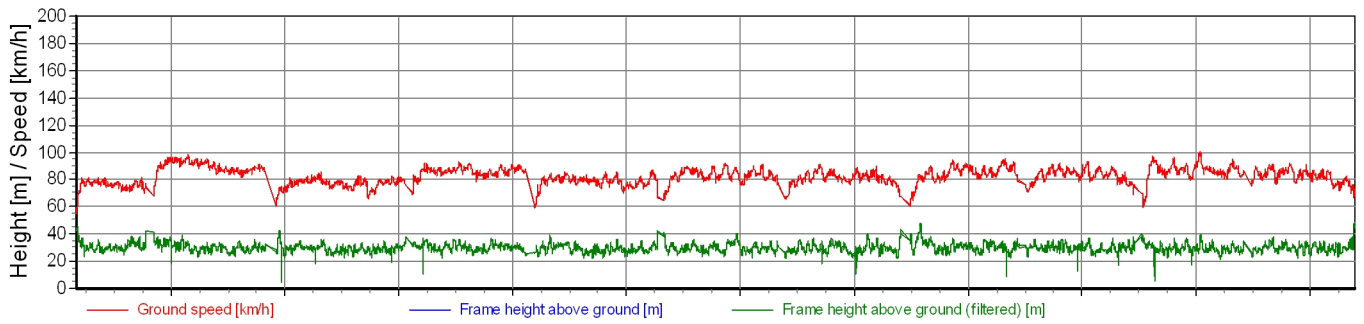


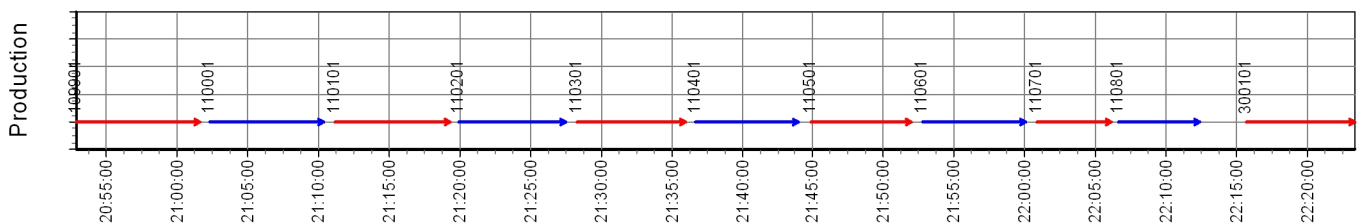
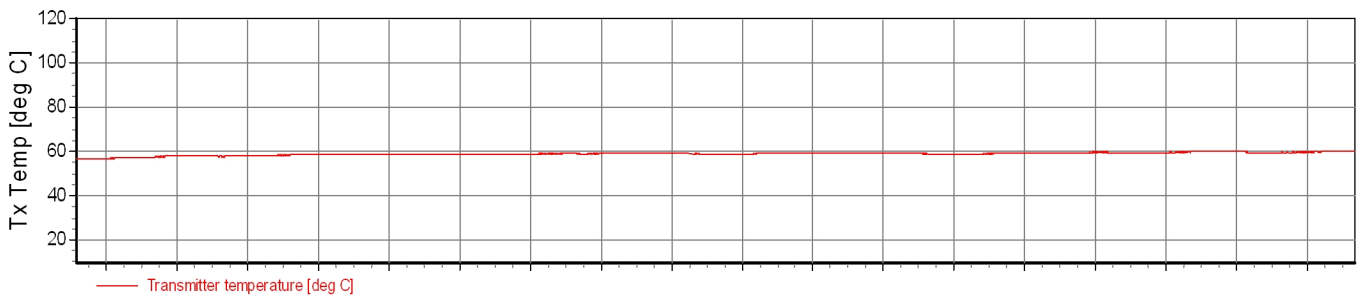
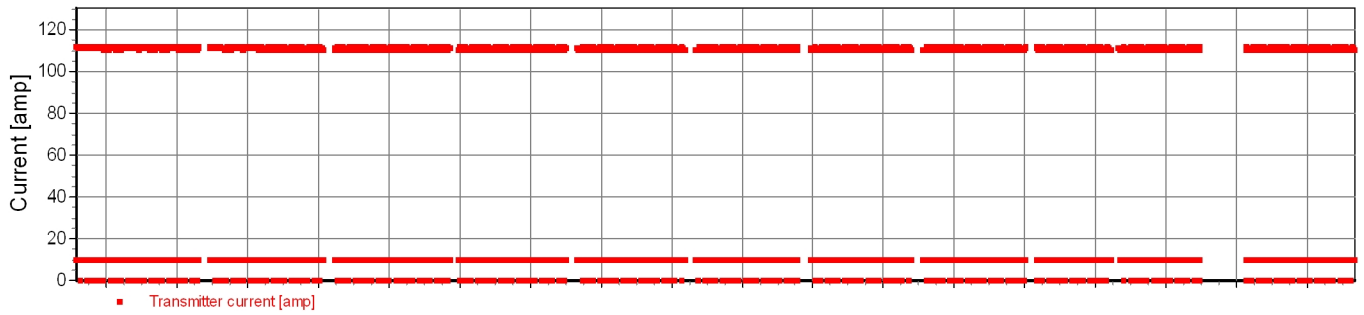
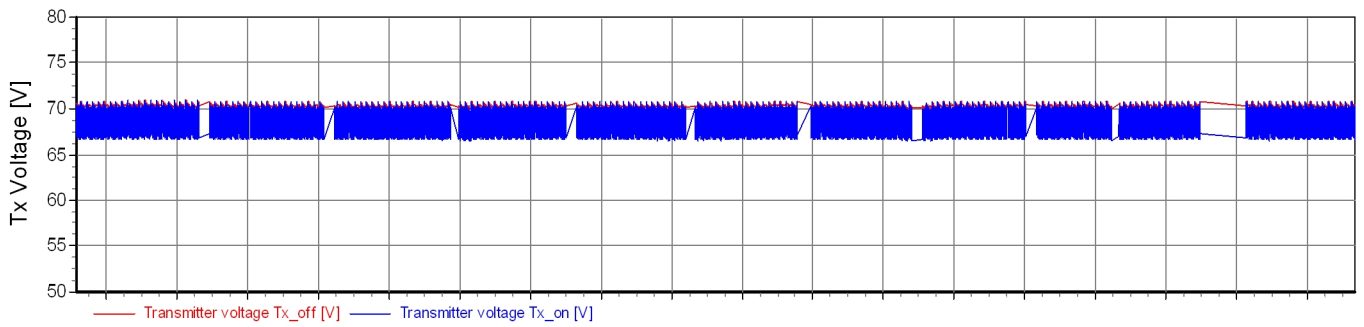
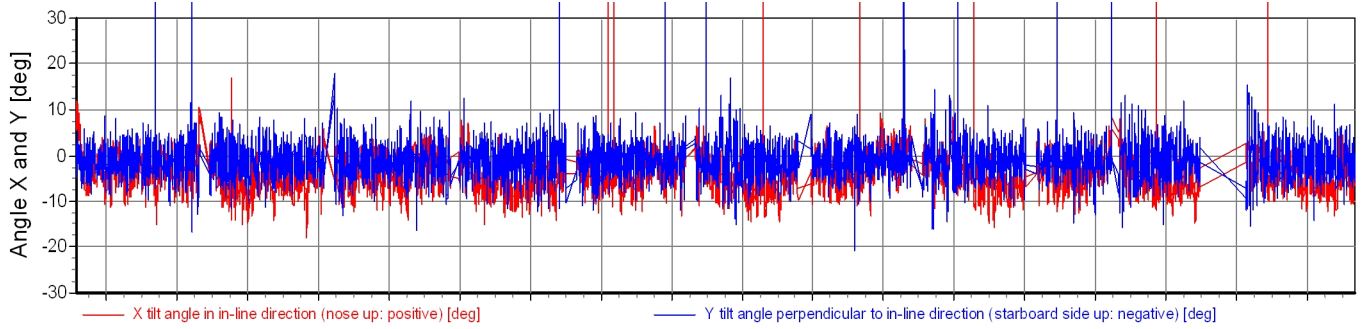
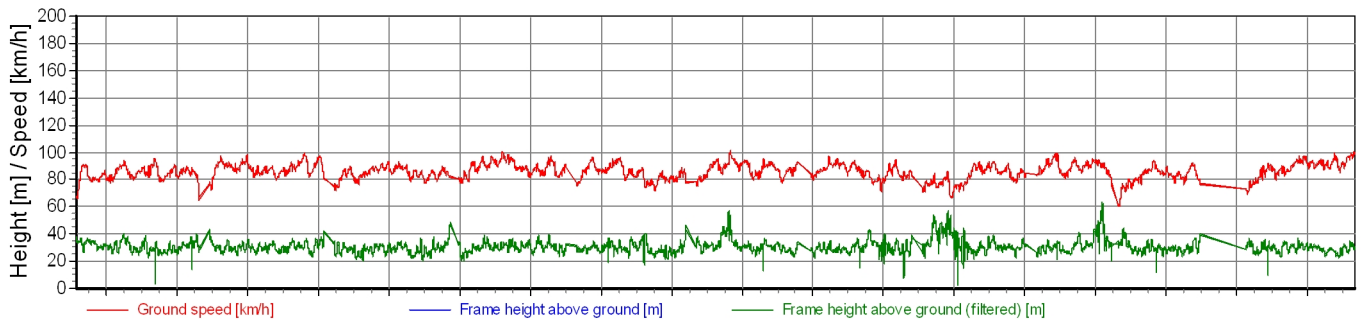


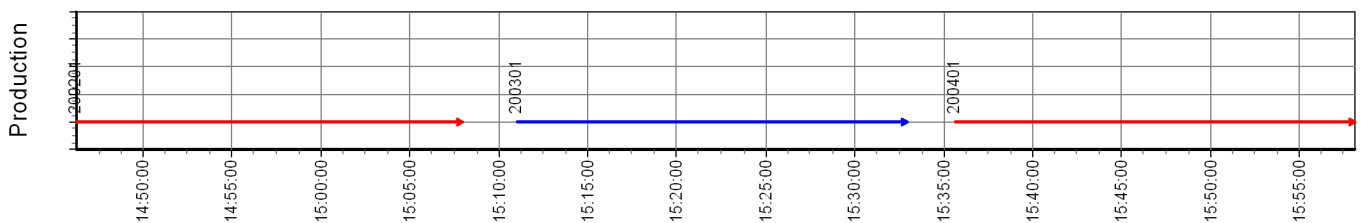
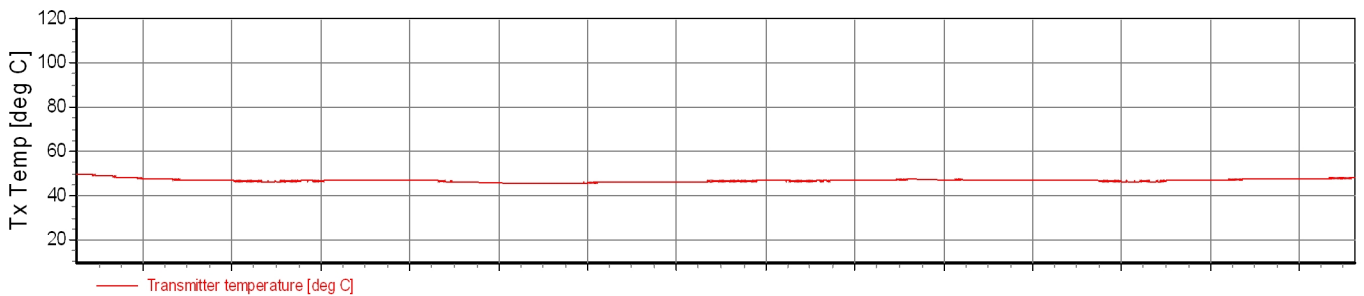
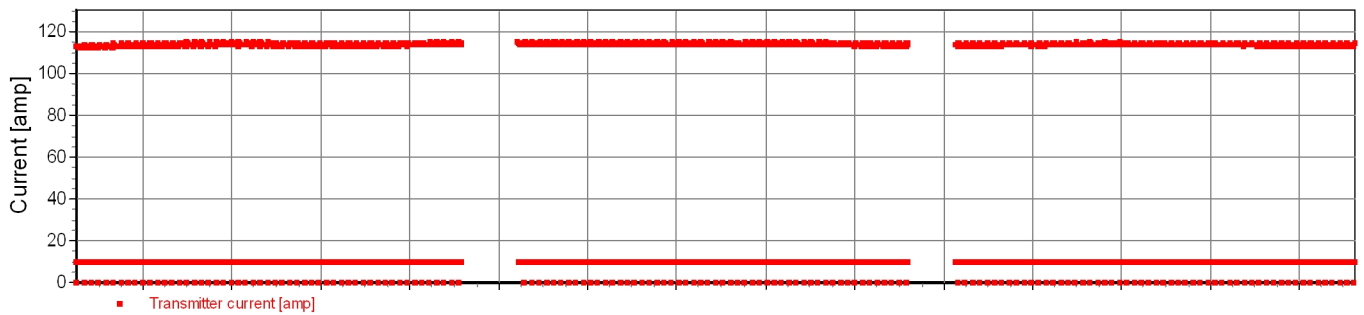
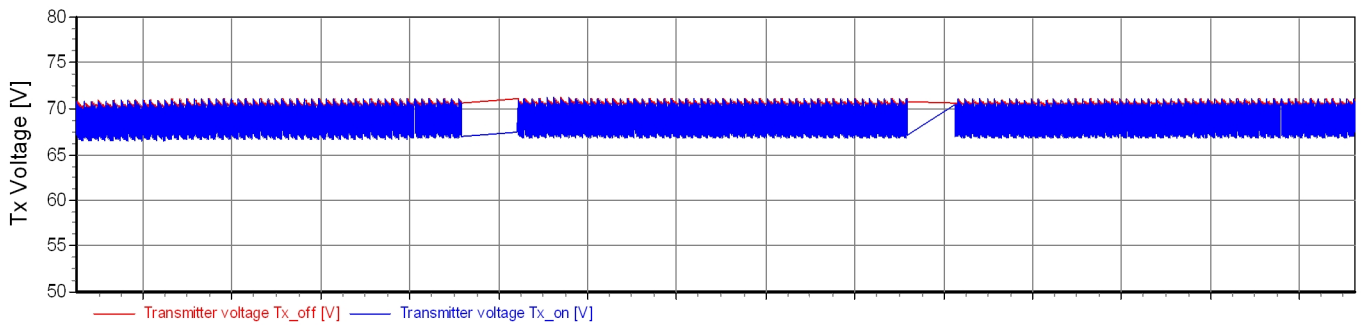
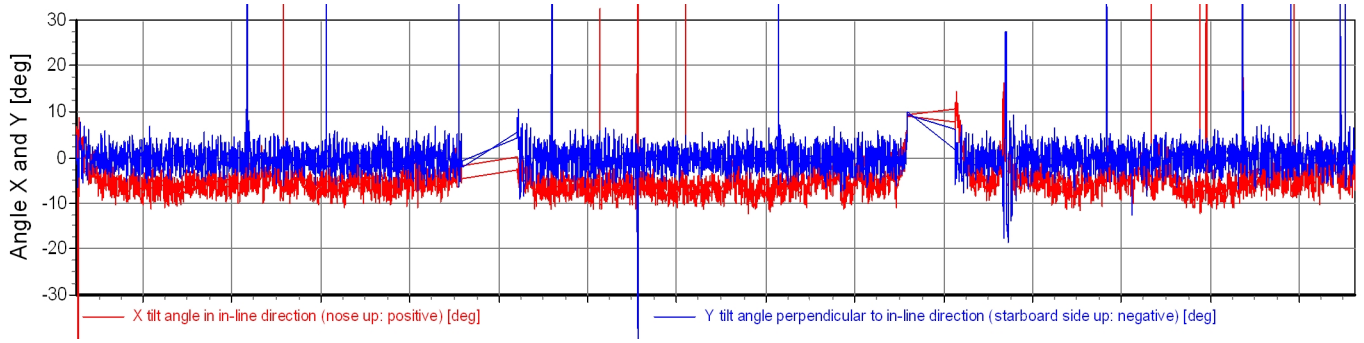
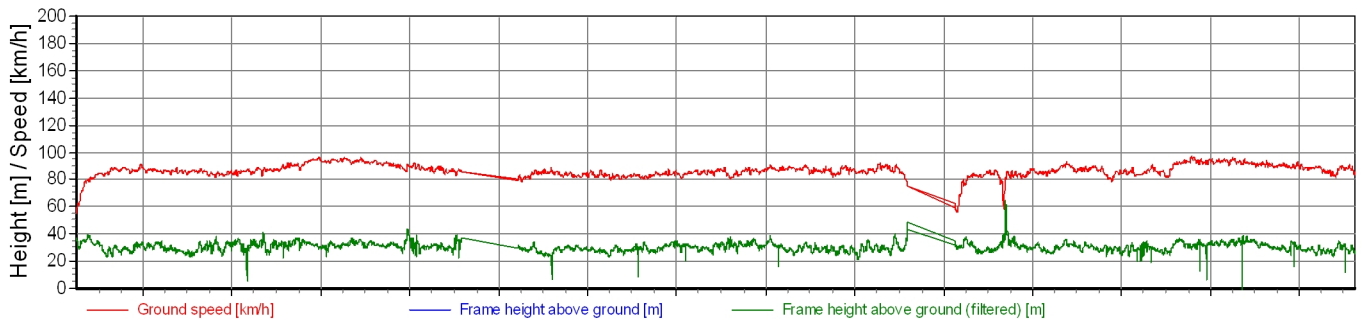


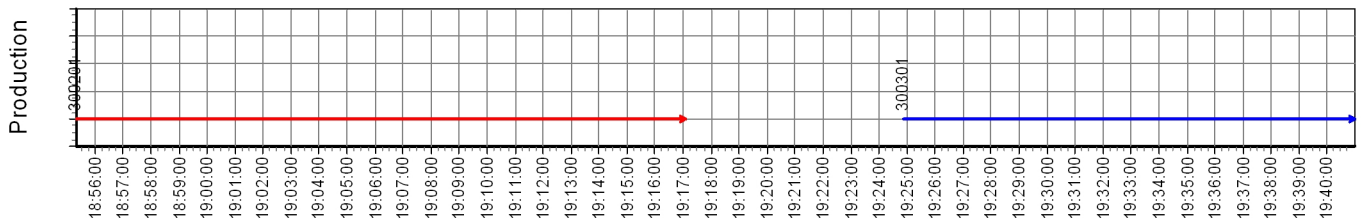
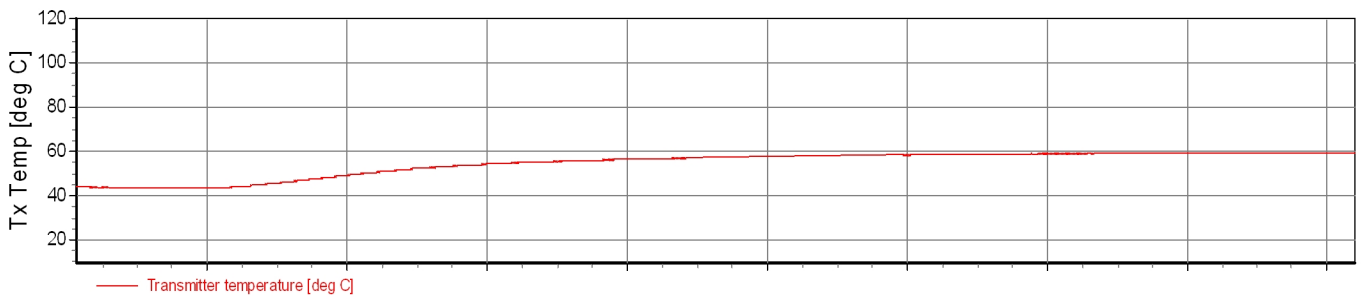
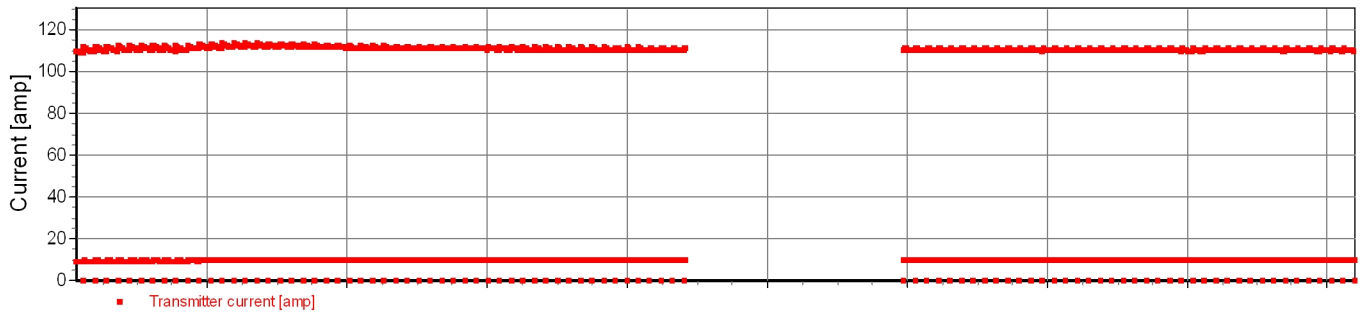
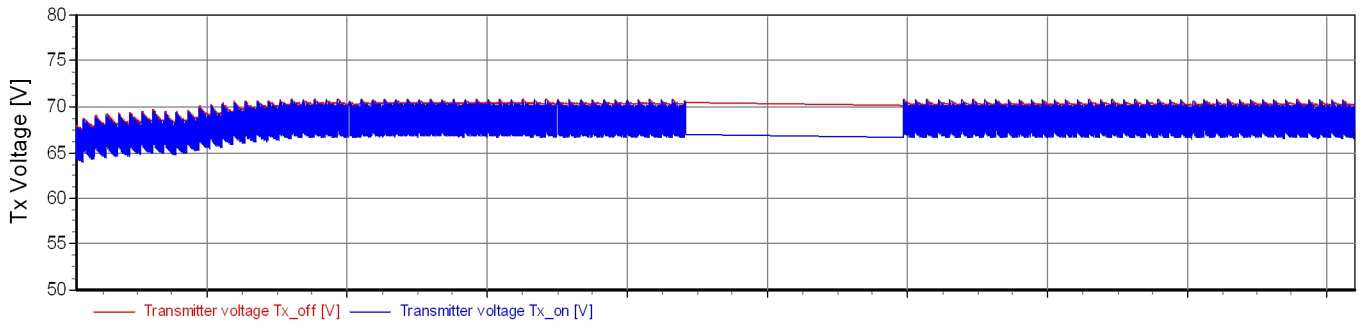
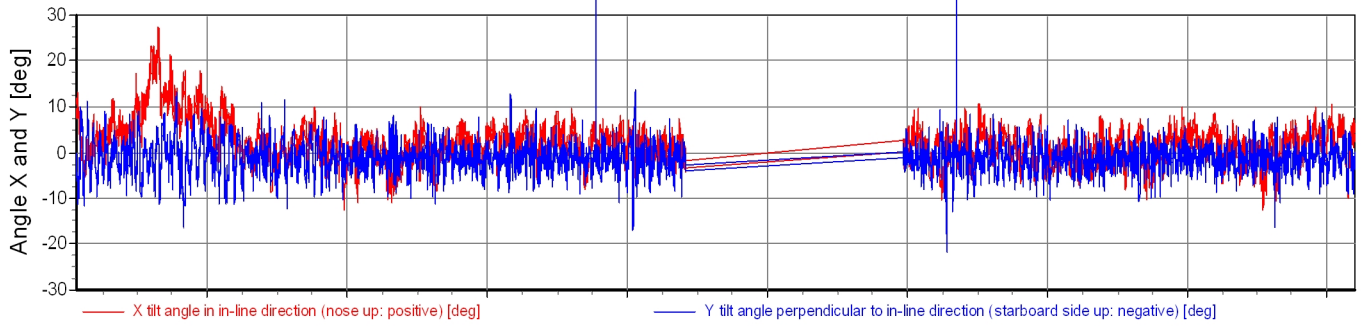


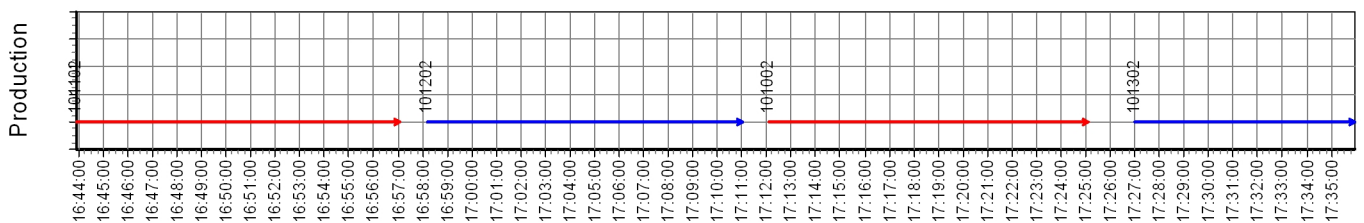
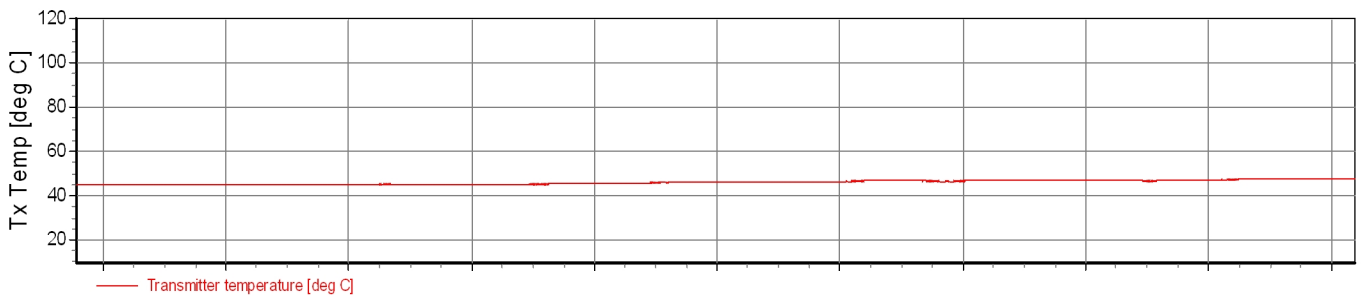
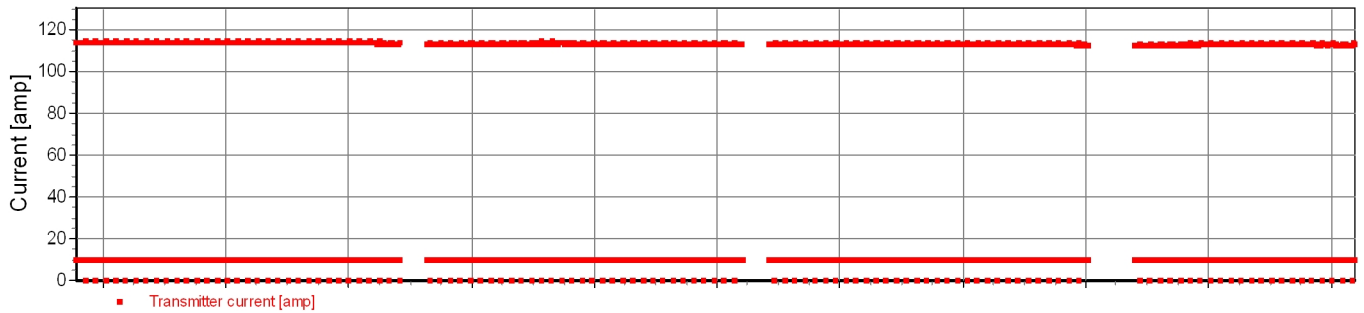
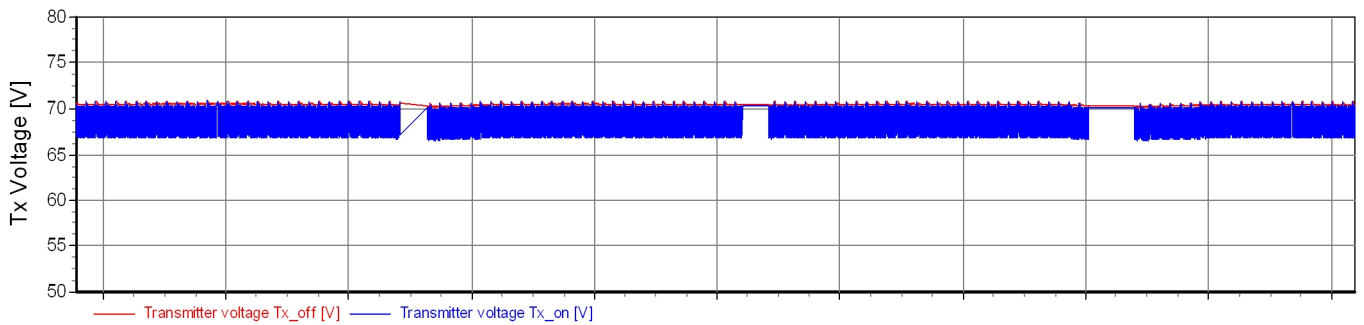
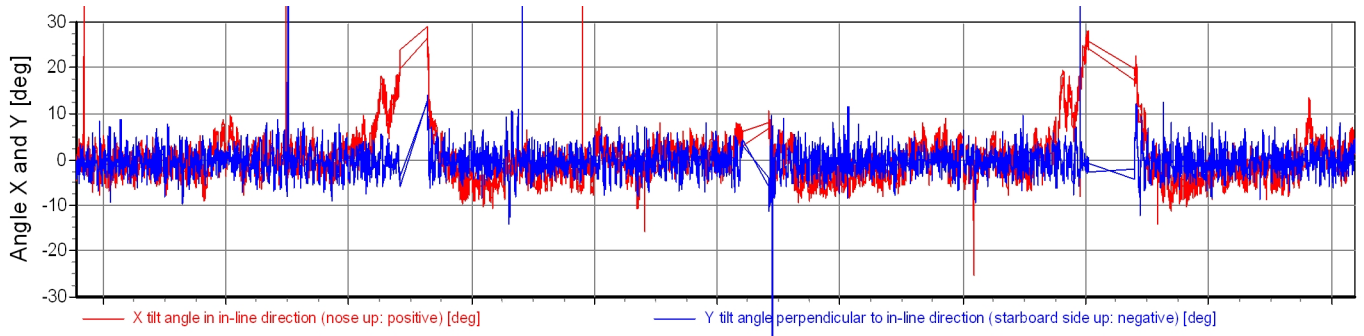
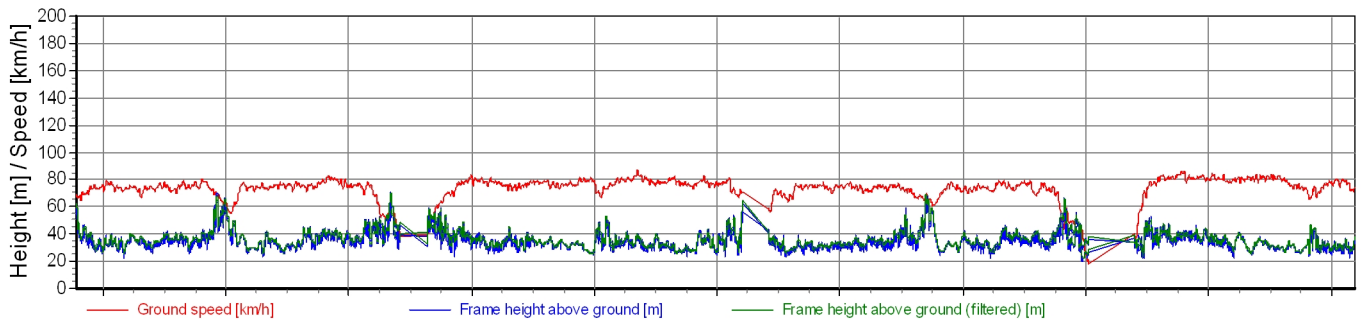


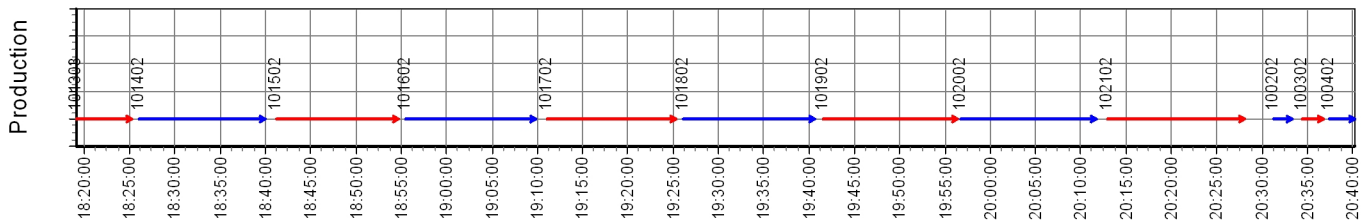
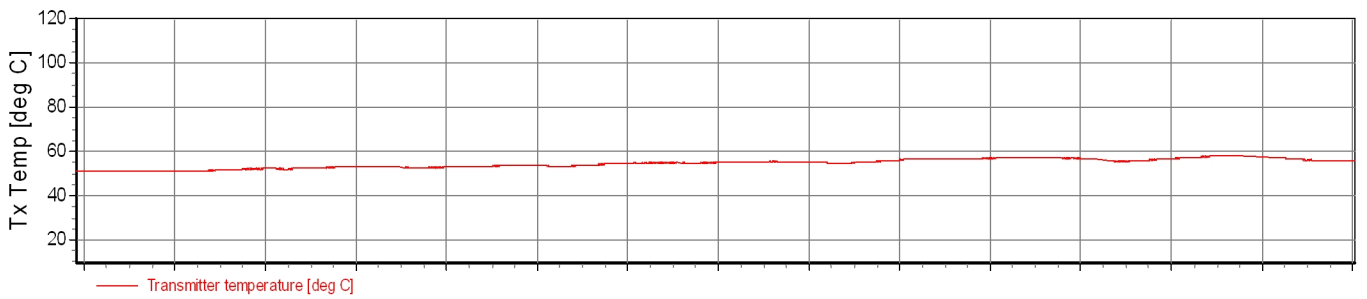
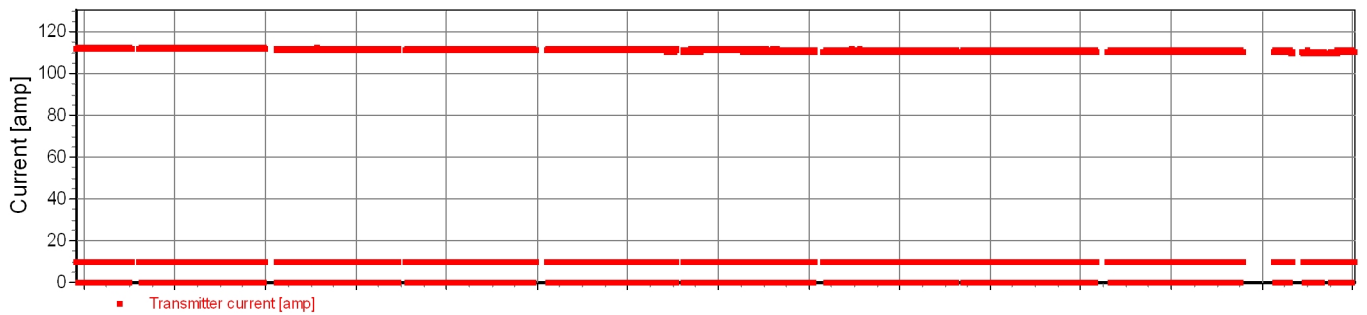
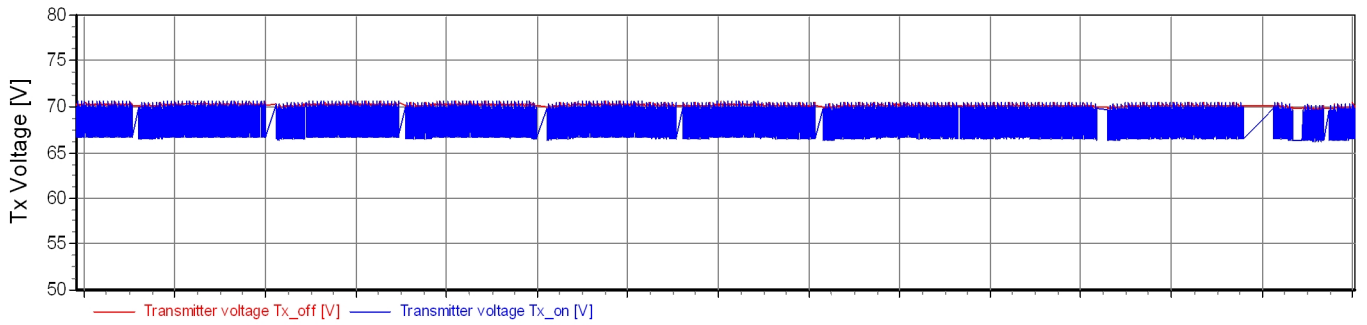
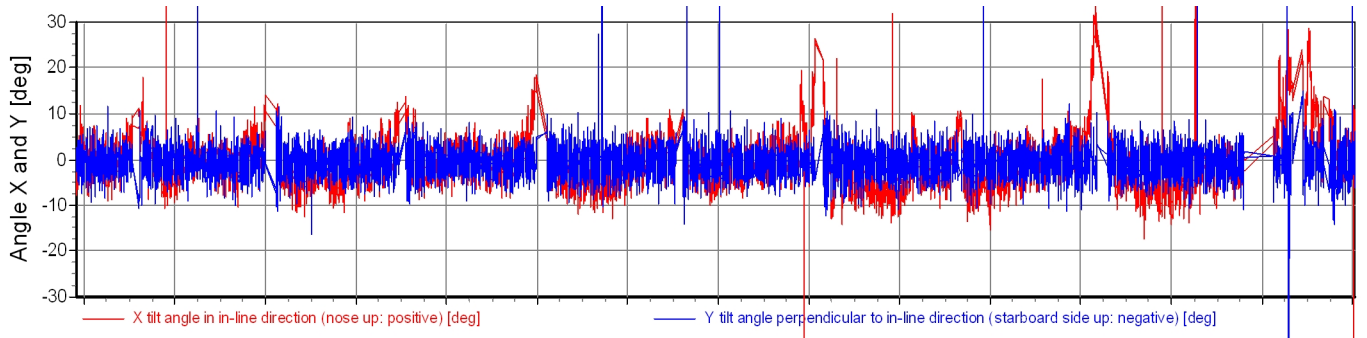
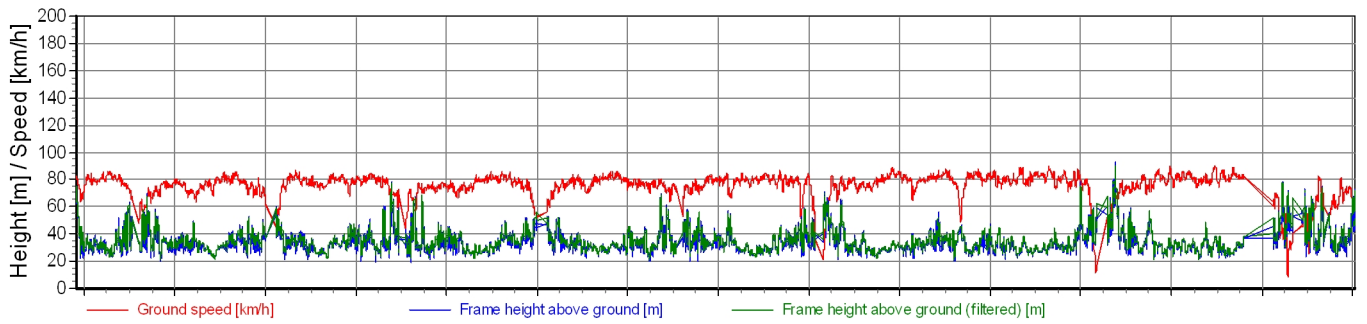


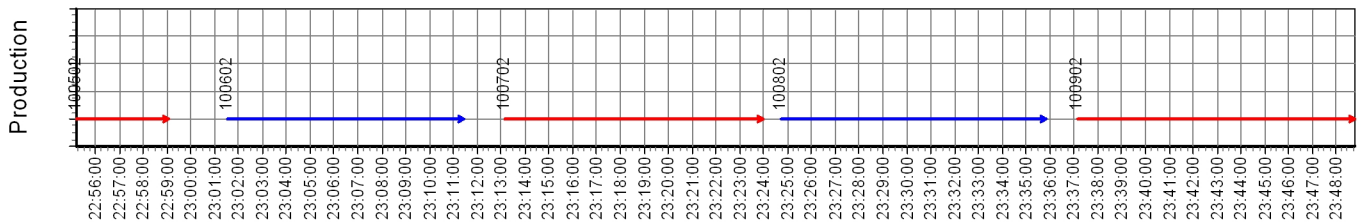
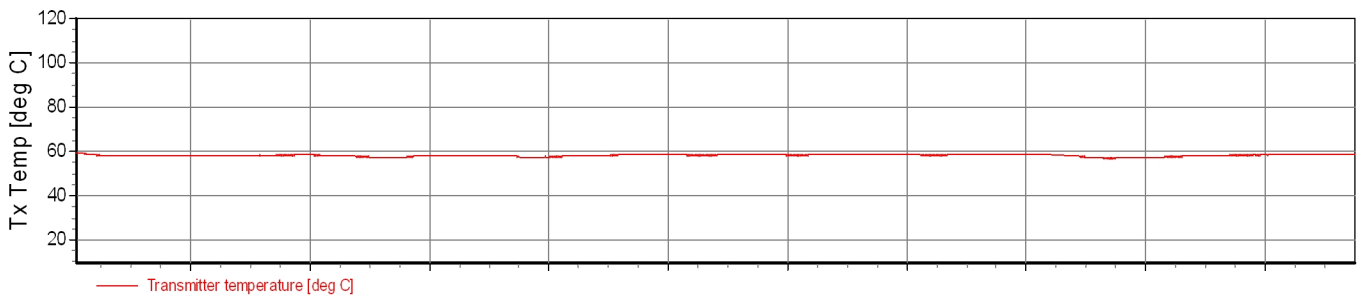
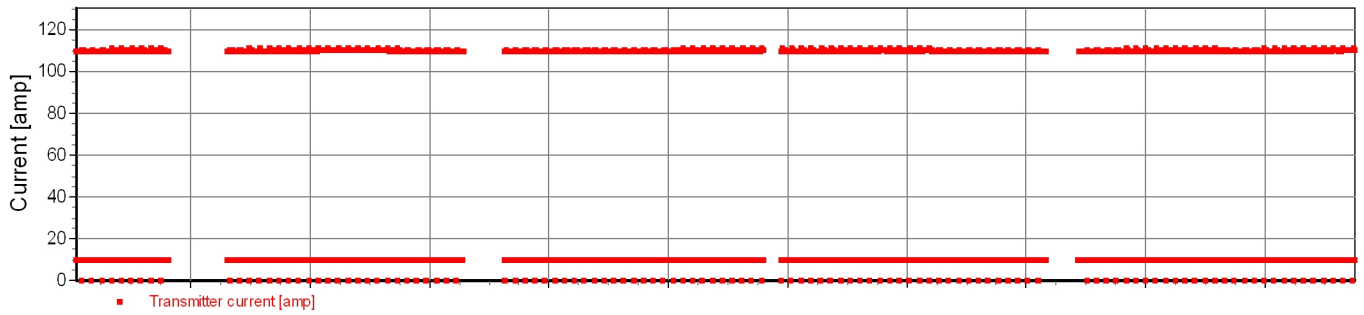
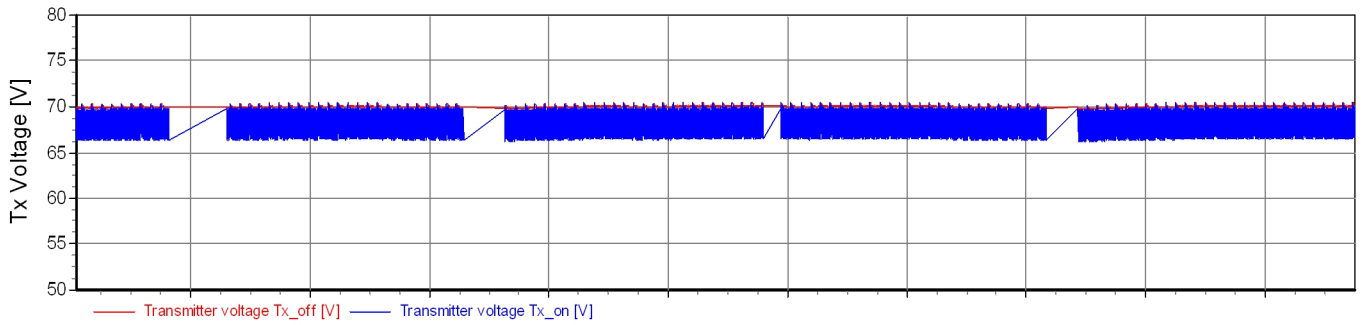
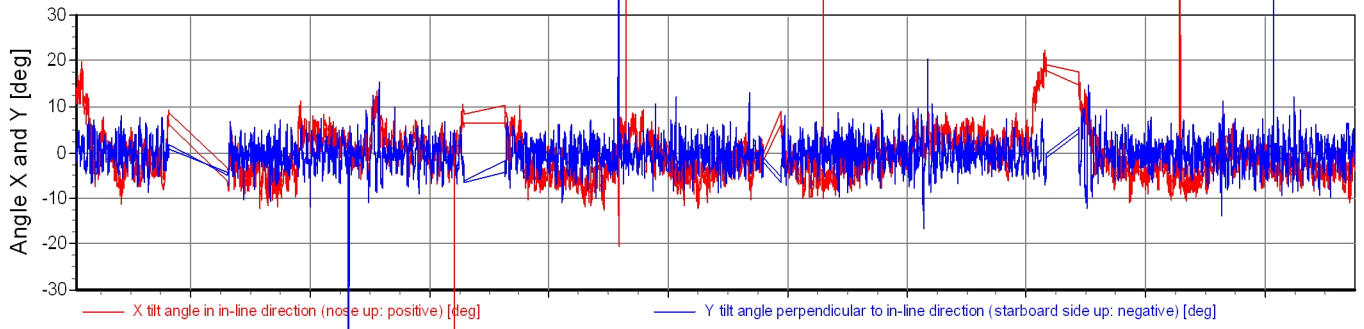
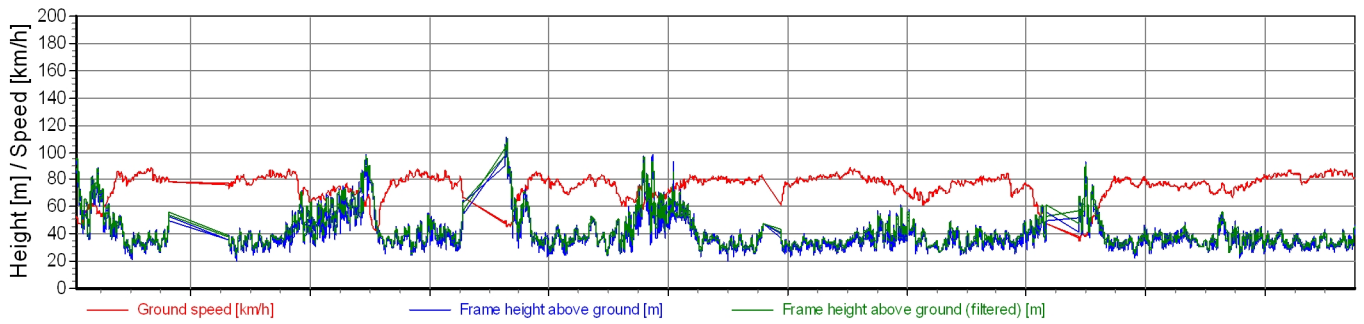


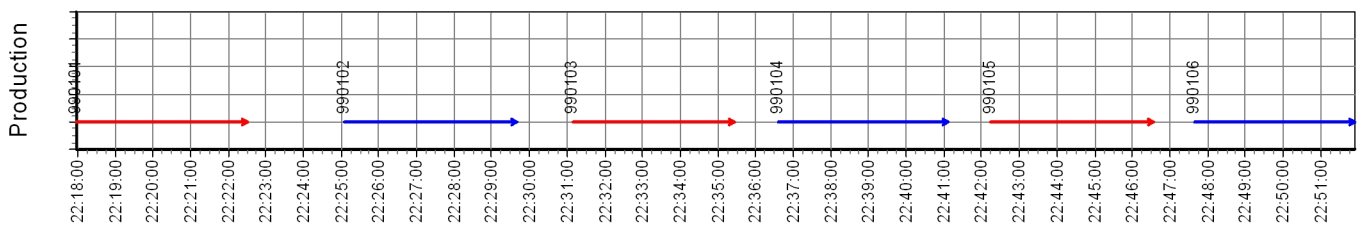
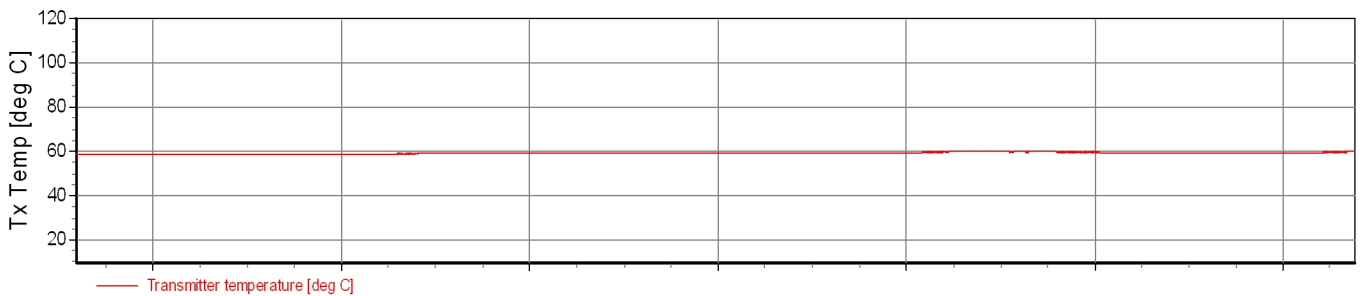
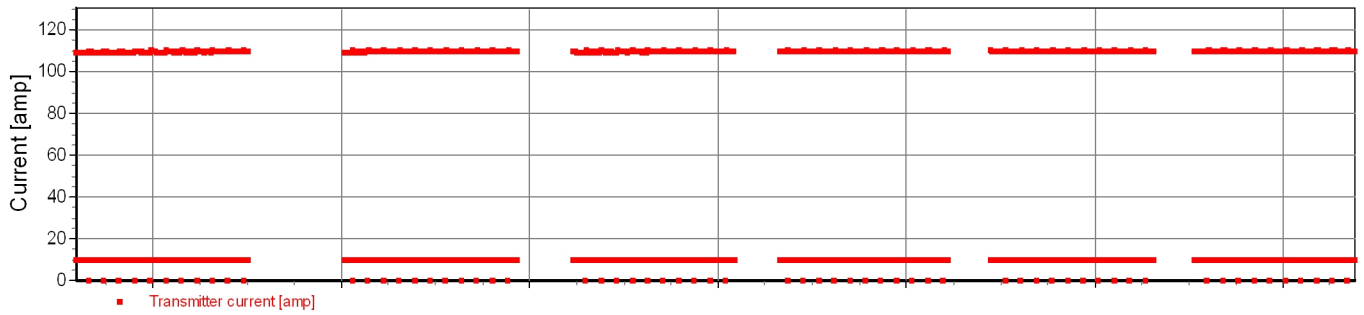
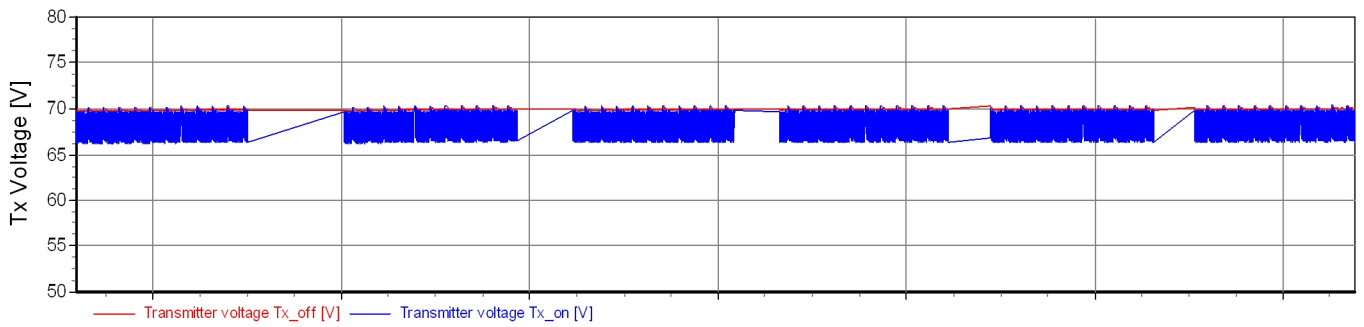
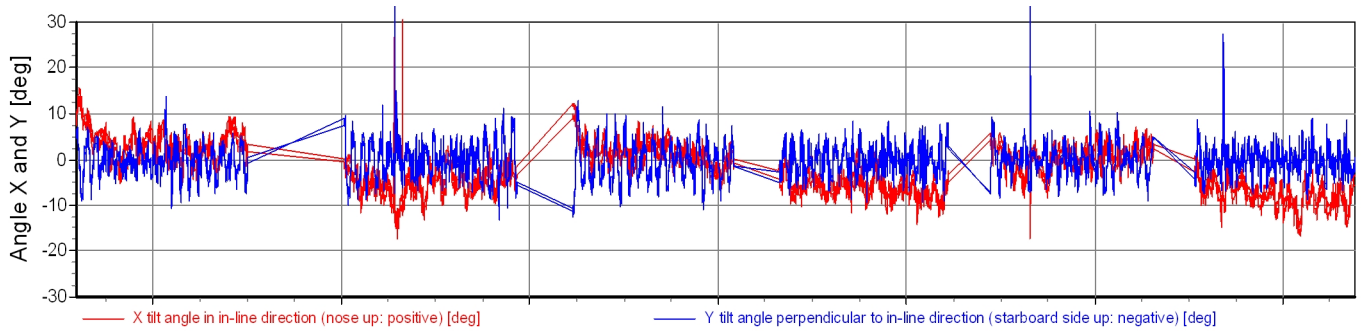
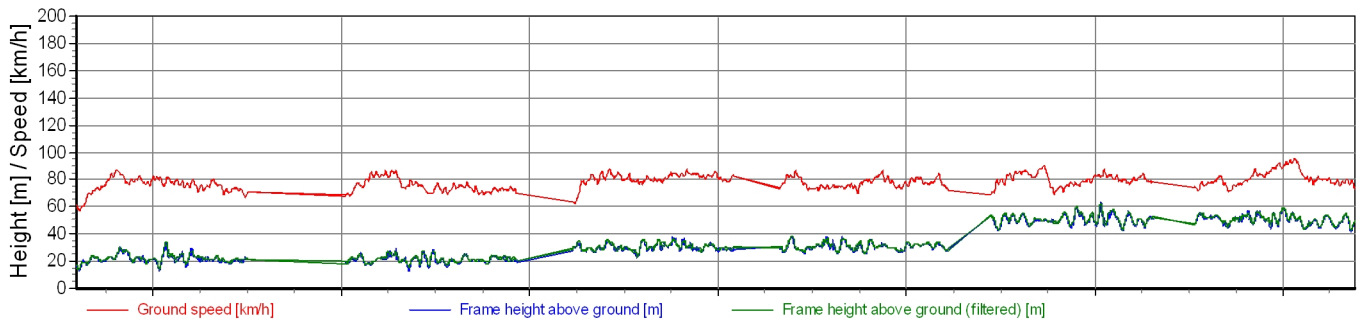


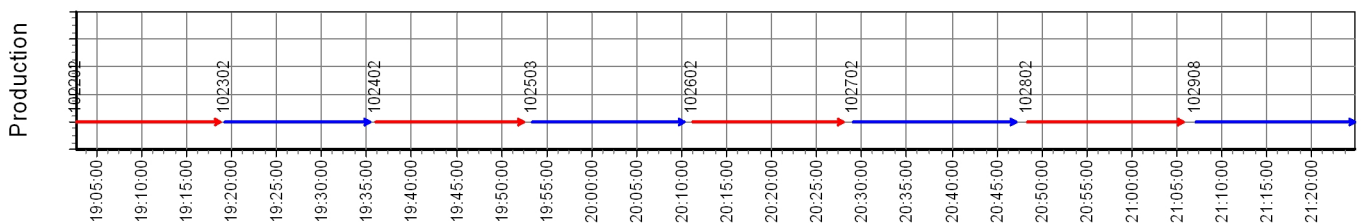
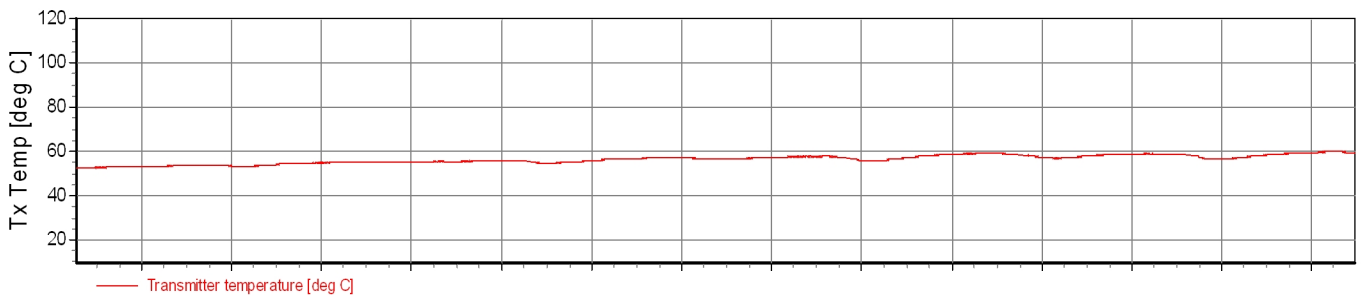
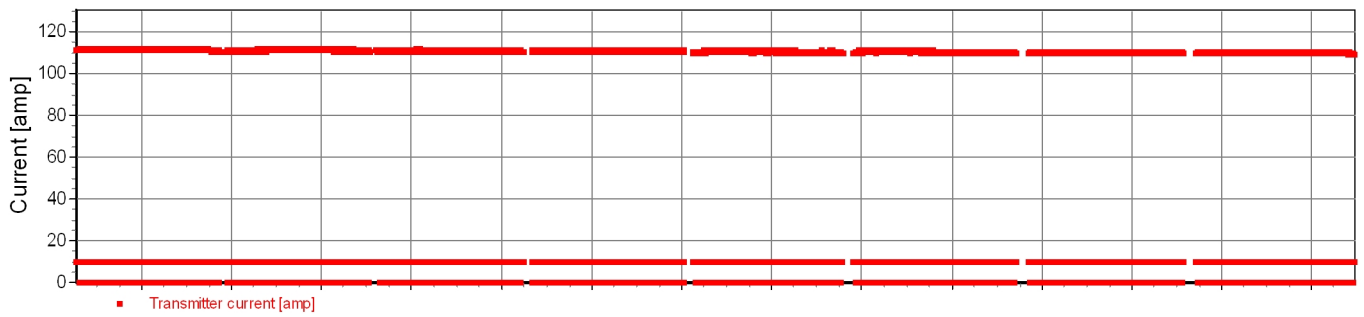
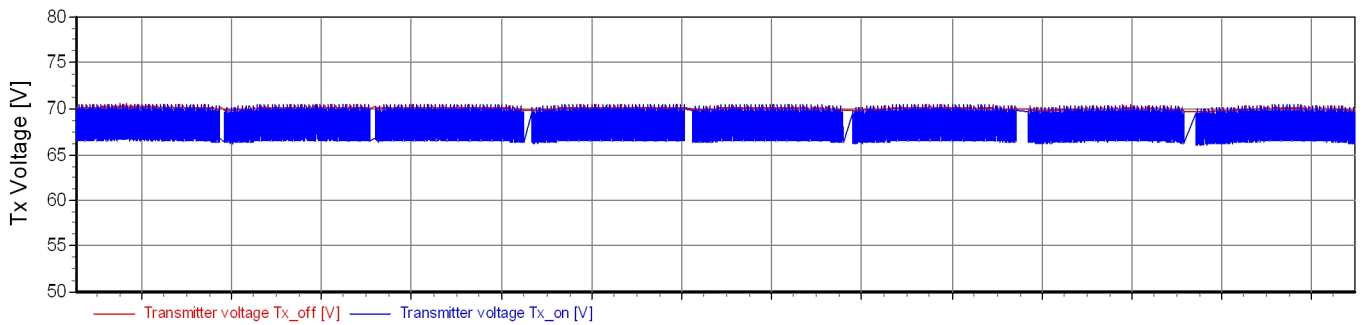
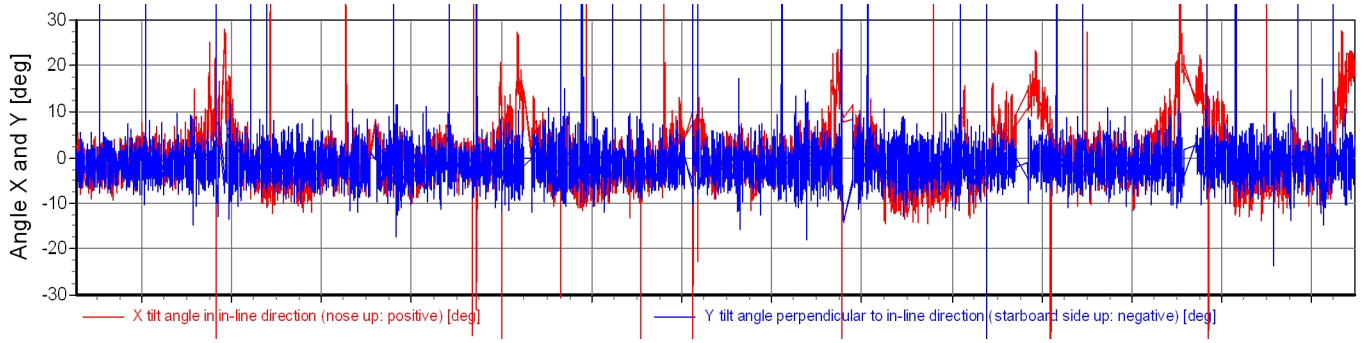
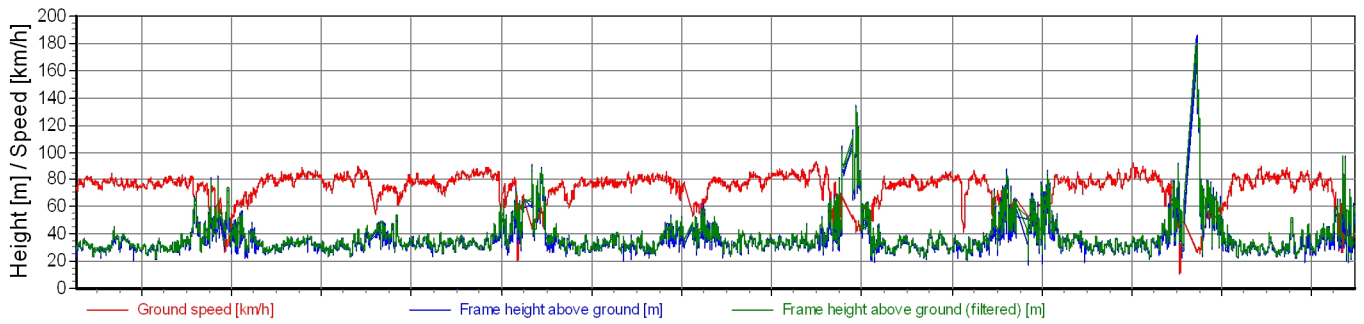


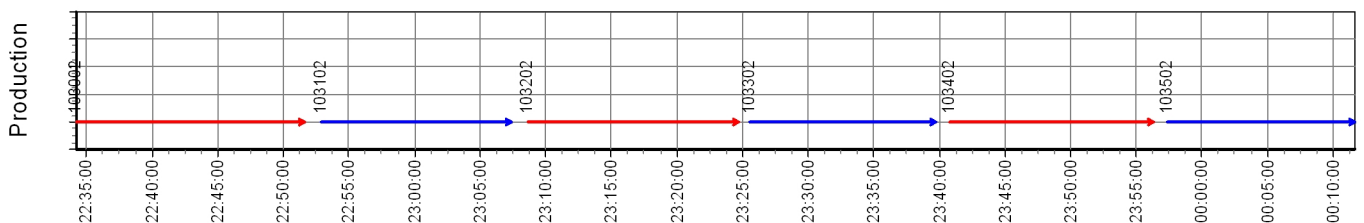
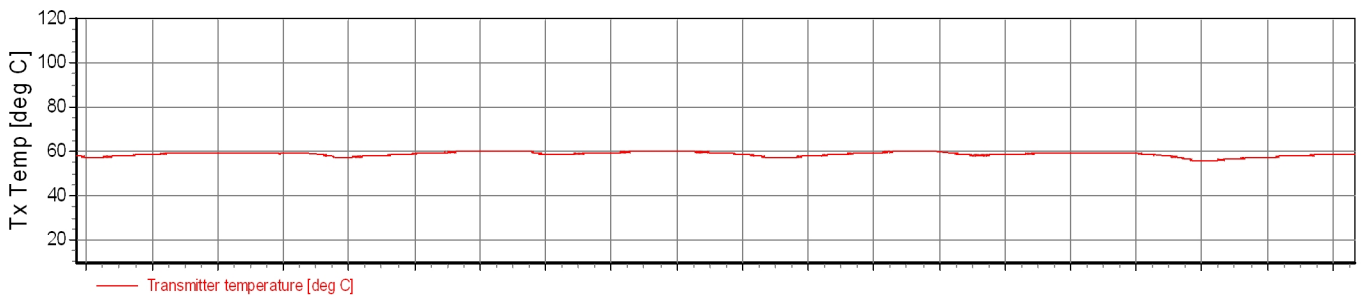
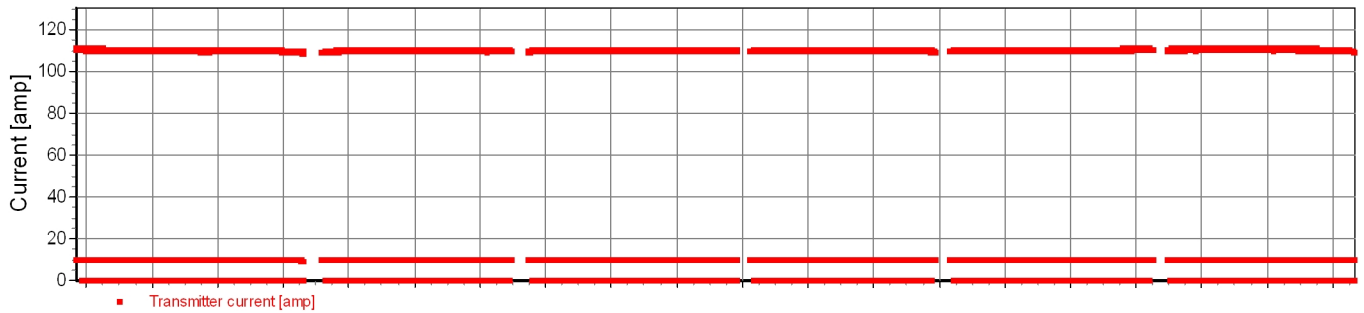
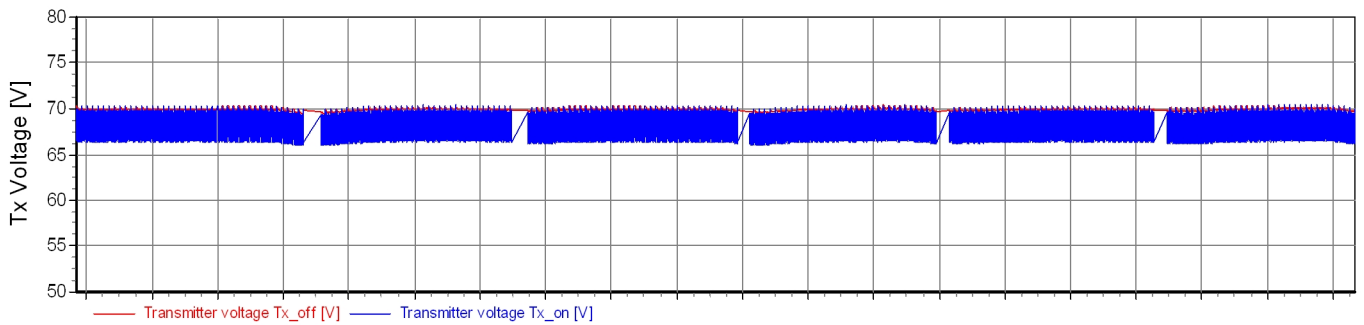
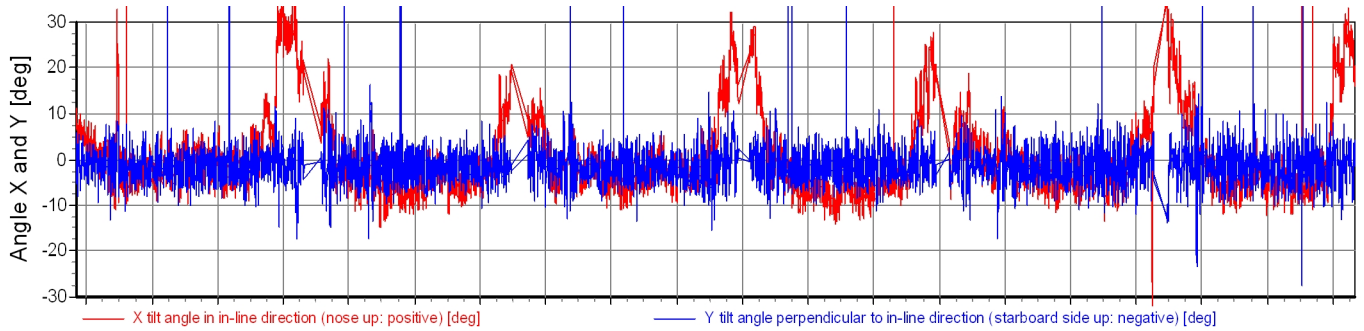
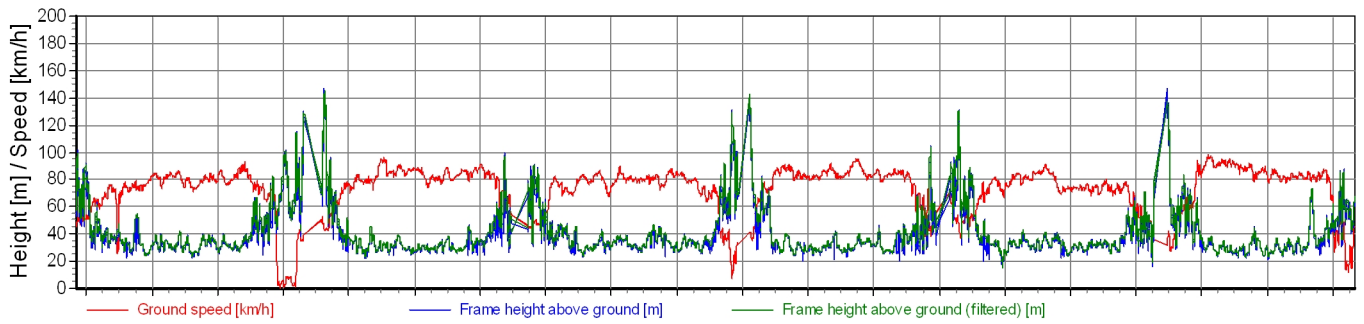


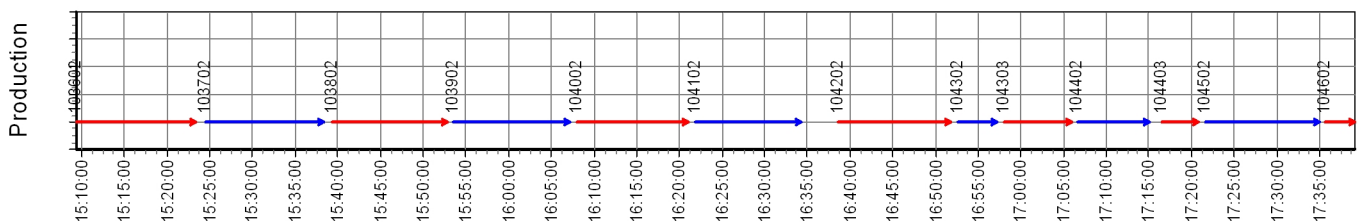
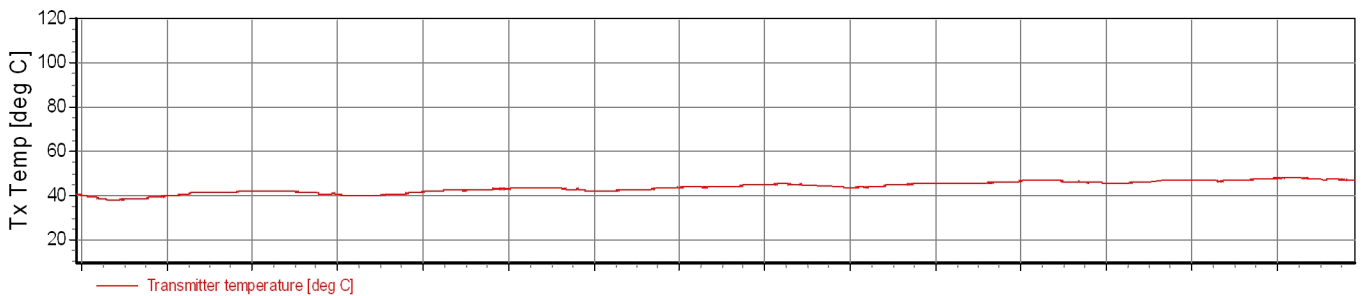
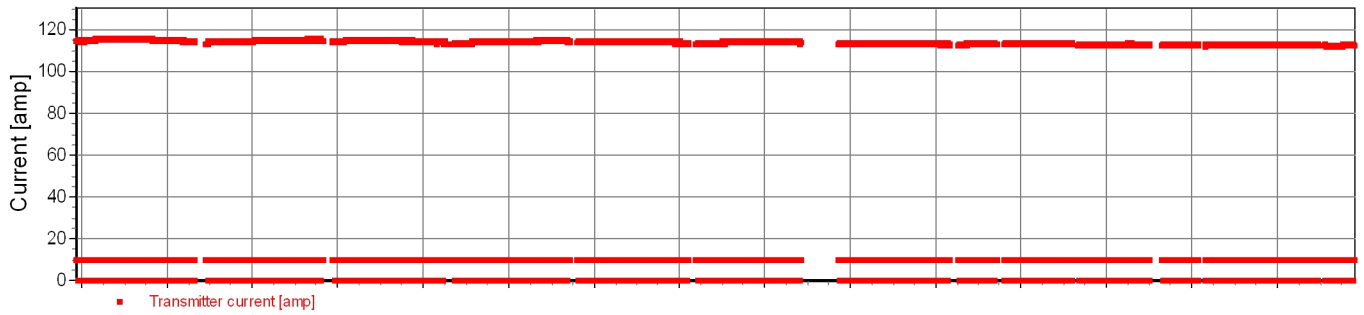
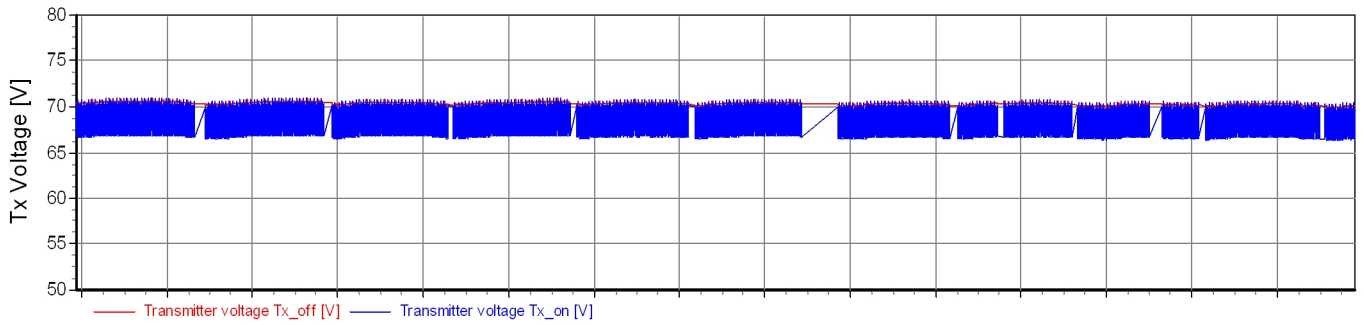
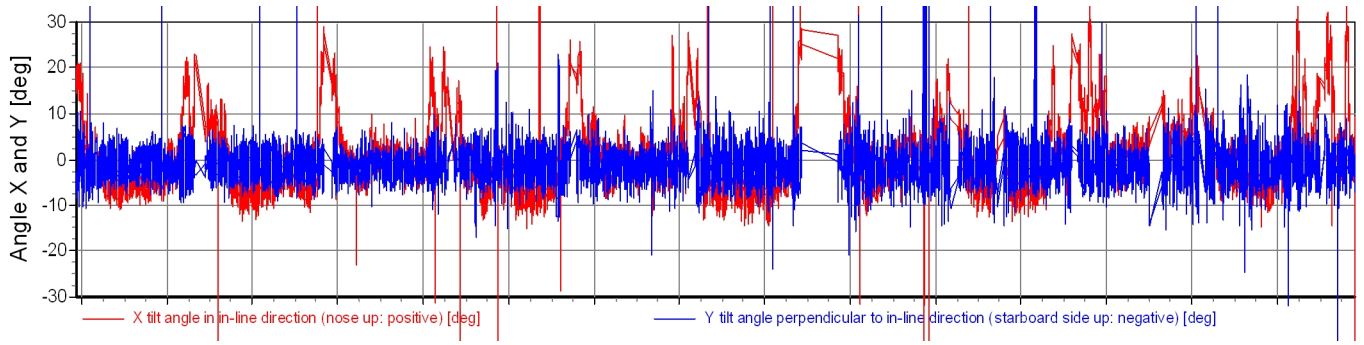
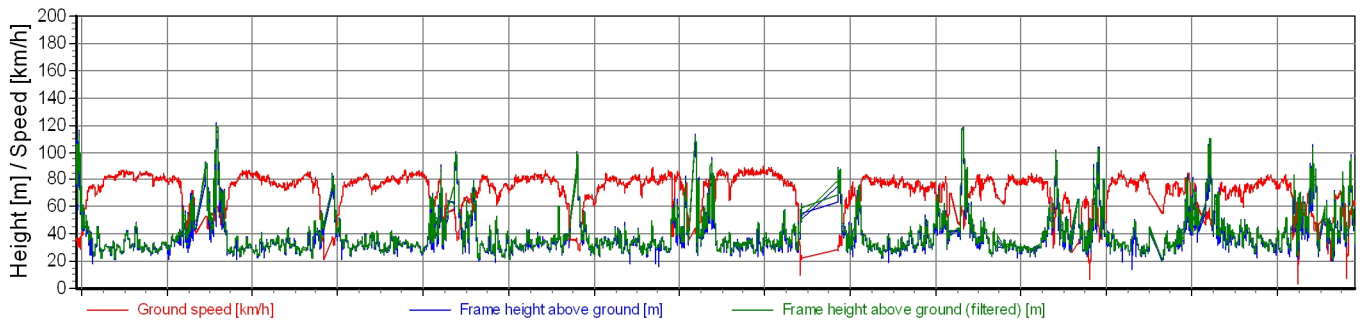


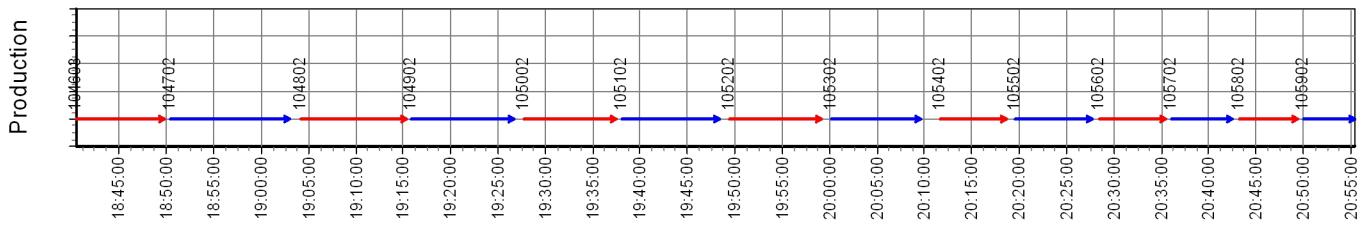
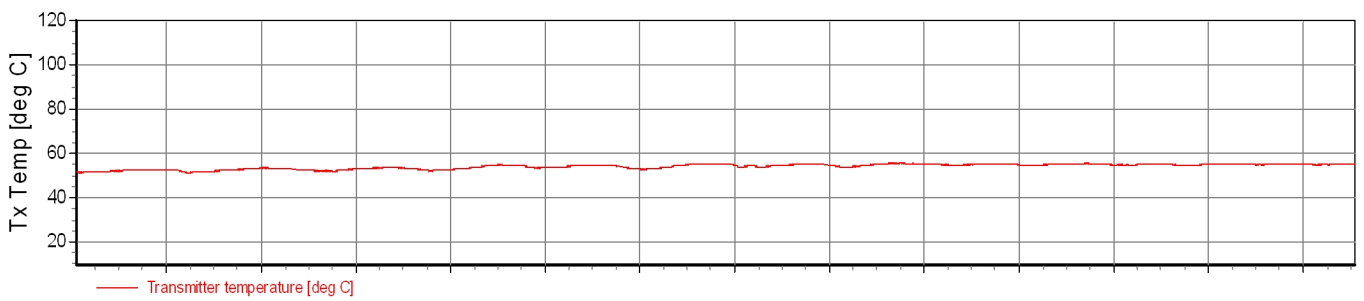
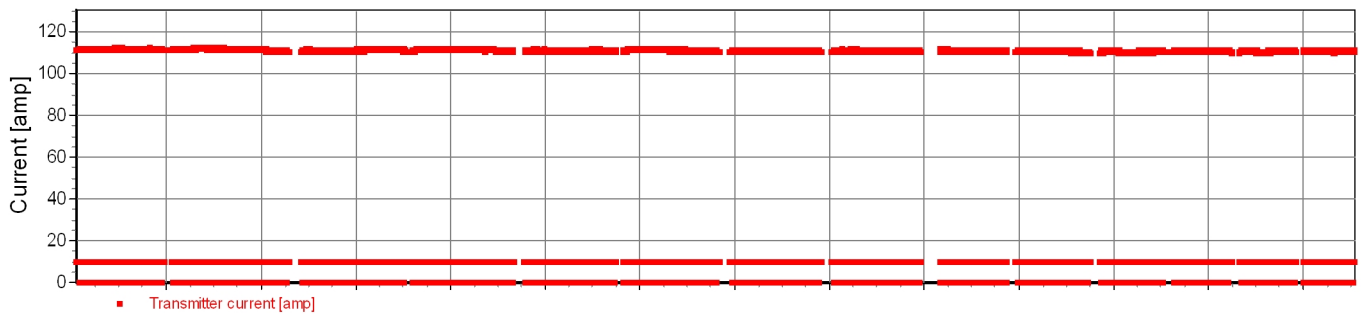
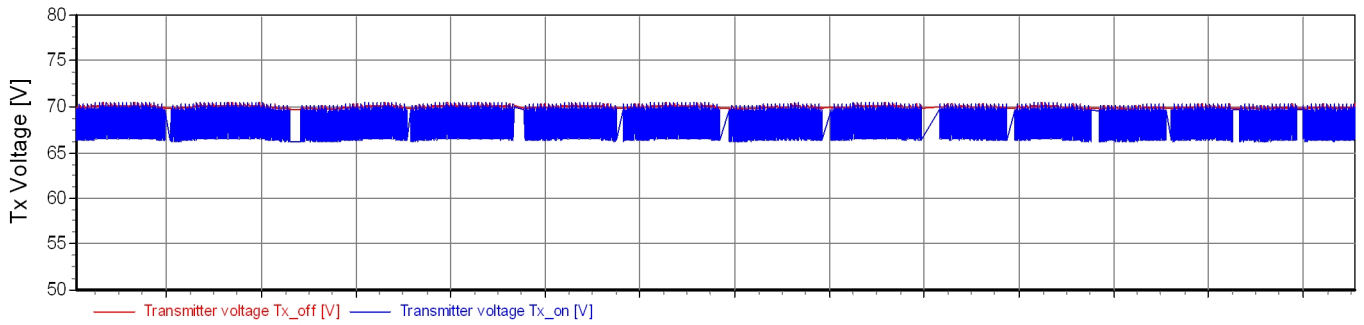
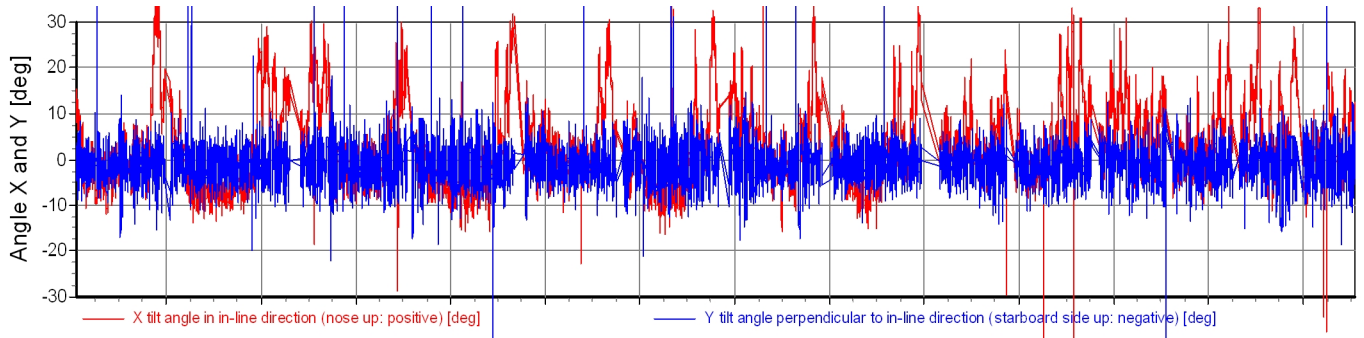
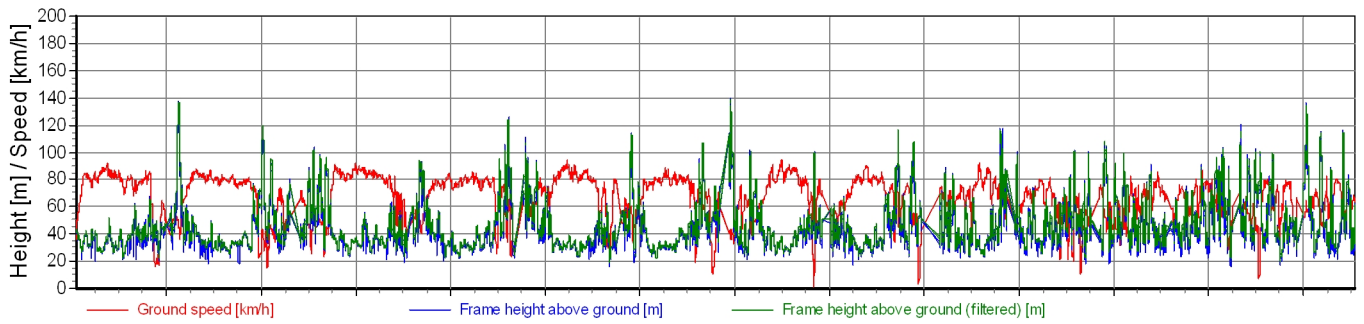


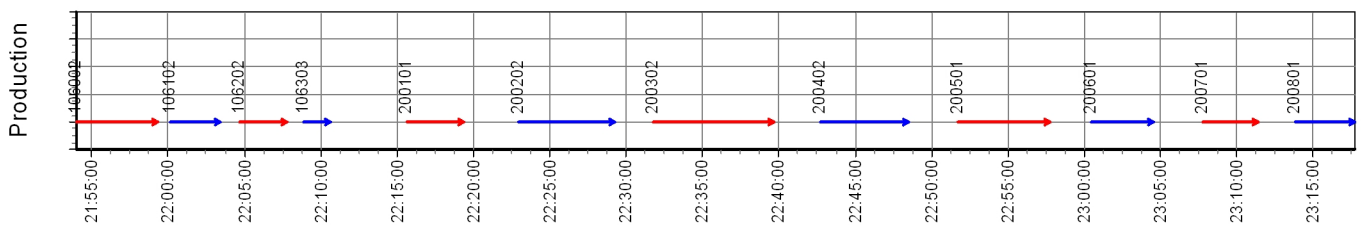
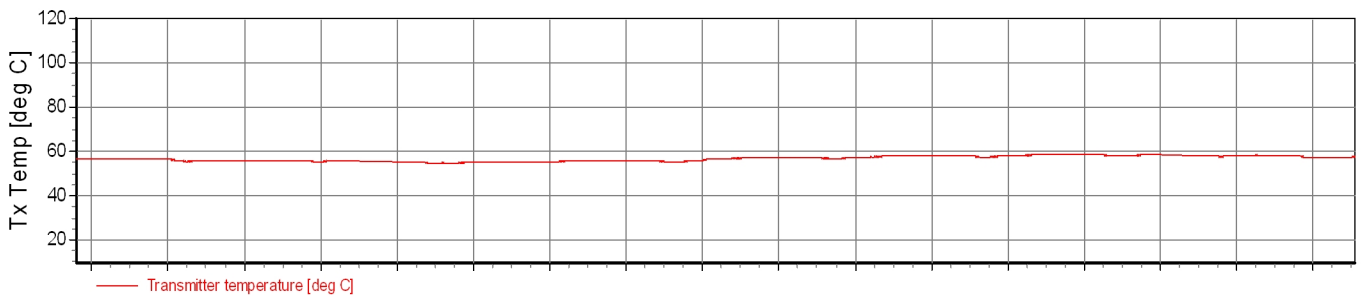
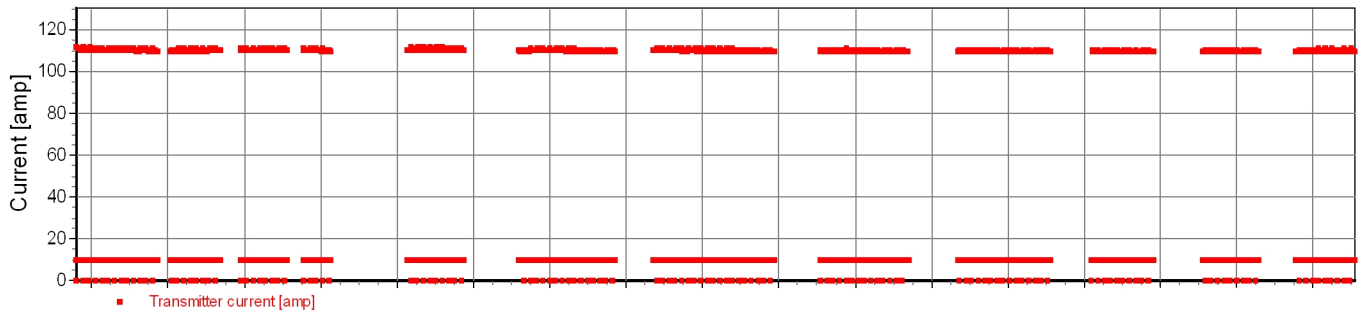
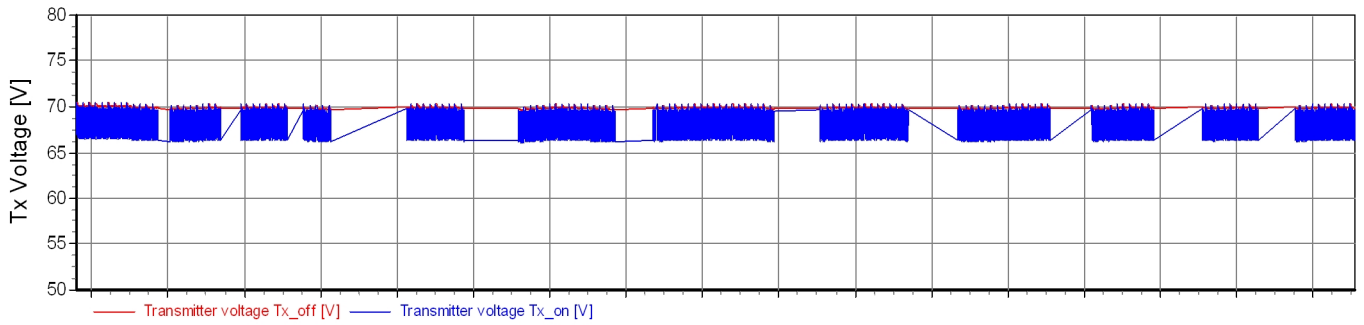
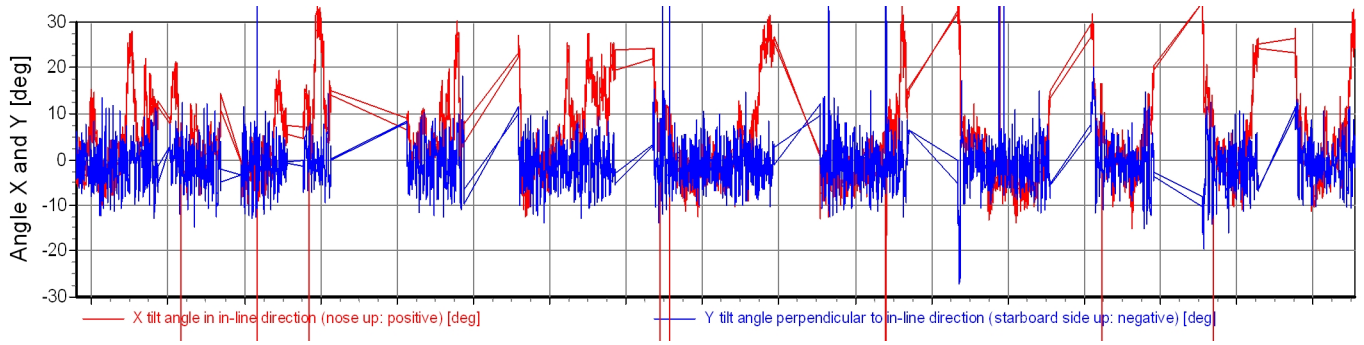
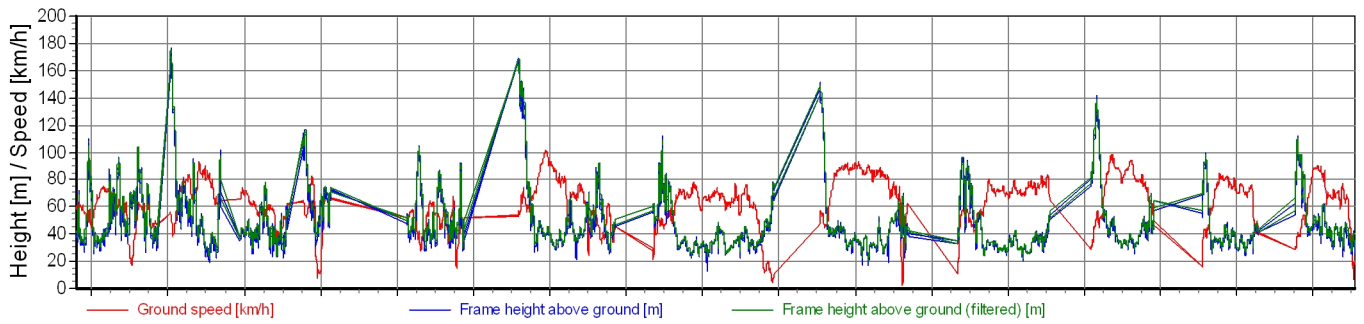


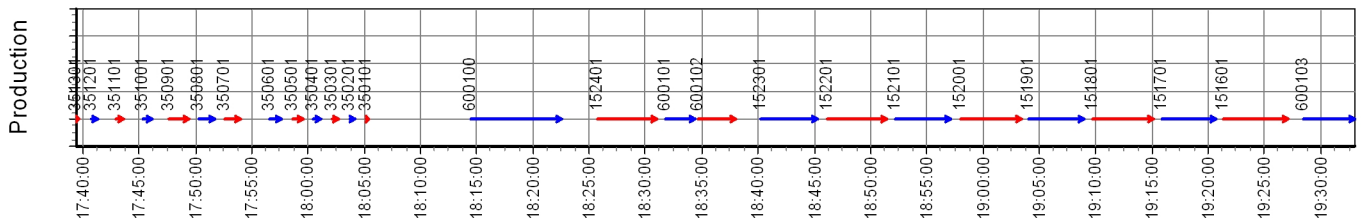
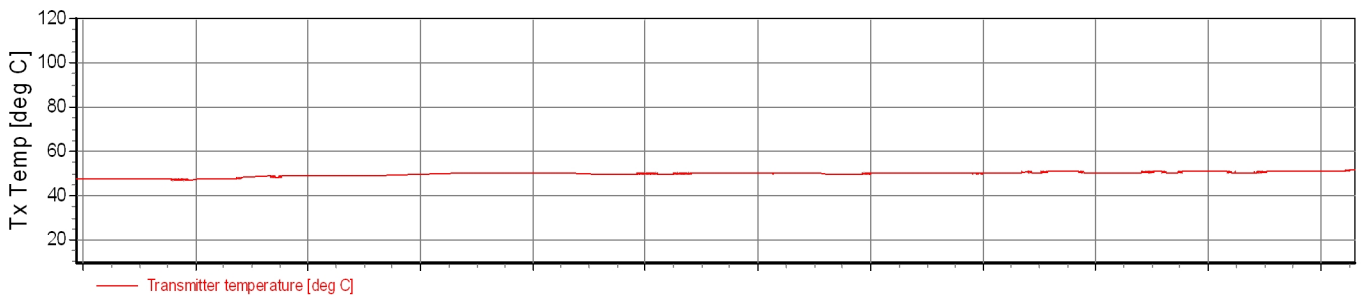
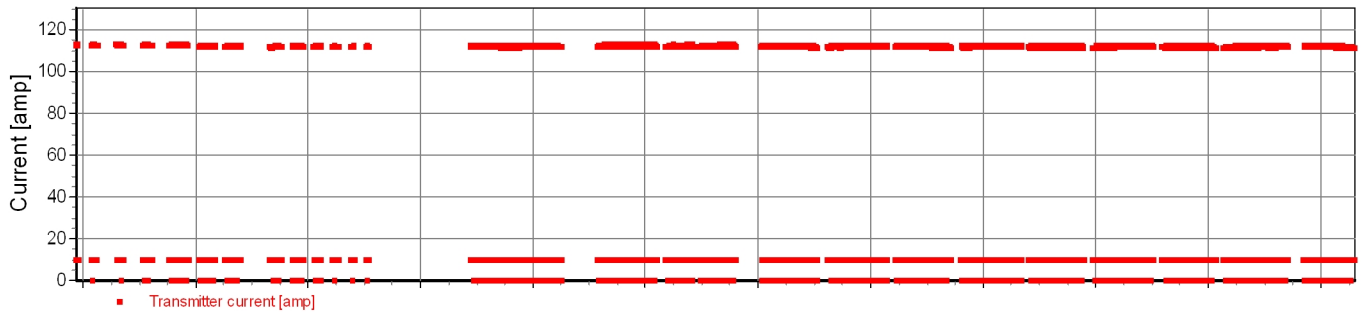
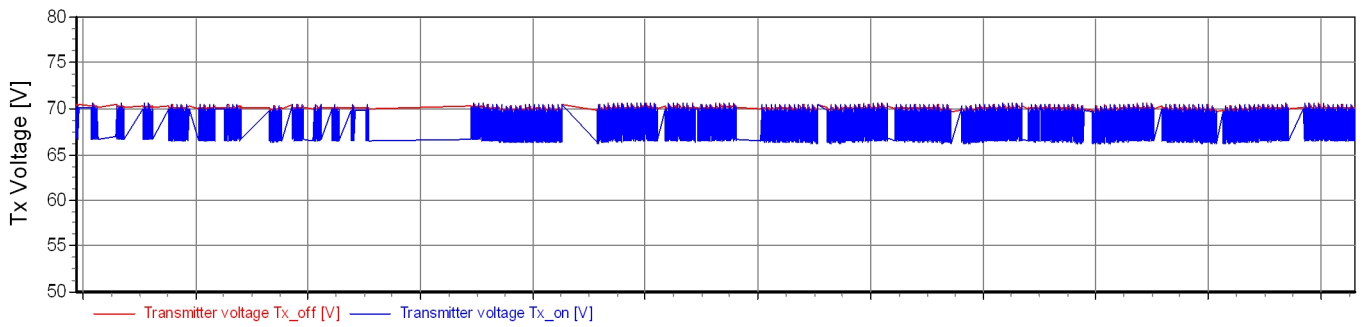
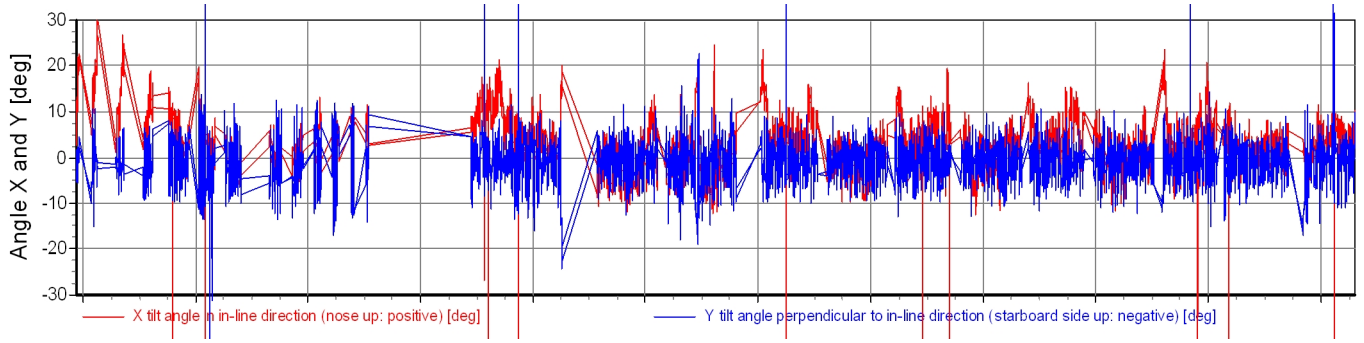
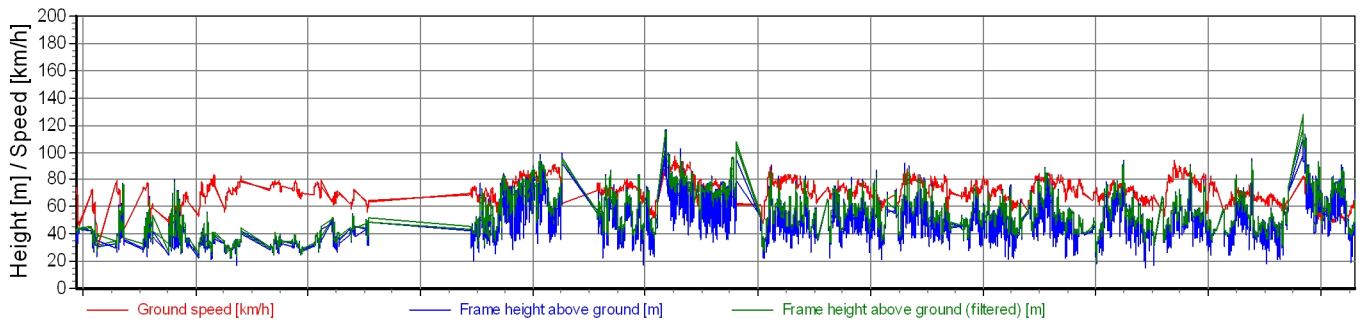


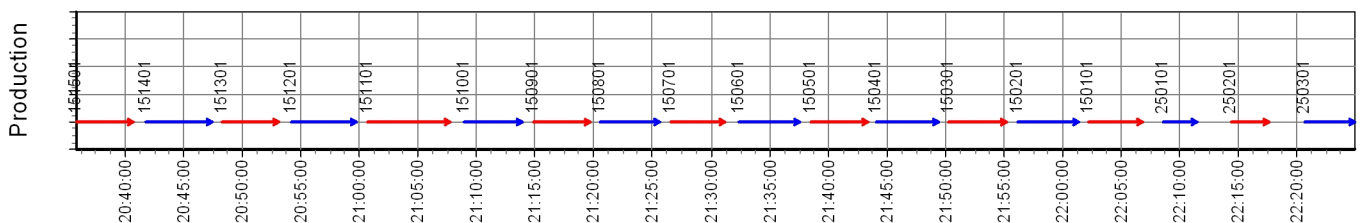
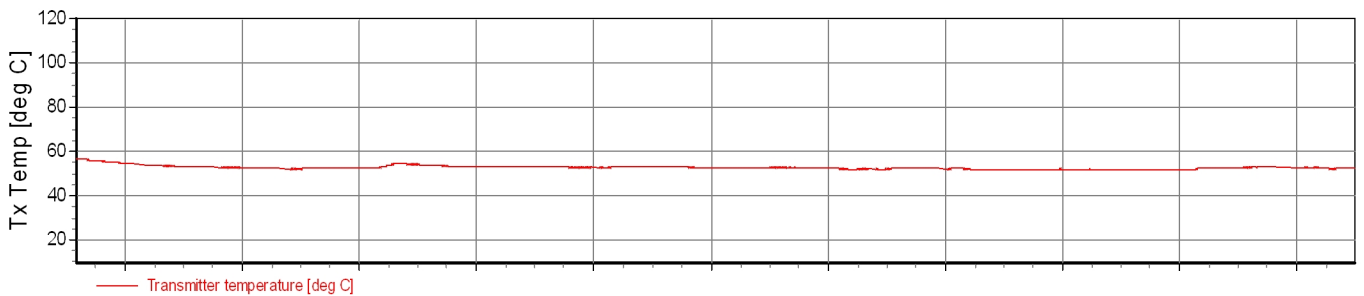
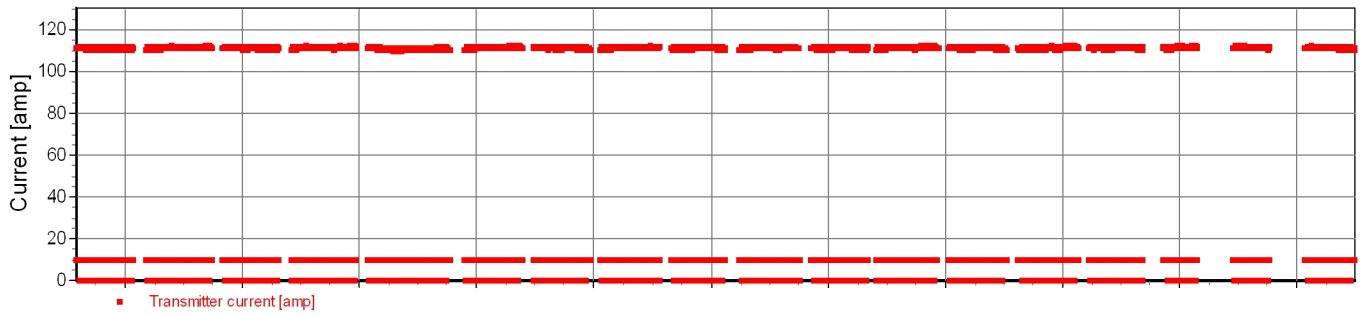
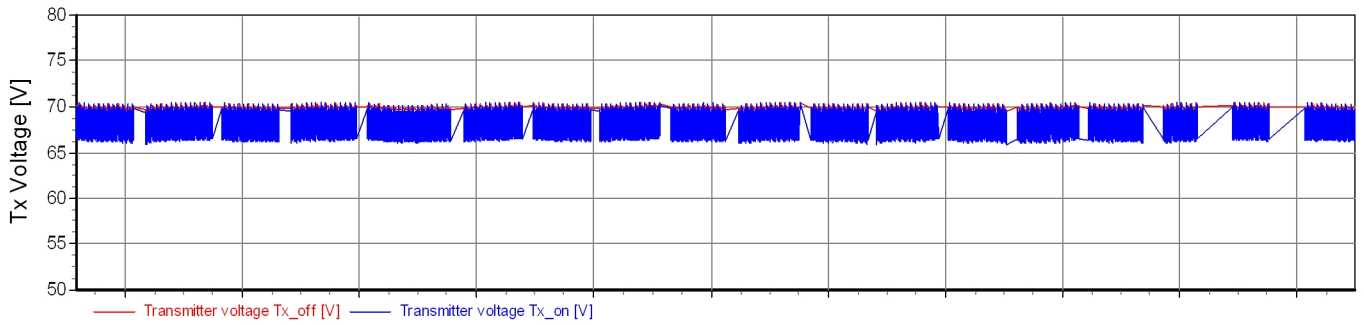
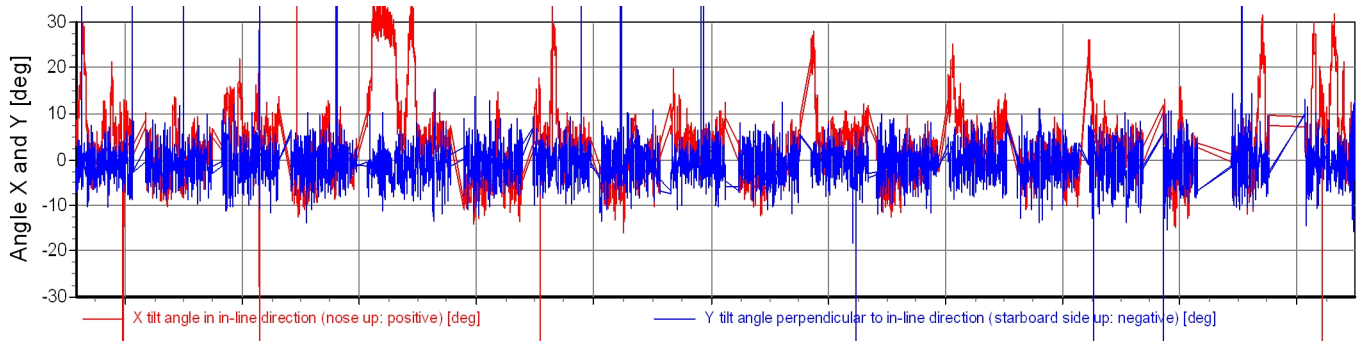
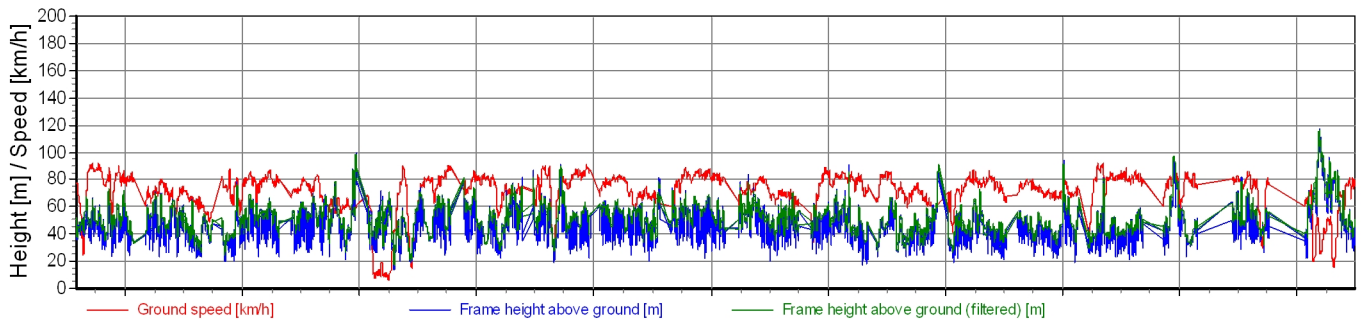












## Appendix 5: Modelling and inversion of TEM Data

This appendix gives a brief introduction to modelling and inversion of SkyTEM data.

### **The model**

The model used for inversion of SkyTEM data is a 1D multi-layer model (MLM) with typically 30 layers. The layer thicknesses increase downwards as a hyperbolic sine function of the layer number. This means that the depth to the layer boundaries increases linearly for small depths, so that the top layers are all of approximately the same thickness. For large depths, the depth to the layer boundaries increases exponentially with depth, so that the thickness of a layer is a factor times the previous one.

### **Inversion - The initial model**

The initial model for the deep inversion is a 30-layer MLM with a homogeneous resistivity for all layers, i.e. the initial model is essentially a homogeneous half space. Model optimization can be carried out in both a L1- and a L2- norm formulation where the former produces more blocky models than the latter.

### **Data and noise model**

The inaccuracy of TEM data is influenced by the ambient noise. This noise is reduced by selective stacking of delay time series, and by applying appropriate filters in the receiver system.

Experience with SkyTEM data suggests that the noise voltage most often can be described with a simple model:  $\log(\text{noise})$  is a linear function of  $\log(\text{time})$ . When the width of the time gates increases proportional to delay time - as is the case with the SkyTEM system - the slope of the linear function is close to -0.5. The noise model used can therefore be described as:

$$V = V_0 \cdot \left( \frac{t}{t_0} \right)^\alpha$$

Where  $V$  is the noise voltage,  $V_0$  is the noise voltage at time  $t_0$  and  $\alpha$  is the slope of the noise voltage as a function of time in a double logarithmic plot. Choosing  $t_0 = 1$  ms, the noise model is defined by the values of  $V_0$  and  $\alpha$ . These values are chosen pragmatically by inspection of a subset of the data volume.

$V_0 = 2.5e-12$  in field units normalized with Tx moment (LM)

$V_0 = 2.5e-13$  in field units normalized with Tx moment (HM)

$t_0 = 1$  ms

slope = -0.5

## **Regularization**

Inversion of TEM data is highly non-linear which means regularization is needed in order to guide the inversion routine to produce feasible geological models. In the initial inversion, a vertical smoothness constraint is implemented through a broadband model covariance matrix. This matrix is constructed by stacking single-scale exponential covariance functions with different correlation lengths, describing the covariance between any two points in the sub-surface. This approach has proven to be very robust and stable as the expected subsurface variability can be described through the prior covariance matrix (/3/).

To obtain laterally smooth model sections, the Lateral Parameter Correlation (LPC) procedure is used (/3/ and /4/). Through an inversion process, a smooth version of the resistivity variation is predicted from the results of the initial inversion. In this approach, all parameter values are correlated with all other values in the plane. After the LPC procedure, data are subjected to a final inversion constrained by the LPC models to improve the data fit.

## **Data insufficiency**

For SkyTEM data, the insufficiency lies primarily in the limited delay time range that can be obtained. The earliest obtainable time gate is determined by the turnoff of the Tx current, and the latest useful time gate is determined by the signal to noise ratio. Increasing the Tx moment will give better measurements at late times, and thus improve the depth penetration, but also increase the turnoff time and thus remove early-time gates, thereby making the near-surface resolution poorer. This trade-off is solved by transmitting an alternating sequence of (1) a low moment that can be turned off quickly to give good near-surface resolution, and (2) a high moment that will improve the signal-to-noise ratio at late times, thus improving depth penetration.

## **Model inconsistency**

When using 1D models in the interpretation of SkyTEM data, inconsistency arises where the lateral gradient of conductivity is not small, e.g. typically in mining applications. However, also in environmental investigations, inconsistencies can arise, typically where near-surface good conductors have abrupt boundaries. Often such inconsistency is indicated by the data residual being high and one should look upon the inversion results with some caution at these locations. 3D effects can also reveal themselves by the so-called 'pant legs', i.e. conductive or resistive structures projecting at an angle of approximately 30 degrees from the horizontal at the edges of high contrast structures.

## Appendix 6: Model sections and resistivity intervals

Model sections and analysis sections are delivered in digital form as PDF files.

## Model sections

The Model sections can be found in the data delivery folder as PDF's.

The model section plot consists of five subplots. The top plot shows the inverted models, with topography, where the resistivity of the individual layers is colour coded according to the colour bar. The resistivity is shown on a logarithmic scale and conductive and resistive features appear with the same weight. The actual flight elevation is shown with a red line above the model section. The white line in the model section indicates the estimated depth of investigation (DOI). Starting from the bottom layer of the model, the DOI is equal to the depth of the first layer having a conductance uncertainty of less than 0.5. If the resistivity uncertainty is too high, the layer resistivity is unresolved.

Below the model section is a plot of the normalized data residual (red line) and normalized total residual (black line) of the inversions. The total residual is a weighted sum of the data residual and the model residual, where the latter is a measure of the roughness of the model, i.e., the deviation of the final model from the initial homogeneous halfspace model.

Below the residual section is the analysis section. The resistivity of the inverted models is determined partly by the measured data and partly by the regularization – the vertical and horizontal smoothness constraints – used in the inversion. To illustrate the relative importance of the data and the smoothness constraints an analysis section is produced. The analysis section has the same appearance as the model section, but rather than plotting the layer resistivities the normalized relative uncertainty of the layer resistivities are plotted. The values of the normalized relative uncertainty are colour coded according to the colour scale. The colour scale consists of four colours: red, yellow, blue, and blue fading into white.

The red colour indicates that data have contributed considerably to the inverted resistivity, i.e., the resistivity is well determined.

The yellow colour indicates that data has had more influence on the inverted resistivity than the regularization, i.e., the resistivity is fairly well determined.

The blue colour indicates that the regularization has had more influence than the data in determining the inverted resistivity, i.e., the resistivity is poorly determined.

Where the blue colour fades into the white, the inverted resistivity is determined almost exclusively by the regularization, i.e., the resistivity is essentially undetermined.

In short, one can say that data has had more influence than the regularization when values are below 1 – the red and yellow colours – and that the regularization has had more influence than the data where the values are above 1 – the blue and white colours.

Please take note that in some parts of the analysis sections, where the near-surface resistivity is very high, the top part of the model can be seen as undetermined. In this situation the TEM method cannot determine the resistivity.

Below the analysis section are two plots of the measured data (dots) together with the response of the inverted models (solid lines). M1 is low moment data and M2 is high moment data. For both plots, every second gate is plotted starting with the earliest gate, and data are plotted with a density of 8 points per centimetre along the profile.

## Layer Resistivity Maps

The Model sections can be found in the data delivery folder as PDF's as well as geosoft . grd files.

The resistivity maps show the inverted resistivity for each of the model layers.

As the thickness of the model layers increases downwards the maps represent a varying thickness interval. The depth interval is stated on the pdf files and is in meters below the surface.

## Appendix 7: Digital data

The digital data are listed in the following folders.

Data delivery folder	Sub folder	Sub folder	File format	Comment
01_TEM_data	01_Data		Geosoft.gdb	EM database ready for import in Geosoft
	02_EM_Channels_grid	Paradox_HM_Z	Geosoft.grd	Channel plots of raw data. Gate 18-34
		Paradox_LM_Z	Geosoft.grd	Channel plots of raw data. Gate 5-26
		SanLuis_HM_Z	Geosoft.grd	Channel plots of raw data. Gate 18-34
		SanLuis_LM_Z	Geosoft.grd	Channel plots of raw data. Gate 5-26
	03_WB_Files	Geofile	.geo	Geometry file
		Maskfile	.lin	Files masking flown lines
Rawdata		.skb .sps	Em and Aux data	
02_MAG_data	01_Data		Geosoft.gdb	Mag database ready for import in Geosoft
	02_Grids		Geosoft.grd	Grids of TMI, RMF
	03_Maps		.pdf .map	Maps and PDF's of RMF, TMI
03_Inversion	01_Data		Geosoft.gdb	Database containing EM inversion results, read for import in Geosoft
	02_Layer_Resistivity_Grids	Paradox	Geosoft.grd	Grids of the resistivity in each layer
		SanLuis		
	03_Layer_Resistivity_Maps	Paradox	.pdf	Maps and pdf's of the resistivity in each layer
		SanLuis	.map	
	04_Sections	Paradox	.pdf	Layer mean resistivity and analysis of all lines
SanLuis		.png		
04_MISC	DEM		Geosoft.grd .pdf .map	Digital Elevation Model (DEM)
	Linepath		.pdf .map	Line Path.
	PlannedFlightLines		.pdf .map	Planned flight lines
05_Report			.pdf	The report and appendices
06_AGG_Report			.pdf	Aarhus Geophysics group report and pdf plots